A COMPARITIVE STUDY OF CONVENTIONAL AND FUZZY LOGIC CONTROL OF DC DRIVE WITH POWER FACTOR CORRECTION

A Thesis submitted in partial fulfillment of the requirements for the award of degree of

Master of Engineering
in
Electronic Instrumentation and Control

Submitted by
ROHIT GUPTA
(Roll No. 801051014)

Under the Guidance of

Ms. Ruchika Lamba
Lecturer

Mr. Moon Inder Singh
Assistant Professor

Department of Electrical and Instrumentation Engineering
Thapar University
(Established under the section 3 of UGC act, 1956)

Patiala, 147004, Punjab, India

July 2012

DECLARATION

I hereby certify that the work which is being presented in the thesis entitled "**A COMPARITIVE STUDY OF CONVENTIONAL AND FUZZY LOGIC CONTROL OF DC DRIVE WITH POWER FACTOR CORRECTION** " in partial fulfillment of award of degree of **Master of Engineering in Electronics Instrumentation and Control** submitted in Electrical and Instrumentation Engineering department, Thapar University, Patiala is an authentic record of my own work carried under the supervision of **Ms. Ruchika Lamba**, Lecturer, Department of Electrical and instrumentation engineering, Thapar University, Patiala, Punjab and **Mr. Moon Inder Singh**, Assistant Professor, Department of Electrical and instrumentation engineering, Thapar University, Patiala, Punjab.

Date: 25/06/12

Rohit Gupta 25/06/12
Rohit Gupta

801051014

I certify that the above made statement made by the student is correct to the best of my knowledge and belief.

Date: 25/06/12

Ruchika 25/6/2012
Ms. Ruchika Lamba
Lecturer
Department of Electrical and
Instrumentation Engineering
Thapar University, Patiala,
Punjab

Moon Inder Singh
Mr. Moon Inder Singh
Assistant Professor
Department of Electrical and
Instrumentation Engineering
Thapar University, Patiala,
Punjab

Countersigned By

S. Ghosh 3/7/12
Dr. Samarjit Gosh
Head of Department
Department of Electrical and
Instrumentation Engineering
Thapar University, Patiala,
Punjab

Dr. S. K. Mohapatra
Dean of Academic Affairs
Thapar University, Patiala,
Punjab

II

ABSTRACT

Power electronics circuits are the major part of the industry and so are the electrical drives. To control the electrical drives power electronics circuits are used dominantly. But there are some disadvantages of power electronics circuits, like mains current in an AC/DC converter contains periodic current pulses due to the action of rectifier and output filter capacitor. The high current peaks cause harmonic distortion of the supply current and low power factor. This results in poor power quality, voltage distortion, poor power factor at input AC mains, slowly varying rippled DC output at load end and low efficiency. So it is very important to improve the power factor of rectifier circuits, and it can be done by reducing the input current harmonics by using some filter or other techniques.

In any of the control application, controller design is the most important part. There are different types of controller architectures available in control literature. The controller can be conventional in nature or can be intelligent in nature. The conventional controller doesn't possess the human intelligence; where in the intelligent controller human intelligence is embed with the help of certain soft computing algorithms. After the design of controller is performed, the performance evaluation part comes in to light. The designed controller has to give optimal control results irrespective of every situation like plant and equipment non linearity, equipment saturation.

So this dissertation looks in to performance evaluation of different conventional and intelligent controllers implemented with a clear objective to control the speed of DC motor including power factor improvement topology. First of all mathematical modeling of the process is performed. After the mathematical modeling the control objective is set and different kind of controllers are designed to meet the control objective. During the design of fuzzy based hybrid controller, the designer meets two key design challenges namely, optimization of existing fuzzy rule base and identification, estimation of new membership function or optimization of existing membership function. These issues play a vital role in controller design in real time.

ACKNOWLEDGEMENT

The real spirit of achieving a goal is through the way of excellence and austere discipline. I would have never succeeded in completing my task without the cooperation, encouragement and help provided to me by various personalities.

With deep sense of gratitude I express my sincere thanks to my esteemed and worthy supervisor, & Co-supervisor **Ms. Ruchika Lamba & Mr. Moon Inder Singh** Department of Electrical and Instrumentation Engineering, Thapar University, Patiala for their valuable guidance in carrying out this work under their effective supervision, encouragement, enlightenment and cooperation. Most of the novel ideas and solutions found in this thesis are the result of our numerous stimulating discussions. Their feedback and editorial comments were also invaluable for writing of this thesis.

I shall be failing in my duties if I do not express my deep sense of gratitude towards **Dr. Smarajit Ghosh,** Professor and Head of the Department of Electrical & Instrumentation Engineering, Thapar University Patiala who has been a constant source of inspiration for me throughout this work.

We express our deep sense of gratitude to **Mr. Subhransu Padhee** for his valuable and encouraging guidance, which played a major role in the formation of this project work. His corporation and timely suggestions have unparallel stimuli for me to travel eventually towards the completion of this project.

I am also thankful to all the staff members of the Department for their full cooperation and help. This acknowledgement would be incomplete if I do not mention the emotional support and blessings provided by my friends. I had a pleasant enjoyable and fruitful company with them.

My greatest thanks are to all who wished me success especially my parents and brother, whose support and care makes me stay on earth.

ROHIT GUPTA

801051014

Place: Thapar University, Patiala

Date: 25/06/12

TABLE OF CONTENTS

LIST OF FIGURES

LIST OF TABLES

CHAPTER 1

INTRODUCTION

1.1 Overview

Electrical drives are the essential part of any manufacturing industry and so as their controlling but it should be controlled in an efficient way so that the losses should be minimum without making any compromise with controlling accuracy. PF is the measure issue with the industry because of that they have to pay extra money to the regulatory departments so to maximize the profit it becomes necessary to maintain the required power factor and take the remedial action for their causes.

1.2 Motivation

The versatile control characteristics of DC motor have contributed in the extensive use of DC motor in the industry. With the increasing use of power semi conductor units, the speed control of DC motor is increasingly getting sophisticated and precise. Speed of the DC motor is controlled by controlling the armature voltage. Armature voltage is controlled using different single phase AC/DC converter. Half converter, semi converter, full converter and dual converter are some of the thyristor based circuits which are used for speed control of DC motor. AC/DC converters are widely used in industrial applications. Input AC voltage is rectified and filtered using filtering circuit which consists of large electrolytic capacitors. These capacitors draw a large amount of current and the efficiency of the converter system decreases drastically. Low power factor, high harmonic distortion and large ripple factor have made the converter system inefficient. This research work studies about different converter topologies by which power factor can be improved and harmonic distortion can be reduced taking DC motor as a load and their time domain analysis is also done by generating transfer function of each component of system with different type of controllers.

1.3 Objective and scope of the dissertation

The objective of this dissertation can be stated in three points:-

- Design and implementation of different types of passive filters to improve the power factor and total harmonic distortion and a comparative study of those topologies in terms of different parameters.
- Incorporate best power factor improvement topology with different open loop thyristor based control topologies of DC drives and studying the reasons of nonlinearity in speed torque characteristic.
- Evaluate the performance of conventional and intelligent controllers. To evaluate the performance of the controller, time response is carried out. The time response analysis consists of unit step response and performance indices analysis.

Fig. 1.1 shows the work flow of this dissertation.

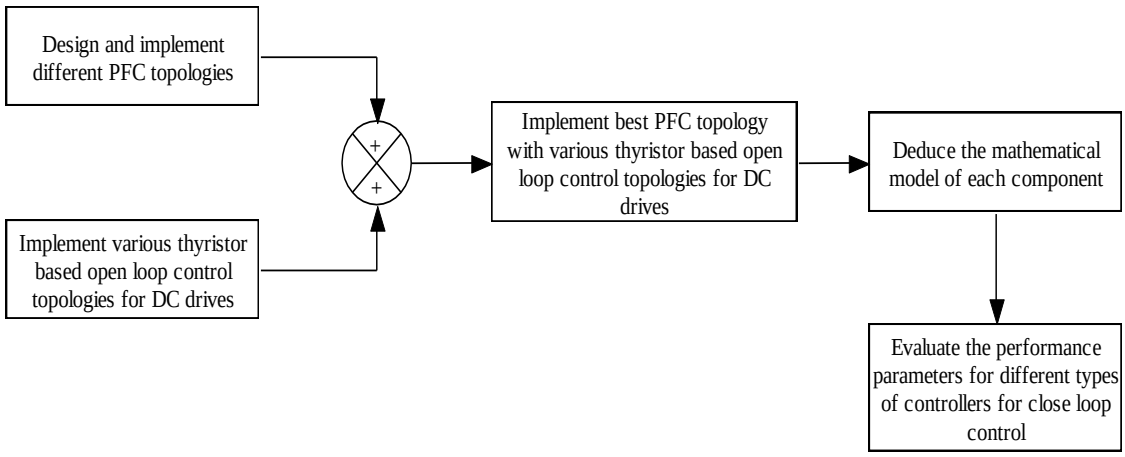

Fig. 1.1 Workflow of dissertation

1.4 Organization of the dissertation

The dissertation is organized as follows.

Chapter 2 takes on AC to DC converter with their poor power factor issues and design different passive filter to improve the power factor and total harmonic distortion as well. A comparative study of different filters is done on the basis of various parameters.

Chapter 3 deals with the different types of DC drives and their thyristor based open loop control methods. In this chapter, the reason of non linear speed torque characteristic is also deduced and the power factor correction filter topology is incorporated to improve the power factor and total harmonic distortion.

In chapter 4 the modeling of all the components is carried out which involves in cascaded close loop control structure of DC motor speed control along with the power factor correction filter.

In chapter 5 conventional and fuzzy controllers for cascade control structured DC motor speed control are designed and a comparative study of conventional controller and fuzzy controller is done basis on the basis of step response analysis and performance indices.

Chapter 6 deals with the performance analysis of power factor correction circuit topologies and time response analysis of conventional controller and Fuzzy based controllers.

Chapter 7 gives the concluding remarks and addresses the issues which can be taken up for further work.

CHAPTER 2

CONVERTERS

2.1 Power converters

Power electronics can be defined as a subject that deals with the apparatus and equipment working on the principle of electronics but rated at power level rather than signal level.

The advantages possessed by power-electronics systems are:-

i. High efficiency due to low loss.
ii. High reliability of power electronics converter system.
iii. Long life and less maintenance.
iv. Fast dynamic response.
v. Small size, light weight.
vi. Low cost due to mass production.
vii. Low cost due to mass production.

But system based on power electronics suffer from harmonics in the supply system as well as in the load circuit.

"***Electronic power converter***" is the term that is used to refer to a power electronic circuit that converts voltage and current from one form to another. The switching characteristics of power semiconductor device permit a power electronic converter to shape the input power of one form to output power of some other form. Broadly power electronics converters are of four types:-

1. Rectifiers (AC to DC)
2. Chopper (DC to DC)
3. Inverters (DC to AC)
4. Cycloconverter (AC to AC)

2.1.1 Rectifiers (AC to DC)

Alternating current is the main source of electrical energy delivered to industrial and domestic facilities. Therefore, it must be changed to a usable form of DC. The AC-DC converter produces a DC output from a AC input while the average power transferred from

an AC source to a DC load. This converter usually also called as a rectifier. The word rectification is used because the current flows in one direction. A rectification circuit is shown in Fig. 2.1.

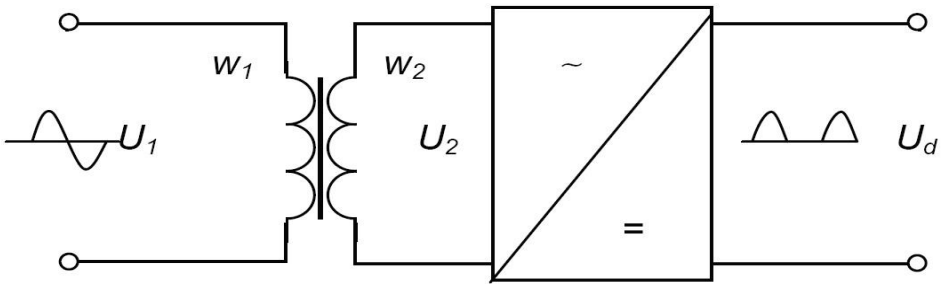

Fig. 2.1 Rectification circuit

Devices with asymmetrical conductance like semiconductor diodes and thyristors are used for rectifier circuits. The rectifiers with diodes are called uncontrolled rectifiers, and the rectifiers with thyristors are called controlled rectifiers as their DC output can be controlled. Further classifications of rectifiers are shown in Fig. 2.2.

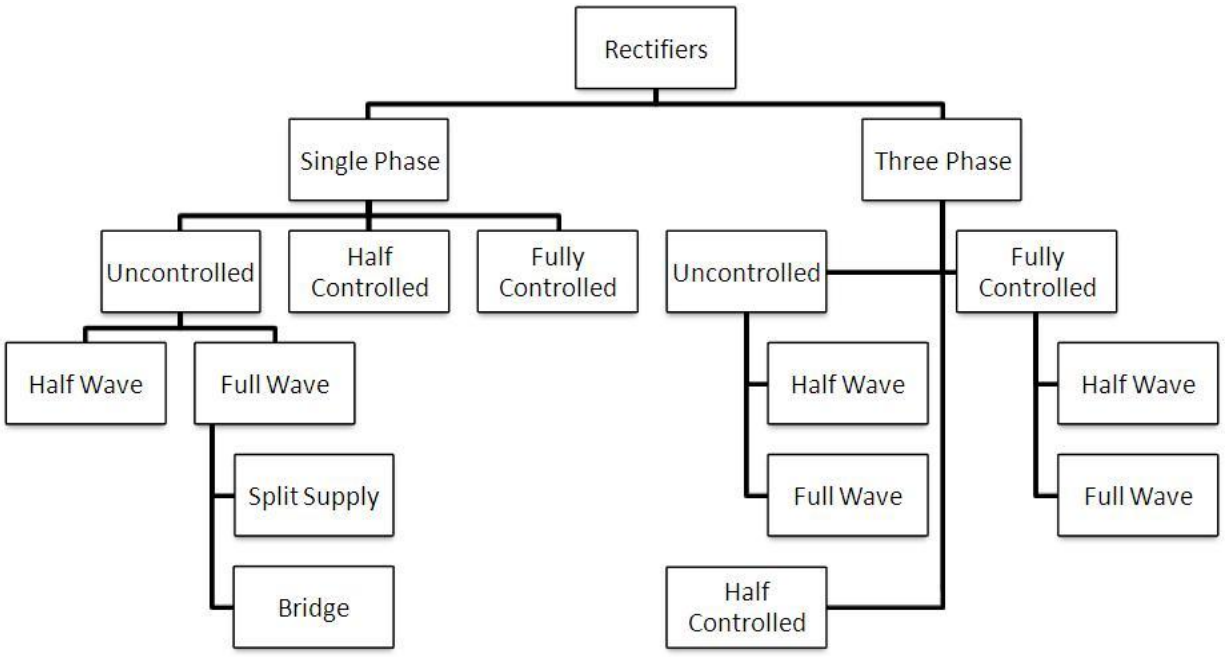

Fig. 2.2 Classifications of Rectifiers

2.1.1.1 Single phase rectifier

A. Uncontrolled single phase rectifier

Uncontrolled rectifiers make use of diodes. Diodes are two-terminal semiconductor devices that allow flow of current in only one direction. The two terminals of a diode are known as the anode and the cathode. The designs are cheap and popular in the industrial applications. In some of these rectifiers, the AC source from the electric utility is directly rectified without using an expensive and bulky transformer. In some applications, the DC voltage from the rectifier is connected to a DC bus for distribution to several different circuit systems, subsystems and other converters as loads [2.1].

A.1 Uncontrolled single phase half-wave rectifier The simplest of the rectifier circuit is a single phase half-wave rectifier which consists of a single diode as shown in Fig. 2.3 with input and output voltage waveform in Fig. 2.4. A diode is the simplest electronic switch. It is uncontrolled in a manner that the on and off conditions are determined by voltages and currents in the circuit [2.2]. By using diode, the DC level output and the power transferred to the load. It produces an output waveform that is half of the incoming AC voltage waveform. The positive pulse output waveform occurs because of the forward-biased condition of the diode. A diode experiences a forward-biased condition when its anode is at a higher potential than its cathode. Reverse bias occurs when its anode is lower than its cathode. During the positive portion of the input waveform, the diode becomes forward biased, which allows current to pass through the diode from anode to cathode, such that it flows through the load to produce a positive output pulse waveform. Over the negative portion of the input waveform, the diode is ideally reverse-biased so no current flows. Thus, the output waveform is zero or nearly zero during this portion of the input waveform.

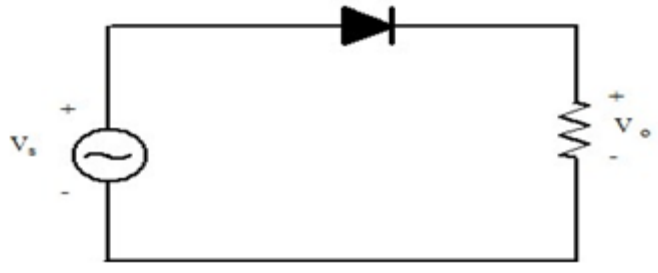

Fig. 2.3 Single Phase Half-Wave Rectifier

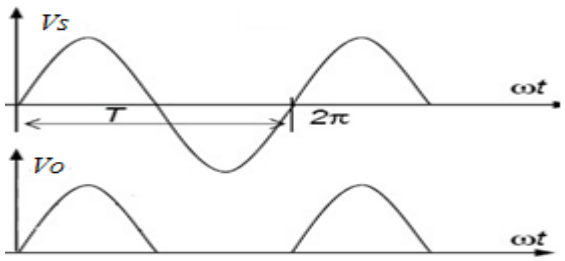

Fig. 2.4 Input and resulting output voltage waveforms of Single Phase Half-Wave Rectifier

The average value of one pulse of the DC output is given by V_o.

$$V_o = \sqrt{2}V_s/\pi \tag{2.1}$$

i.e., 0.318 of the peak value of ac voltageV_{max} . The PIV of a diode should be π times larger than the average DC voltage developed. In this circuit,

$$V_r = V_s/\sqrt{2} \tag{2.2}$$

The ripple factor of the output waveform is given by.

$$r = \frac{V_r}{2V_o} = 1.57 \tag{2.3}$$

A.2 Uncontrolled single phase full-wave rectifiers The purpose of the full-wave rectifier is basically same as that of the half wave rectifier but full-wave rectifiers have some fundamental advantages. The two types of full-wave rectifiers that the bridge rectifier and the center-tapped rectifier, these are shown in Fig. 2.5 and Fig. 2.6.

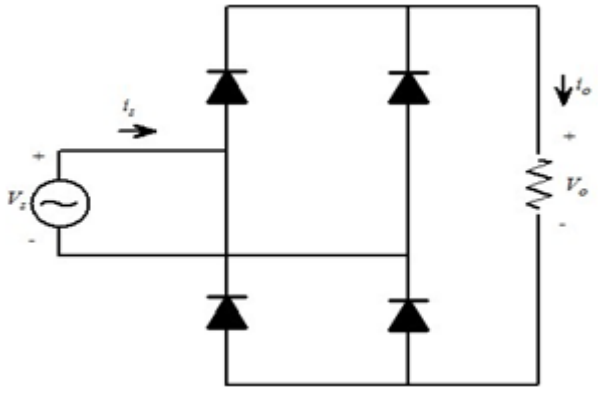

Fig. 2.5 The full wave Bridge Rectifier

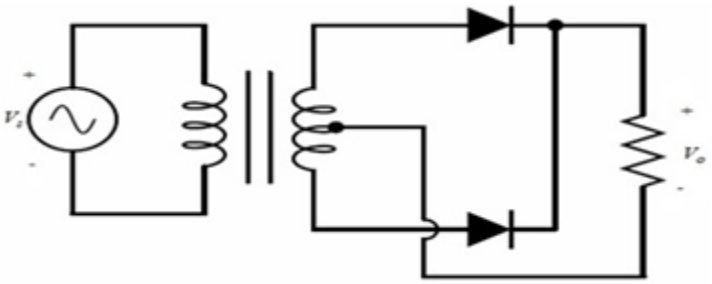

Fig. 2.6 Center-Tapped Transformer Rectifier

The lower peak diode voltage in the bridge rectifier which consists of arrangement of four diodes makes it more suitable for high-voltage applications. Thus, the center-tapped transformer rectifier in addition to including electrical isolation has only one diode voltage drop between the source and load making it desirable for low-voltage and high current applications.

B. Controlled single phase rectifier

The previous rectifiers are classified as uncontrolled rectifiers but once the source and the load parameters are established, the DC level of the output and the power transferred to the load are fixed quantities. As mentioned before, the output voltage of the AC-DC converters using diodes is not controllable because the diodes are not self controlled switch [2.1]. Thus, there is a way to control the output by using thyristor instead of a diode. A thyristor is a four-layer (*pnpn*), three-junction device that conducts current only in one direction similar to a diode.

B.1 Controlled single phase half-wave rectifiers Unlike the diode, the thyristor does not to begin to conduct as soon as the source becomes positive. Gate trigger current is the minimum current required to switch silicon controlled rectifiers from the off-state to the on-state at the specified off-state voltage and temperature. Once the thyristor conducts, the gate current can be removed and the thyristor remains on until the current becomes zero [2.2]. Here the rectified voltage on the load depends on the firing angle α,

$$V_d = \frac{V_{max}}{2\pi}(1 + cos\alpha) \qquad (2.4)$$

Fig. 2.7 and Fig. 2.8 shows the basic controlled half-wave rectifier and its output voltage waveform with gate pulse.

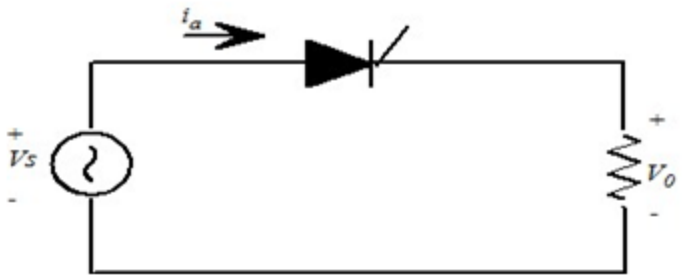

Fig. 2.7 A Basic Half-Wave Controlled Rectifier

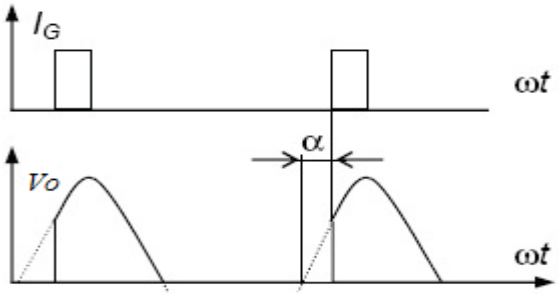

Fig. 2.8 Output voltage waveforms of Single Phase Half-Wave Rectifier with gate pulse

The control curve which represents the relation between output voltage and firing angle is shown in Fig. 2.9. The firing angle is measured from the point of the sine waveform when the positive anode voltage appears on the thyristor.

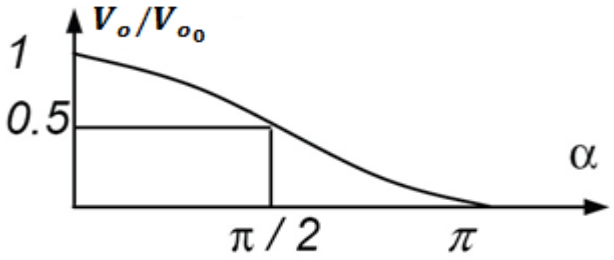

Fig. 2.9 Control curve of Single phase Half-Wave controlled rectifier

In the above Fig. V_{O_0} is the DC output voltage for α=0°.

The main advantage of the single-phase half-wave rectifier is its simplicity. But, it is rarely used in practice because of following reasons:

i. This circuit has the low use of transformer due to the poor secondary current shape.
ii. The use of diode is not appropriate, that is, PIV significantly excels V_o.

iii. Quality of the rectified voltage is low because of very high ripples and very low power factor.

B.2 Controlled single phase full-wave rectifiers Popular AC-DC converters use full-bridge topologies [2.1]. Full-bridge converters are designed for delivering constant but controllable DC current or DC voltage to the load. Similar to the diode bridge rectifier topology, a versatile method of controlling the output of a full-wave rectifier is to substitute controlled switches such as thyristors for the diode. Because of their unique ability to be controlled, the output voltage and hence the power can be controlled to desire levels. The triggering of the thyristor has to be synchronized with the input sinusoidal voltage in an AC to DC rectifier circuit. The delay angle α is the angle interval between the forward biasing of the thyristor and the gate signal application [2.2]. Otherwise, if the delay angle is zero, the rectifiers behave exactly like uncontrolled rectifiers with diodes. Fig. 2.10 shows a basic controlled full wave rectifier.

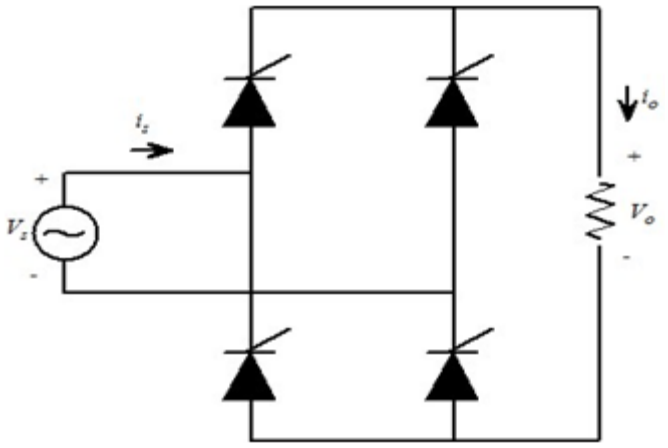

Fig. 2.10 A Basic Full-Wave Controlled Bridge Rectifier

2.1.1.2 Three phase rectifiers

Single-phase rectifiers are suitable up to power loads of about 15kW. For higher power demands three phase rectifiers are preferred due to the following reasons.

i. Higher DC voltage.
ii. Better transformer utilization factor.
iii. Better input power factor.
iv. Less ripple content in output current.

A. Three phase uncontrolled rectifiers

Three phase rectifiers are commonly used in industry to produce a DC voltage and current for large loads [2.2]. Like single phase rectifiers, three phase rectifiers can be classified as uncontrolled and controlled. The three phase full-bridge uncontrolled rectifier is shown in Fig. 2.11. As mentioned before in single phase uncontrolled rectifier, three phase full-bridge rectifier uses diodes as switch. Three phase rectifier is divided into two groups, the top group and the bottom group. For top group, diode with its anode at the highest potential will conduct at one time, the other two will be reversed. For bottom group, diode with its cathode at the lowest potential will conduct. The other two will be reversed. Fig. 2.11 and Fig. 2.12 shows the three phase full bridge uncontrolled rectifier with its phase and resulting combinations of line-to-line voltages from a balanced three phase source.

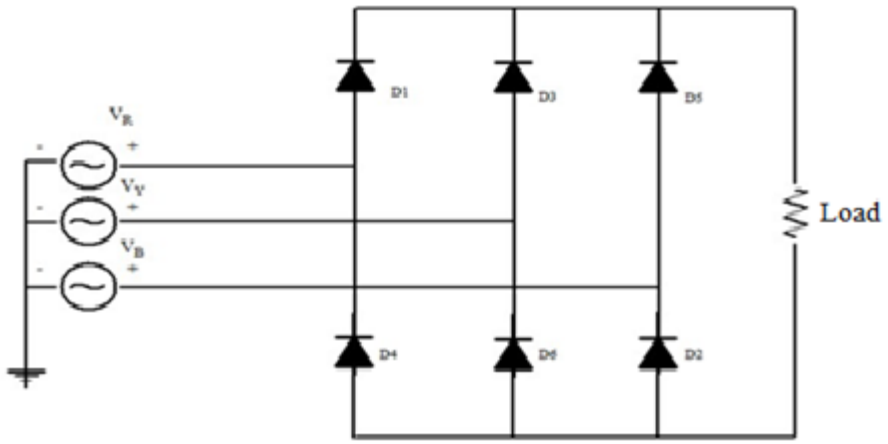

Fig. 2.11 Three Phase Full-Bridge Uncontrolled Rectifier

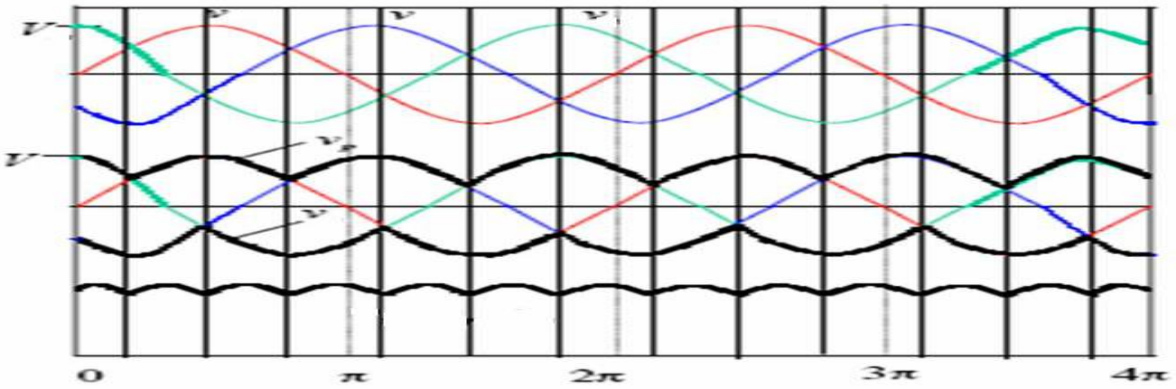

Fig. 2.12 Source and Output Voltage

B. Three phase controlled rectifiers

Similar to single phase controlled rectifier, the output of the three phase rectifier can be controlled by substituting thyristors instead of diodes. Fig. 2.13 shows a controlled six pulse three phase rectifier. As mentioned before in single phase controlled rectifier, thyristors will conduct until a gate signal is applied but the thyristor should be forward biased. Thus, the transition of the output voltage to the maximum instantaneous line-to-line source voltage can be delayed [2.2].

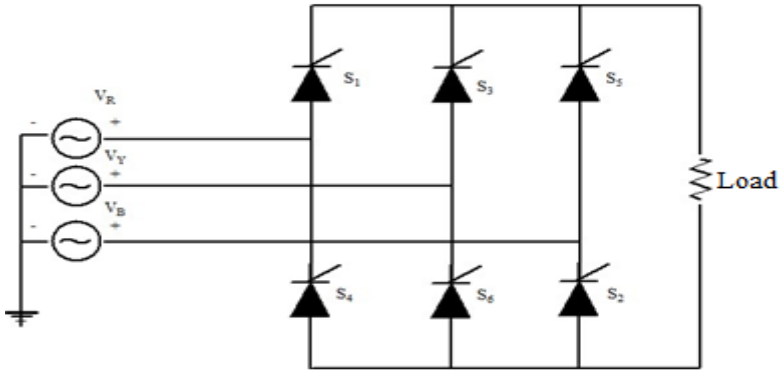

Fig. 2.13 Three Phase Full-Bridge Controlled Rectifier

2.2 Basic power factor and harmonic concepts

Harmonics is an increasing problem in electric power systems because of the expanding demand of nonlinear load such as power electronic equipment. Harmonics can cause a number of unwanted effects. Electric utility transmission and distribution equipment may be adversely affected by ac line harmonics which may cause higher transformer loss, capacitor failure or failure of protective relay operation. Sensitive electronic loads also may malfunction when connected to an ac line which has severe harmonics. Another concern is interference with communication circuits. The power line harmonics current can be coupled into the communication circuits by either induction or direct conduction.

Major sources of harmonics in utility or industrial systems include rectifiers, motor drives, UPS and Arc furnaces. For this research, the harmonics due to rectifier loads are considered and analyzed. The wide spread application of power electronics is resulting in an increasing number of electrical load which include rectifiers to produce DC power. Inverter motor drives, uninterruptible power supplies and computer power supplies generally have rectifier

inputs. The most common ac to DC converter used in power electronics is single phase diode rectifier.

2.2.1 Harmonics

A harmonic is defined as a sinusoidal component of a periodic wave having a frequency that is an integral multiple of the fundamental frequency. We define harmonics as voltages or currents at frequencies that are a multiple of the fundamental frequency. In most systems, the fundamental frequency is 60 Hz. Therefore, harmonic order is 120 Hz, 180 Hz, 240 Hz and so on. (For European countries with 50 Hz systems, the harmonic order is 100 Hz, 150 Hz, 200 Hz, etc.)We usually specify these orders by their harmonic number or multiple of the fundamental frequency.

For example, a harmonic with a frequency of 180 Hz is known as the third harmonic (60x3 = 180). In this case, for every cycle of the fundamental waveform, there are three complete cycles of the harmonic waveforms. The even multiples of the fundamental frequency are known as even-order harmonics while the odd multiples are known as the odd-order harmonics.

2.2.1.1 Effects of harmonics

The biggest problem with harmonics is voltage waveform distortion. We can calculate a relationship between the fundamental and distorted waveforms by finding the square root of the sum of the squares of all harmonics generated by a single load, and then dividing this number by the nominal 60 Hz waveform value. We can do this by a mathematical calculation known as a Fast Fourier Transform (FFT) theorem. This calculation method determines the total harmonic distortion (THD) contained within a nonlinear current or voltage waveform. Electronic equipment generates more than one harmonic frequency. For example, computers generate 3rd, 9th, and 15^{th} harmonics. These are known as triplen harmonics. They are of a greater concern to engineers and building designers because they not only distort the voltage waveforms but also overheat the building wiring, overheat transformer units, and cause random end-user equipment failure.

Harmonics can cause overloading of conductors and transformers and overheating of utilization equipment such as motors. Triplen harmonics can especially cause overheating of neutral conductors on 3-phase, 4-wire systems. While the fundamental frequency and even

harmonics cancel out in the neutral conductor, odd order harmonics are additive. Even in a balanced load condition, neutral currents can reach magnitudes as high as 1.73 times the average phase current. This additional loading creates more heat, which breaks down the insulation of the neutral conductor. In some cases, it can break down the insulation between windings of a transformer. In both cases, the result is a fire hazard. But this potential damage can be diminished by using sound wiring practices.

2.2.2 Power Factor

Power factor (PF) is defined as the ratio of the real power (P) to apparent power (S), or the cosine (for pure sine wave for both current and voltage) that represents the phase angle between the current and voltage waveforms (Fig. 2.27). The power factor can vary between 0 and 1, and can be either inductive (lagging, pointing up) or capacitive (leading, pointing down). In order to reduce an inductive lag, capacitors are added until PF equals 1. When the current and voltage waveforms are in phase, the power factor is 1 (cos (0°) = 1). The whole purpose of making the power factor equal to one is to make the circuit look purely resistive (apparent power equal to real power).

Real power (watts) produces real work; this is the energy transfer component (example electricity-to-motor rpm). Reactive power is the power required to produce the magnetic fields (lost power) to enable the real work to be done, where apparent power is considered the total power that the power company supplies, as shown in Fig. 2.14. This total power is the power supplied through the power mains to produce the required amount of real power.

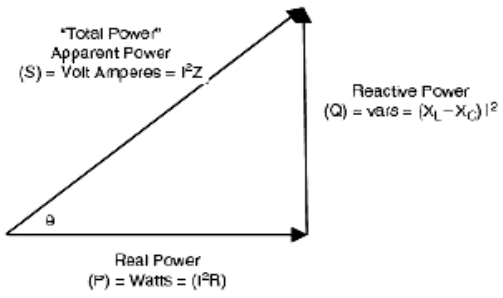

Fig. 2.14 Power factor triangle (lagging)

The previously-stated definition of power factor related to phase angle is valid when considering ideal sinusoidal waveforms for both current and voltage; however, most power

supplies draw a non-sinusoidal current. The purpose of the power factor correction circuit is to minimize the input current distortion and make the current in phase with the voltage.

When the power factor is not equal to 1, the current waveform does not follow the voltage waveform. This result not only in power losses, but may also cause harmonics that travel down the neutral line and disrupt other devices connected to the line. The closer the power factor is to 1, the closer the current harmonics will be to zero since all the power is contained in the fundamental frequency.

2.2.2.1 Causes of inefficiencies

One problem with switch mode power supplies (SMPS) is that they do not use any form of power factor correction and that the input capacitor C_{in} shown in Fig. 2.15 will only charge when V_{in} is close to V_{Peak} or when V_{in} is greater than the capacitor voltage VC_{in} [2.6].

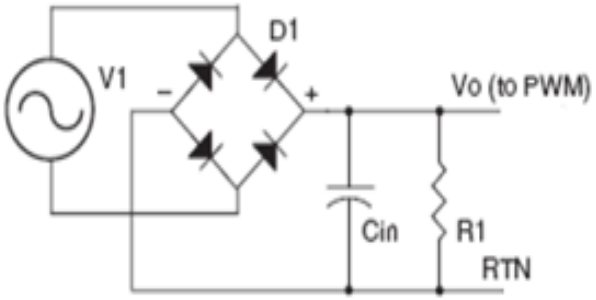

Fig. 2.15 SMPS input without PFC

If C_{in} is designed using the input voltage frequency, the current will look much closer to the input waveform, however, any little interruption on the mainline will cause the entire system to react negatively. In saying that, in designing a SMPS, the hold-up time for C_{in} is designed to be greater than the frequency of V_{in}, so that if there is a glitch in V_{in} and a few cycles are missed, C_{in} will have enough energy stored to continue to power its load.

As previously stated, C_{in} will only charge when V_{in} is greater than its stored voltage, meaning that a non-PFC circuit will only charge C_{in} a small percentage of the overall cycle time. After 90 degrees as shown in Fig. 2.16 the half cycle from the bridge drops below the capacitor voltage (VC_{in}); which back biases the bridge, inhibiting current flow into the capacitor (via V_{in}), a noticeable big input current spike is observed so all the circuitry in the

supply chain (the wall wiring, the diodes in the bridge, circuit breakers, etc) must be capable of carrying this huge peak current [2.6].

During these short periods the C_{in} must be fully charged, therefore large pulses of current for a short duration are drawn from V_{in}. There is a way to average this spike out so it can use the rest of the cycle to accumulate energy, in essence smoothing out the huge peak current, by using power factor correction.

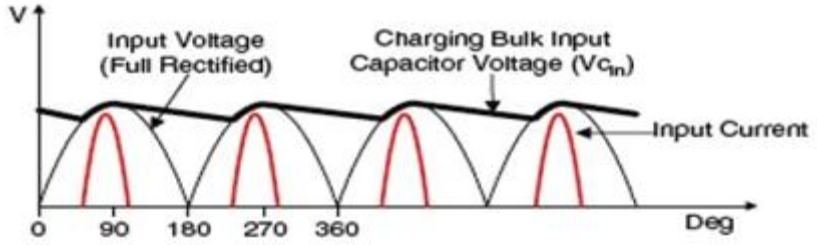

Fig. 2.16 Voltage and current waveform of full wave rectifier

In order to follow V_{in} more closely and not have these high amplitude current pulses, C_{in} must charge over the entire cycle rather than just a small portion of it. Today's non-linear loads make it impossible to know when a large surge of current will be required, so keeping the inrush to the capacitor constant over the entire cycle is beneficial and allows a much smaller C_{in} to be used. This method is called power factor correction.

2.2.2.2 Need for power factor correction

The input stage of any AC-DC converter comprises of a full-bridge rectifier followed by a large filter capacitor. The input current of such a rectifier circuit comprises of large discontinuous peak current pulses that result in high input current harmonic distortion. The high distortion of the input current occurs due to the fact that the diode rectifiers conduct only for a short period. This period corresponds to the time when the mains instantaneous voltage is greater than the capacitor voltage. Since the instantaneous mains voltage is greater than the capacitor voltage only for very short periods of time, when the capacitor is fully charged, large current pulses are drawn from the line during this short period of time.

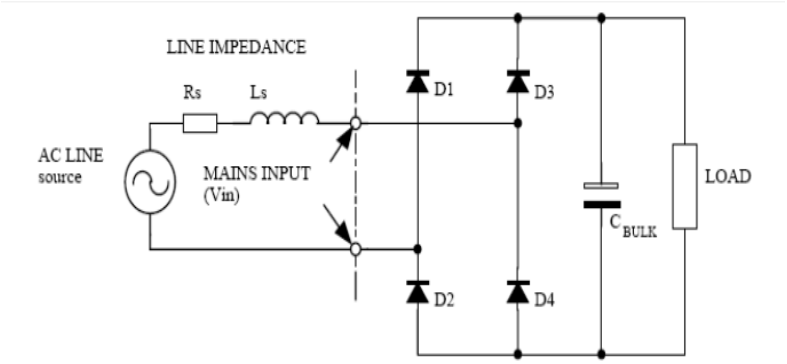

Fig. 2.17 Schematic diagram of a single phase diode rectifier with capacitor filter circuit

Fig 2.17 shows the schematic of a typical single phase diode rectifier filter circuit while Fig. 2.18 shows the typical simulated line voltage and current waveforms [2.7]. The typical input current harmonic distortion for this kind of rectification is usually in the range of 55% to 65% and the power factor is about 0.6 [2.8]. The actual current wave shape and the resulting harmonics depend on the line impedance.

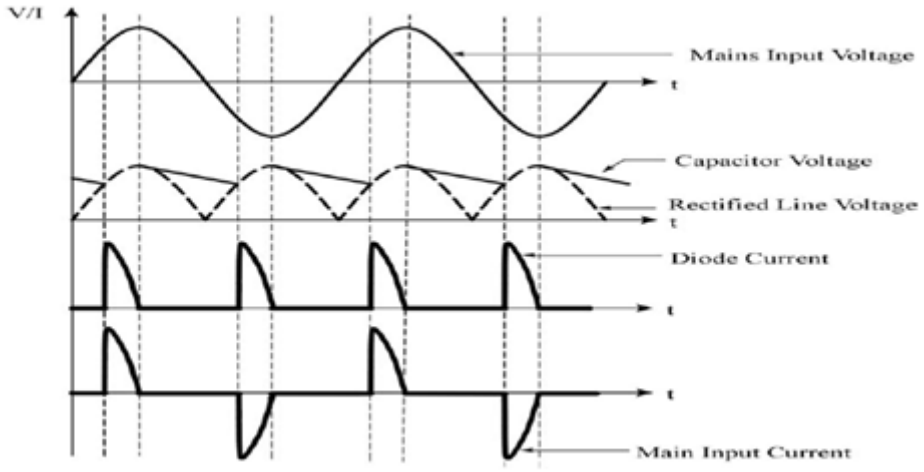

Fig. 2.18 Typical line current and voltage waveforms [2.7]

Conventional AC rectification is thus a very inefficient process, resulting in waveform distortion of the current drawn from the mains. A circuit similar to that shown in Fig 2.17 is used in most mains-powered AC-DC converters. At higher power levels (200 to 500 watts and higher) severe interference with other electronic equipment may become apparent due to these harmonics sent into the power utility line. Another problem is that the power utility line cabling, the installation and the distribution transformer, must all be designed to

withstand these peak current values resulting in higher electricity costs for any electricity utility company.

Thus, summarizing, conventional AC rectification has the following main disadvantages:

- It creates harmonics and electromagnetic interference (EMI).
- It has poor power factor.
- It produces high losses.
- It requires over-dimensioning of parts.
- It reduces maximum power capability from the line.

2.3 Literature review

Francisc C. Schwarz did a time-domain analysis of power factor for rectifier filter system for different values of inductance through which exact and complete characterizations of significant voltage and current waveforms for different range of inductance were generated [2.9].

Ray P. Stratford showed the effect of rectifier harmonics current on power systems with related case studies and concluded that by understanding the physical characteristics of power system and static power converters, shunt filters can be designed and applied to provide reactive power and control the flow of harmonic currents produced by the nonlinear characteristics of static power converters [2.10].

Shashi B. Dewan presented a design example of LC filter with optimum value of inductance and capacitance for single phase uncontrolled bridge rectifiers and verified the theoretical result with experimental model [2.11].

Joseph S. Subjak et.al, presented a update on harmonics with its cause, effects, measurements and analysis generated in drive systems taking the data logging system in account [2.12].

Atluri Rama Prasad et.al, proposed a new passive waveshaping method for single-phase diode rectifiers which maintains a high-input power factor, lowers rectifier current stress, and lowers the volt-ampere (VA) rating of the associated reactive components as compared with the standard diode rectifier [2.8].

A.R. Prasad et.al, proposed and analyzed a novel active power factor correction method for power supplies with three-phase front-end diode rectifiers, but drawback of this method is that this method requires the use of an additional single switch boost chopper [2.13].

Arthur W. Kelley et.al, worked on a quantitative analysis of single three phase rectifier line-current harmonics and power factor as a function of the output filter inductance which introduces significant error in the estimation of line-current harmonics and power factor if not considered [2.14].

Thomas S. Key et.al, compared the major standards and power supply design options for limiting harmonic distortion and also listed the several difficulties and uncertainties that appeared in the application of those standards [2.15].

Richard Redl et.al, concluded that power factor correction and the related line-harmonics reduction of bridge rectifiers can be achieved with passive means by using only inductive and capacitive components with simplicity and reliability through their research work [2.16].

Ji Yanchao et.al, proposed an improved passive input current waveshaping method for single phase diode rectifier which performed better as compared with the novel passive input current waveshaping method for single-phase diode rectifiers proposed by P.D. Ziogas (novel method) [2.17].

Richard Redl described a novel passive power factor correction circuit that ensures the compliance of the capacitively filtered signal phase rectifier with the EN61000-3-2 norm at low cost with additional components like small inductor, capacitor and diode [2.18].

G. A. Karvelis et.al, compared five single phase high power factor switch mode rectifier topologies with respect to their generated current harmonics, efficiencies, ratings of power semiconductor devices and passive elements and complexity of power and control circuit [2.19].

Oscar Garcia et.al, proposed an alternative to the typical two-stage ac/DC power conversion in which high efficiency and improved energy management is achieved by splitting the input power in two parts, Moreover, the division of the power is done automatically without any complex control strategy [2.20].

Bhim singh et.al, gave a comprehensive review of improved power quality converters configurations, control approaches, design features, selection of components, other related considerations, and their suitability and selection for specific applications [2.21].

Huai Wei et.al, presented a new single-stage, single-switch power factor correction converter topology with output electrical isolation which is derived by combining a boost circuit and a forward circuit in one power stage [2.22].

O. Garcia et.al, proposed a new converter named harmonic reducer which was derived from the classical power active filters, acts as a current source and it is able to obtain a sinusoidal line current in ac/dc applications without any change in the existing system [2.23].

Miaosen Shen et.al, presented novel single stage PFC converter which employs two auxiliary windings to achieve low input current THD, low voltage stress across the bulk capacitor, and high efficiency [2.24].

H. M. Suryawanshi et.al, devised a circuit for power factor improvement of an AC-to-DC resonant converter without active control of input line current. The proposed circuit is most suitable for high-voltage DC application [2.25].

Bhim Singh et.al, presentd a review of an single-phase improved power quality AC-DC converters, in which he provides a classified list of more than 450 research publications on the art of IPQC. In his paper, he classified IPQCs into eight categories with further sub classifications [2.26].

Hussein A. Kazem et.al, derived different methods for estimation of the harmonic current of the single-phase diode bridge rectifier i.e. simple and advanced methods and both gave the convincing results when compared with the real application [2.27].

Bhim singh et.al, presented a novel method of reducing harmonic currents at the point of common coupling in a three-phase diode bridge rectifier type utility interface. The proposed configuration consists of a current injection device, which is a newly designed current injection network and a properly tuned passive shunt filter [2.28].

Mehjabeen A. Khan et.al, presented a simple yet effective scheme for improving the power factor and whaveshape of input current drawn by a single phase bridge rectifier in which a

single MOSFET switch on ac side is used to provide an alternate path for the input current to flow and hence make it continuous [2.29].

Hussein A. Kazem classified the various available current waveshaping methods for single phase rectifiers with their advantages, disadvantages and designing consideration [2.30].

Ali M. Eltamaly presented a detailed analysis for determining the relation between the optimal amplitude and phase angle of the injection current along with the firing angle which played an important role in third harmonics injection technique for reducing the THD of the utility line of three-phase controlled converters [2.31].

V. Suresh Kumar et.al, focused on the evaluation of active power filter which is controlled by fuzzy logic and neural network based controller for harmonic reduction and power factor enhancement [2.32].

Mohammad Mahdavi et.al, proposed a new zero-current-switching high-power-factor rectifier with pulse width-modulation control in which all semiconductor devices are soft switched. Moreover, there is no extra stress on the switches [2.33].

R.Balamurugan et.al, presentd a comparative evaluation of five topologies of single-phase AC-DC boost converters having power factor correction(PFC) and also describes techniques for minimizing the input current distortion of current-controlled single phase boost rectifiers. The mathematical models of all topologies for evaluation were used [2.34].

Przemyslaw Janik proposed an efficient and theoretically fully justified approach to filter design for circuit with high harmonic content. Using the proposed approach, the filter can be easily triggered to handle harmonics in a way desired by user, even for enter harmonics [2.35].

Abbas A. Fardoun et.al, presented a new ac-DC converter and its topology derivation with an efficiency of 94.3% and a THD of 5% at prototype level as the components of the presented topology are fully utilized over the whole line cycle [2.36].

2.5 Simulation Results

Some assumptions were made to analyze the circuits which are the following:-

- Load is purely resistive.

- Ideal filter components.
- The forward voltage drop and reverse leakage current of diodes are neglected.

Table 2.1 shows the specifications of the components used in the topologies.

Table2.1 Specification of the components

Components	**Specifications**
AC supply	220V/50Hz
Diodes	DIN4936
Resistances	100Ω
Capacitors	60mF/0.1mF/100mF/500µF
Inductor	1mH/50mH/5mH/.005mH

Five different passive power factor improvement topologies for low power output with 220volt/50 Hz AC input have been considered.

The five different topologies are:-

i. Conventional single phase diode rectifier with filter capacitor.

ii. Single phase diode rectifier with LC filter.

iii. Single phase diode rectifier circuit with parallel input resonant filter.

iv. Single phase diode rectifier circuit with series input resonant filter.

v. Single phase diode rectifier circuit with improved parallel input resonant filter.

All methods are compared in terms of THD (Total harmonic distortion), Input current distortion, Input current harmonic factor, Input displacement factor, and Power factor. Fig. 2.19 shows the conventional single phase diode rectifier circuit with load of 100Ω.

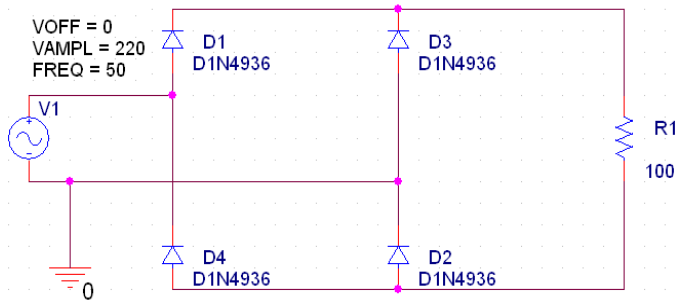

Fig. 2.19 Conventional single phase diode rectifier

From the conventional single phase diode rectifier shown in Fig. 2.32, the values of all the five parameters are calculated, which are kept as reference to compare the parameters of other five topologies. Fig. 2.20 shows the waveform of input current and input voltage, and there are no harmonic distortions in input current.

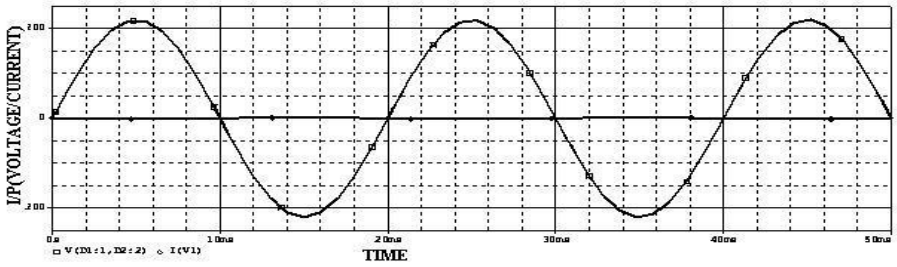

Fig. 2.20 I/P voltage and current waveform for conventional single phase diode rectifier

Table 2.2 shows the values of all the calculated parameters with which the parameters of rest of the topologies will be compared.

Table 2.2 Values of parameters for conventional single phase diode rectifier

Parameters	Values
PF	0.991
DF	0.999
CDF	0.9925
HF	0.123
THD	0.033%

Fig. 2.21 shows the simulated prototype of a conventional single phase diode rectifier with filter capacitor. The output filter capacitor value (C_1) is calculated using eq. 2.5.

$$C_1 = \frac{1}{4fR}\left[1 + \frac{1}{\sqrt{2RF}}\right] \tag{2.5}$$

RF:- ripple factor

R:- output resistance

f:- frequency of AC source

To get minimum ripple factor we have chosen C_1=60 mF (milli farads).

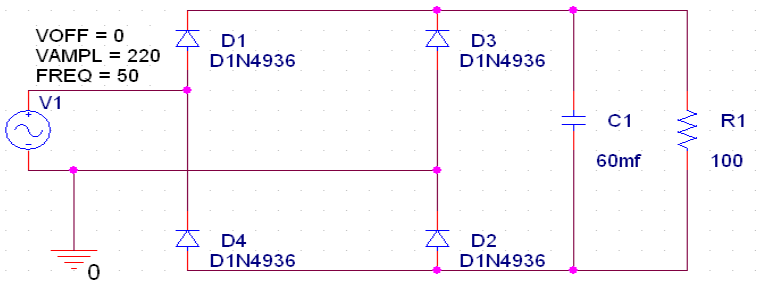

Fig. 2.21 Conventional single phase diode rectifier with filter capacitor

Fig. 2.22 shows the waveform of input current and input voltage for filter capacitor circuit, in which the harmonics of input current which are highly undesirable are seen.

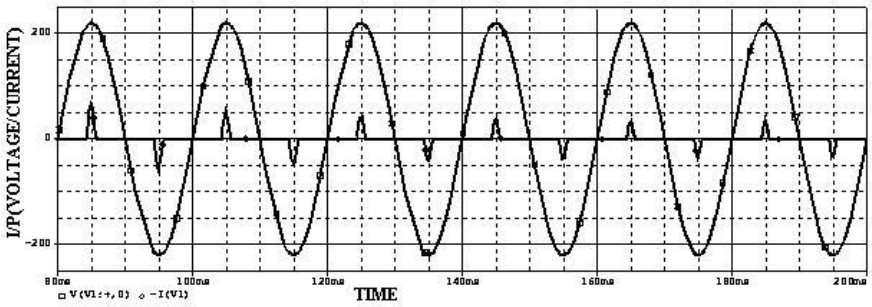

Fig. 2.22 I/P voltage and current waveform for conventional single phase diode rectifier with filter capacitor

Table 2.3 shows the values of all the calculated parameters for a conventional single phase diode rectifier with filter capacitor in a tabulated form.

Table 2.3 Values of parameters for conventional single phase diode rectifier with filter capacitor

Parameters	Values
PF	0.215
DF	0.999
CDF	0.215
HF	4.527
THD	176.9%

From the calculated values, it is clear that the Total Harmonic Distortion is 176.9% which is very high which needs to be reduced which is achieved in the proceeding methods. The power factor is also very low which should be improved.

Fig. 2.23 shows the simulated prototype of a conventional single phase diode rectifier with LC filter. The inclusion of the inductor results in larger conduction angle of the current pulse and reduced peak and r.m.s values.

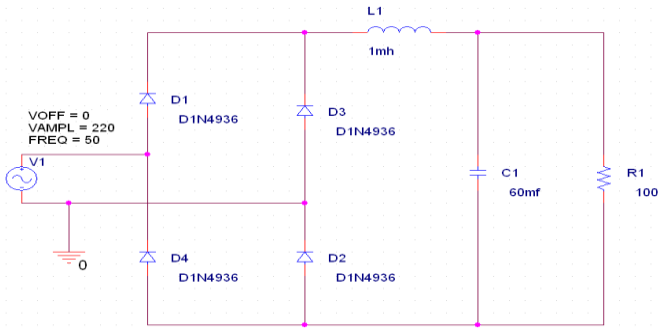

Fig. 2.23 Single phase diode rectifier with LC filter

For low values of inductance the input current is discontinuous and pulsating. However, it is shown [13] that even for infinite value of the inductance; the PF cannot exceed 0.9 for this kind of arrangement.

Fig. 2.24 shows the waveform of input current and input voltage for circuit with LC filter, and the harmonics of input current are reduced as compared to the previous topology.

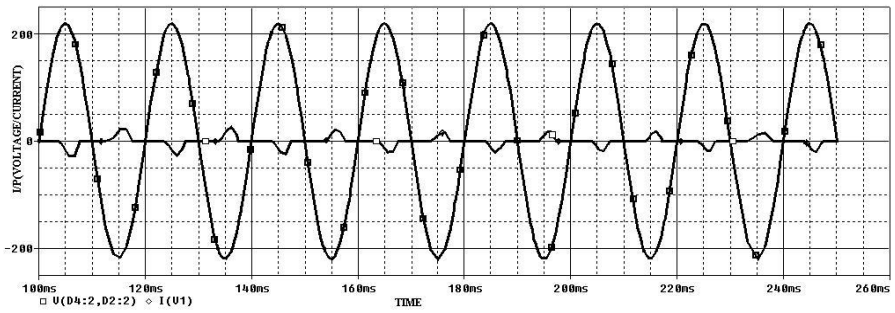

Fig. 2.24 I/P voltage and current waveform for single phase diode rectifier with LC filter

Table 2.4 shows the values of all the calculated parameters for a conventional single phase diode rectifier with LC filter in a tabulated form.

Table 2.4 Values of parameters for conventional single phase diode rectifier with LC filter

Parameters	Values
PF	0.3629
DF	0.967
CDF	0.375
HF	2.471
THD	84.09%

It is clear from the above calculated parameters that LC filter topology gives better results than the previous topology as the value of Total Harmonic Distortion decreased and Power Factor improves but still not up to very satisfactory level, so we will proceed towards other topologies.

Fig. 2.25 shows the simulated prototype of single phase diode rectifier using parallel resonant circuit as a passive wave shaping method. The value of inductor and capacitor are calculated using the analysis discussed below.The n^{th} harmonic component of the equivalent impedance of the input parallel resonant filter is given by eq.

$$Z_n = \frac{nX_{L_2} * \frac{X_{C_2}}{n}}{jnX_{L_2} - j\frac{X_{C_2}}{n}} \qquad (2.6)$$

X_{L_2}:-impedance of input resonant inductor L at fundamental frequency.

X_{C_2}:- impedance of input resonant capacitor C at fundamental frequency.

The third harmonic impedance of the input resonant filter will be infinity (theoretically). Therefore,

$$3X_{L_2} = \frac{X_{C_2}}{3}$$

And $$L_2 = \frac{1}{9\omega^2 C_2}$$

Where $\omega = 2\pi f$ and f is in Hz.

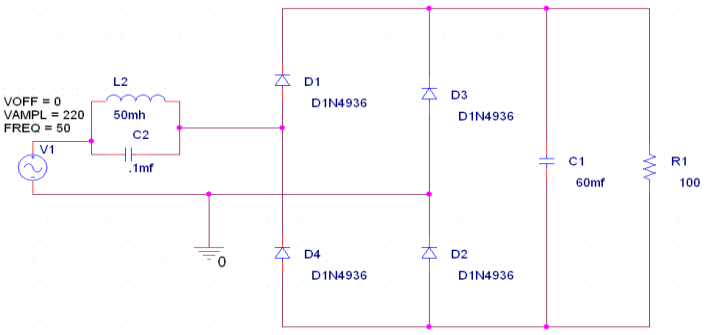

Fig. 2.25 Single phase diode rectifier circuit with parallel input resonant filter

Fig. 2.26 shows the waveform of input current and input voltage for single phase diode rectifier circuit with parallel input resonant filter. It is clear that the input current harmonics are reduced as compared to the previous topology.

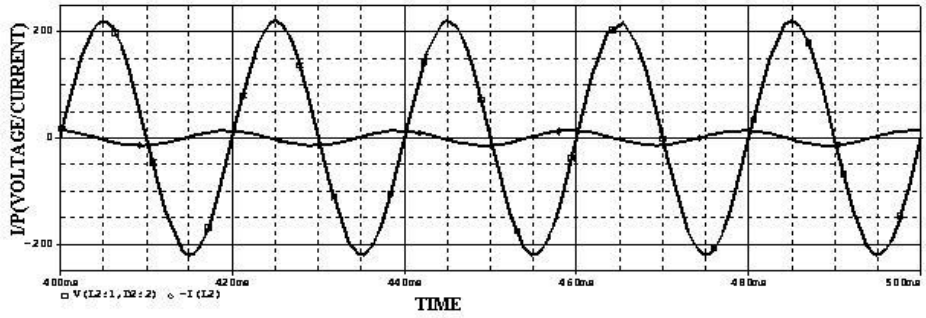

Fig. 2.26 I/P voltage and current waveform for single phase diode rectifier with parallel input resonant filter

Table 2.5 shows the values of all the calculated parameters for single phase diode rectifier with parallel input resonant filter in a tabulated form.

Table2.5 Values of parameters for single phase diode rectifier with parallel input resonant filter

Parameters	Values
PF	0.592
DF	0.919
CDF	0.644
HF	1.186
THD	23.39%

The input Total Harmonic Distortion is reduced to 23.39% which was 84% in previous topology, but power factor is still non-unity. Therefore, some more efficient topologies are required.

The simulated prototype of a single phase diode rectifier with series input resonant filter is shown in the Fig. 2.27. The values considered in the prototype are calculated using the analysis discussed below.

For a series resonant filter at the input end of a single phase rectifier, the capacitance C_2 and L_2 is chosen such that the resonance condition is satisfied, and the minimum ripple is achieved.

$$\omega = \frac{1}{\sqrt{L_2 C_2}} \tag{2.7}$$

Where $\omega = 2\pi f$ and f is in Hz.

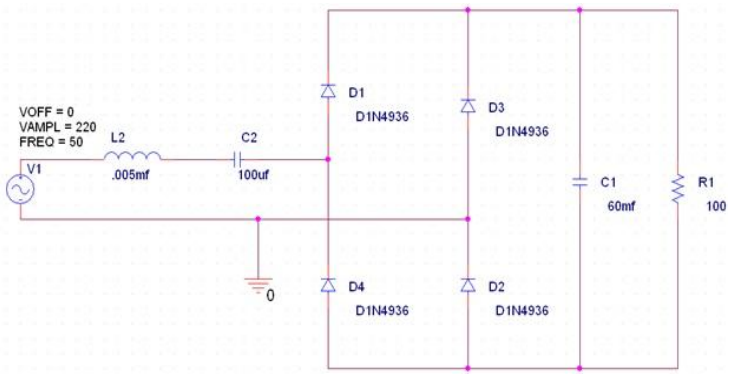

Fig. 2.27 Single phase diode rectifier circuit with series input resonant filter

The waveform of input current and input voltage for single phase diode rectifier circuit with series input resonant filter is shown in Fig. 2.28, in which harmonics in input current are very less as compared to the previous topologies.

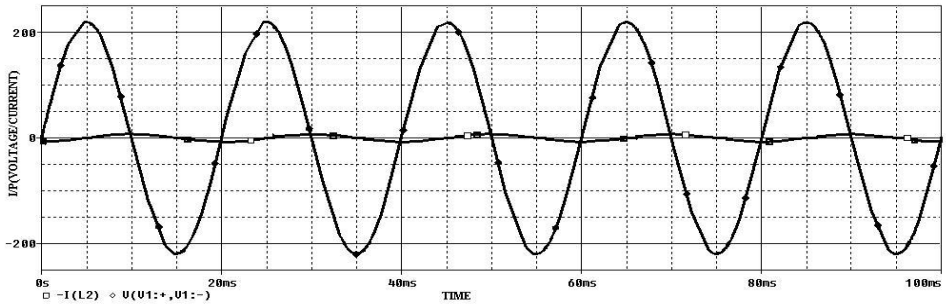

Fig. 2.28 I/P voltage and current waveform for single phase diode rectifier with series input resonant filter

Calculated parameters for single phase diode rectifier with series input resonant filter circuit are shown in Table 2.6 in a tabulated form.

Table2.6 Values of parameters for single phase diode rectifier with series input resonant filter

Parameters	Values
PF	0.64
DF	0.953
CDF	0.679
HF	1.08
THD	10.12%

It is clear from Fig. 2.28 that the harmonics in input current is greatly reduced and power factor reached 0.64 with Total Harmonic Distortion 10.12% which is shown in Table 2.11, but still power factor is very less than unity.

Fig. 2.29 shows the simulated prototype of a proposed single phase diode rectifier circuit with improved parallel input resonant filter, in which values of C_3 are chosen ranging from 100µf(micro farads) to 1mf(milli farads) and is selected such that the input power factor at rated output power reaches its peak value.

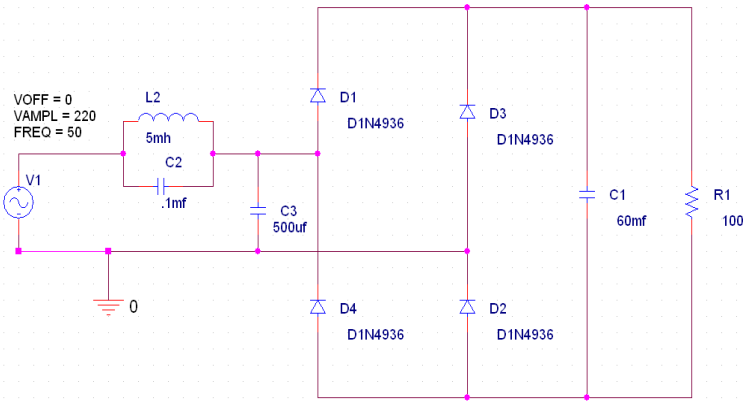

Fig. 2.29 Single phase diode rectifier circuit with improved parallel input resonant filter

The input current and voltage waveform for single phase diode rectifier circuit with improved parallel input resonant filter is shown in Fig. 2.30. For different values of C_3, different waveforms are obtained.

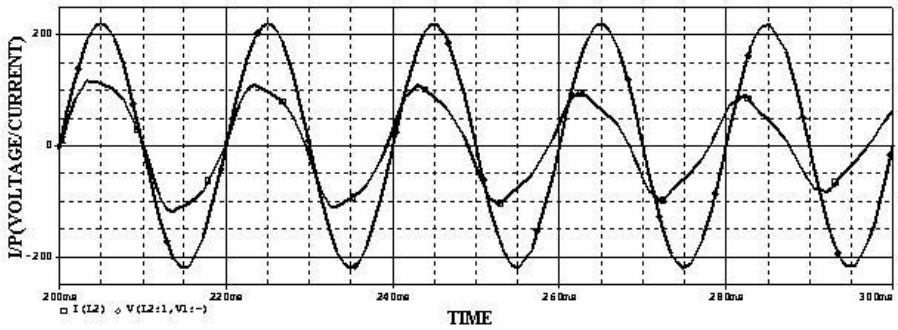

Fig. 2.30 I/P voltage and current waveform for Single phase diode rectifier circuit with improved parallel input resonant filter

Table 2.7 shows the calculated parameters for single phase diode rectifier circuit with improved parallel input resonant filter in tabulated form.

Table2.7 Values of parameters for Single phase diode rectifier with improved parallel input resonant filter

Parameters	Values
PF	0.931
DF	0.99
CDF	0.94
HF	0.36
THD	5.591

The results obtained from single phase diode rectifier with improved parallel input resonant filter are closest to the reference values obtained from conventional single phase rectifier circuit.

The calculation of all five parameters are done by the below written formulise.

Input current distortion factor (CDF):-

$$CDF = \frac{I_{s_1}}{I_s} \tag{2.8}$$

Input current harmonic factor (HF):-

$$HF = \sqrt{\left[\frac{I_s}{I_{s_1}}\right]^2 - 1} \tag{2.9}$$

$$HF = \sqrt{\frac{1}{CDF^2} - 1} \tag{2.10}$$

Power factor (PF):-

$$PF = \frac{I_{s_1}}{I_s} Cos\varphi_1 \tag{2.11}$$

Where: - φ_1 is the phase angle between the 1st harmonic of current and the voltage

Input displacement factor (DF):-

$$DF = Cos\varphi_1 \tag{2.12}$$

Total Harmonic Distortion (THD):-

$$THD = \frac{\sqrt{I_{2rms}^2 + I_{3rms}^2 \ldots . + I_{nrms}^2}}{I_{1rms}} \quad (2.13)$$

Where I_{nrms} is the rms value of the n[th] harmonic of the current. Fourier series expansion is used to get the harmonic components of i/p current.

References

[2.1] Jai P. Agrawal, *Power Electronic Systems: Theory and Design,* 1st ed. Prentice Hall, 2000.

[2.2] Timothy L. Skvarenina, *The Power Eelectronics Handbook,* CRC Press, 2001.

[2.3] Muhammad H. Rashid, *Power Electronics Circuits, Devices and Applications,* 3rd ed. Prentice Hall, 2008.

[2.4] Sandeep Pande , Harshit Dalvi, "Simulation of Cycloconverter Based Three Phase Induction Motor," *International Journal of Advances in Engineering & Technology (IJAET),* vol. 1, pp. 23-33, July 2011.

[2.5] Abhishek Pratap Singh and V. K. Giri, " Simulation of Cycloconverter Fed Split Phase Induction Motor", *International Journal of Engineering Science and Technology (IJEST),* vol. 4, pp. 367-372, January 2012.

[2.6] Application Note 42047, Power Factor Correction (PFC) Basics, Available: www.fairchildsemi.com/an/AN/AN-42047.pdf.

[2.7] Supratim basu, "Single Phase Active Power Factor Correction Converters: Methods for Optimizing EMI, Performance and Costs," *Department of Energy and Environment, Division of Electric Power Engineering, Chalmers University of technology, Göteborg, Sweden,* June 2006.

[2.8] A. R. Prasad, P. D. Ziogas and S. Manias, "A novel Passive wave-shaping method for single phase Diode Rectifiers", *IEEE Trans. on Industrial Electronics*, Vol.37,

No.6, pp. 521-530, Dec.1990.

[2.9] Francisc C. Schwarz, “A Time-Domain Analysis of the Power Factor for a Rectifier Filter System with Over- and Subcritical Inductance”, *IEEE Trans. On Industrial Electronics and Control Instrumentation*, Vol. 20, No.2, pp. 61-68, May 1973.

[2.10] Ray P. Stratford, “Rectifier harmonics in power systems,” *IEEE Trans. Ind.Appl.* Vol. IA-16:271-276, 1980.

[2.11] S. B. Dewan, “Optimum Input and Output Filters for a Single-phase Rectifier Power Supply”, *IEEE Trans. Industry Appl.*, vol. IA-17, no. 3, pp. 282-288, 1981.

[2.12] Joseph.S. Subjak. Jr. and John. S. McQuilkin, “Harmonics - Causes, effects, measurements, and analysis: An update,” *IEEE Trans. Ind. Appl.* IA-26:1034-1042, 1990.

[2.13] A. R. Prasad, Phoivos D. Ziogas and Stefanos. Manias, “An Active Power Factor Correction Technique for Three Phase Diode Rectifiers”, *IEEE Trans. On Power Electronics*, vol. 6, no. 1, pp. 83-92, January 1991.

[2.14] Arthur W. Kelley and William F. Yadusky, “Rectifier Design for Minimum Line Current Harmonics and Maximum Power Factor”, *IEEE Trans. on Power Electronics*. vol. 7, no. 2, pp. 332-341, 1992.

[2.15] Thomas. S. Key and Jih-Sheng Lai, “Comparison of standards and power supply design options for limiting harmonic distortion in power systems,” *IEEE Trans. Ind. Appl.* Vol. 29, pp. 688-695, 1993.

[2.16] R. Redl and L. Balogh, “Power-factor correction in bridge and voltagedoubler rectifier circuits with inductors and capacitors,” *IEEE Appl. Power Electronics Conf., Rec.*, pp. 466-472, 1995.

[2.17] Ji Yanchao, Liang Xiaobing, Liu Zhuo, Jin Jisheng and Liu Xinhua, "An improved Passive Input Current Waveshaping Method for Single-Phase Rectifier," *Industrial*

Electronics, Control and Instrumentation, IEEE IECON, Vol. 2, pp 695-699, 1996.

[2.18] Redl and Richard, "An Economical Single-phase Passive Power-Factor-Corrected Rectifier: Topology, Operation, Extensions, and Design for Compliance*", Proc. of IEEE Applied Power Electronics Conference, APEC'98*. pp. 454-460, 1998.

[2.19] G. A. Karvelis, S. N. Manias, and G. Kostakis, "A comparative evaluation of power converters used for current harmonics elimination," *in Proc. IEEE HQP'98*, pp. 227–232, 1998.

[2.20] Oscar Gercia, Jose A. Cobos, Roberto Prieto, Pedro Alou and Javier Uceda, "An alternative to Supply DC Voltages with High Power Factor", *IEEE Trans. on Industrial Electronics*, vol. 46, no. 4, pp. 703-709, August 1999.

[2.21] Bhim Singh, Kamal Al-Haddad and Ambrish Chandra, "A Review of Active Filter for Power Quality Improvement", *IEEE Transaction on Industrial Electronics*, Vol. 46, no. 5, pp.960-971, Oct. 1999.

[2.22] Huai Wei and Issa Batarseh, "A Single-switch AC-DC Converter with Power Factor Correction", *IEEE Transactions on Power Electronics*, vol. 15,no. 3, pp. 421-430, 2000.

[2.23] O. Garcia, M. D. M. Avail, J. A. Cobos, J. Uceda, J. Gonzalez, and J. A. Navas, "Harmonic reducer converter," *in Proc. IEEE PESC '00*, pp. 583-587, 2000.

[2.24] Miaosen Shen and Zhaoming Qian, "A novel high efficiency single stage PFC converter with reduced voltage stress," *in Proc. IEEEAPEC'01*, pp. 363-367, 2001.

[2.25] H.M. Sut-yawanshi, K.L. Thakre, S.G. Tarnekar, D.P. Kothari and A.G. Kothari, "Power factor improvement and closed loop control of an AC-to-DC sonant converter", *IEE Proc-Electr, Power Appl*, Vol 149, No. 2, March 2002.

[2.26] Bhim Singh, Brij N. Singh, Ambrish Chandra, Kamal Al-Haddad, Ashish Pandey, Dwarka P. Kothari, "A Review of Single-Phase Improved Power Quality AC-DC Converters", *IEEE Transactions On Industrial Electronics*, Vol. 50, NO. 5,

October 2003.

[2.27] Hussein A. Kazem, Abdulhakeem Abdullah. Alblushi, Ali. Said Ali Al-Jabri and Khmaisis Humaid Alsaidi, "Simple and Advanced Models for Calculating Single-Phase Diode Rectifier Line-Side Harmonics", *Transactions on Engineering, Computing and Technology*, Vol.9, pp. 179-183, November 2005.

[2.28] Bhim Singh, Vipin Garg, and G. Bhuvaneshwari, "Third harmonic current injection for power quality improvement in rectifier loads," *in Proc IEEE Conf. Power Electron., Drives, Energy Syst. Ind. Growth (PEDES'06)*, New Delhi, India, pp. 1–5, paper 4B-08, Dec. 2006.

[2.29] Mehjabeen A. Khan, Akeed A. Pavel, M. Rezwan Khan and M. A. Choudhury, "Design of a single phase rectifier with switching on AC side for high power factor and low total harmonic distortion", *IEEE Region 5 Technical Conference, April 20-21, Fayetteville, AR, 2007.*

[2.30] Hussein A. Kazem, "Input Current Wave shaping Methods Applied to Single Phase Rectifier," *Proceeding of International Conference on Electrical Machines and Systems*, Oct 8-11, Seoul, Korea, 2007.

[2.31] C.-M. Wang, "A novel single-stage high-power-factor electronic ballast with symmetrical half-bridge topology," *IEEE Trans. Ind. Electron.*, vol. 55, no. 2, pp. 969–972, Feb. 2008.

[2.32] V. Suresh Kumar, D. Kavitha, K. Kalaiselvi, P. S. Kannan, "Harmonic Mitigation and Power Factor Improvement using Fuzzy Logic and Neural Network Controlled Active Power Filter", *Journal of Electrical Engineering & Technology*, Vol. 3, No. 3, pp. 520~527, 2008.

[2.33] M. Mahdavi and H. Farzanehfard, "Zero-Current-Transition Bridgeless PFC without Extra Voltage and Current Stress," *IEEE Trans. on Ind. Electron.*, vol. 56, no. 7, pp. 2540-2547, Jul. 2009.

[2.34] R.Balamurugan, Dr.G.Gurusamy, "Harmonic Optimization by Single Phase Improved Power Quality AC-DC Power Factor Corrected Converters", *International Journal of Computer Applications (0975 – 8887),* Volume 1 – No. 5, 2010.

[2.35] Przemyslaw Janik, "Effective Approach to Analogue Filter Design Dedicated to Current Harmonics Reduction in Nonlinear Circuits",*IEEE, 10th International Conference on Environmental and Electrical Engineering,* May 2011.

[2.36] Abbas A. Fardoun, Esam H. Ismail, Mustafa A. AL-Saffar and Ahmad J. Sabzali, "New "real" Bridgeless High Efficiency AC-DC Converter", *IEEE, 27th Applied Power Electronics Conference and Exposition,* Feb. 2012.

CHAPTER 3

ELECTRICAL DRIVES

Drives can be defined as systems used for motion control e.g.-fans, robots, pumps, etc. Prime mover is the main part of any drive which provides the movement, so it can be diesel engines, petrol engines, hydro motors, electric motors etc.

Drivers using electric motor as the prime movers are known as electrical drives. There are several advantages of electrical drives:

i. Easy to control.
ii. High efficiency (switch mode converters and electrical motors are very efficient).
iii. Lesser pollution.
iv. Easy to store or transport energy.

3.1 Components of electrical drives

Fig 3.1 shows the mainly four components of electrical drives.

- Motors
- Source
- Power processor or power modulator
- Control unit.

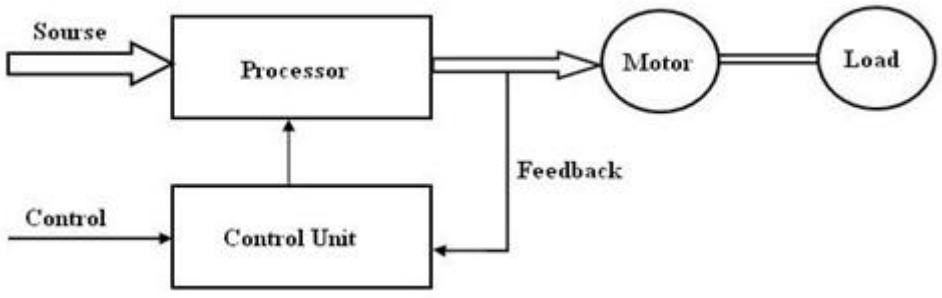

Fig 3.1 Components of electrical drives

3.2 Motors

Motors take the power from electrical source and convert that energy into mechanical energy, so these can be considered as energy converters. Fig. 3.2 shows the types of motors

which are used in electrical drives. The choice of motor depends on electrical source and application.

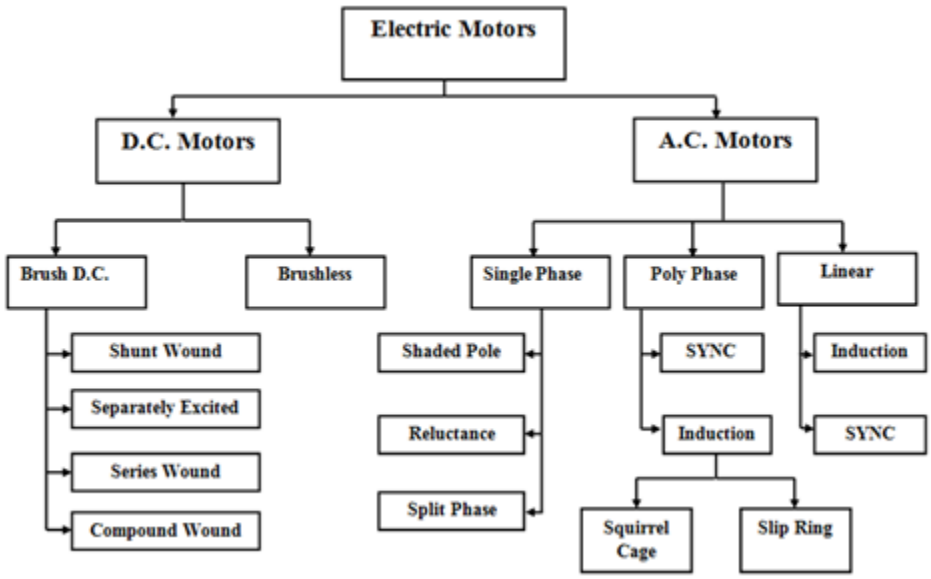

Fig 3.2 Classification of electric motors

3.2.1 DC Motors

A machine that converts DC power into mechanical power is known as a DC motor. Its operation is based on the principle that when a current carrying conductor is placed in a magnetic field, the conductor experiences a mechanical force. The direction of this force is given by Fleming's left hand rule and magnitude is given by

$$F = BIl \text{ newtons} \qquad (3.1)$$

B = magnetic flux density in Wb/m^2.

l = length of the conductor in meters.

I = current in the conductor in Amp.

Working of DC Motor Consider a part of a multipolar DC motor as shown in Fig. 3.3. When the terminals of the motor are connected to an external source of DC supply,

- The field magnets are excited developing alternate N and S poles.

- The armature conductors carry currents. All conductors under N-pole carry currents in one direction while all the conductors under S-pole carry currents in the opposite direction.

Let the conductors under N-pole carry currents into the plane of the paper and those under S-pole carry currents out of the plane of the paper as shown in Fig. 3.3. Since each armature conductor is carrying current and is placed in the magnetic field, mechanical force acts on it. Referring to Fig. 3.3 and applying Fleming's left hand rule, it is clear that force on each conductor is tending to rotate the armature in anticlockwise direction. All these forces add together to produce a driving torque which sets the armature rotating. When the conductor moves from one side of a brush to the other, the current in that conductor is reversed and at the same time it comes under the influence of next pole which is of opposite polarity. Consequently, the direction of force on the conductor remains the same [3.1].

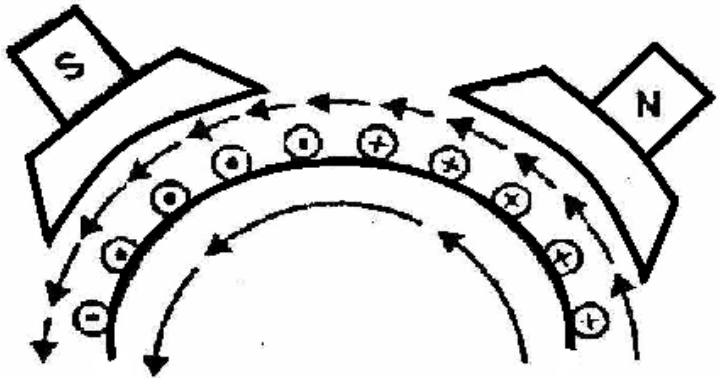

Fig. 3.3 Multipolar DC motor

The types of DC motors characterized by the connections of field winding in relation to the armature are described as follows:

A. Separately Excited The field coil contains a relatively large number of turns which minimizes the current required to produce a strong stator field. It is connected to separate DC power supply, thus making field current independent of load or armature current. The connection diagram of separately excited DC motor is shown below in Fig. 3.4.

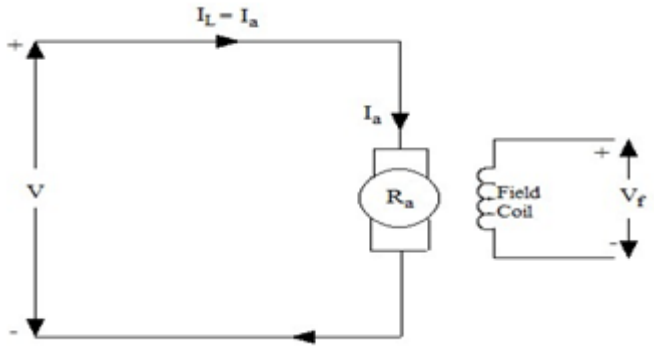

Fig. 3.4 Separately excited DC motor

B. Shunt-wound motor In shunt wound motor the field winding is connected in parallel with the armature as shown in Fig. 3.5. The current through the shunt field winding is not the same as the armature current. Shunt field windings are designed to produce the necessary m.m.f. by means of a relatively large number of turns of wire having high resistance. Therefore, shunt field current is relatively small compared with the armature current.

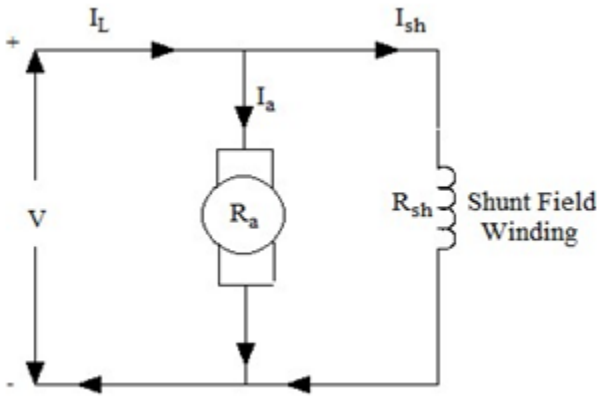

Fig. 3.5 Shunt wound DC motor

C. Series-wound motor In series wound motor the field winding is connected in series with the armature as shown in Fig. 3.6. Therefore, series field winding carries the armature current. Since the current passing through a series field winding is the same as the armature current, series field windings must be designed with much fewer turns than shunt field windings for the same m.m.f. Therefore, a series field winding has a relatively small number of turns of thick wire and, therefore, will possess a low resistance.

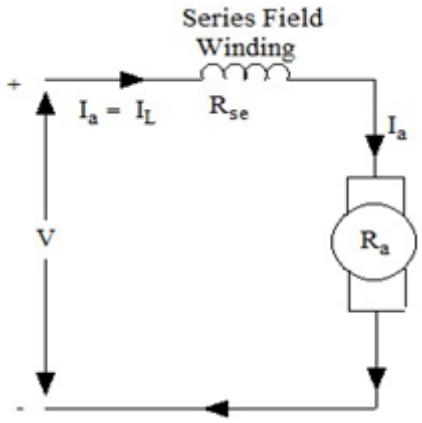

Fig. 3.6 Series wound DC motor

D. Compound-wound motor Compound wound motor has two field windings; one connected in parallel with the armature and the other in series with it. There are two types of compound motor connections. When the shunt field winding is directly connected across the armature terminals it is called short-shunt connection shown in Fig. 3.7. When the shunt winding is so connected that it shunts the series combination of armature and series field it is called long-shunt connection shown in Fig. 3.8. The compound machines are always designed so that the flux produced by shunt field winding is considerably larger than the flux produced by the series field winding. Therefore, shunt field in compound machines is the basic dominant factor in the production of the magnetic field in the machine.

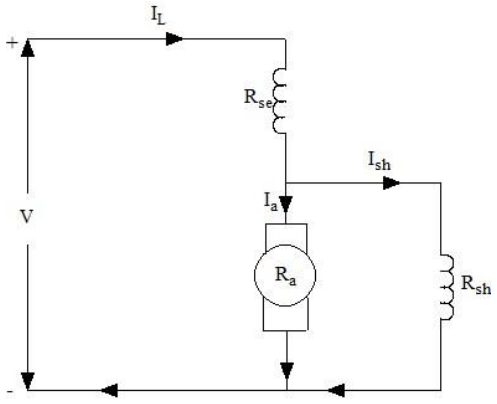

Fig. 3.7 Sort shunt connection of compound wound DC motor

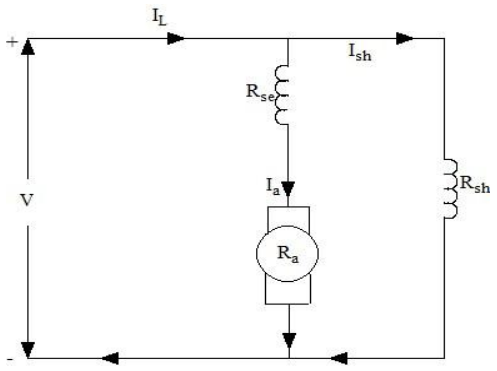

Fig. 3.8 Sort shunt connection of compound wound DC motor

3.2.2 Comparison of characteristics of DC Motors

- The speed regulation of a shunt motor is better than that of a series motor. However, speed regulation of a cumulative compound motor lies between shunt and series motors as shown in Fig. 3.9.

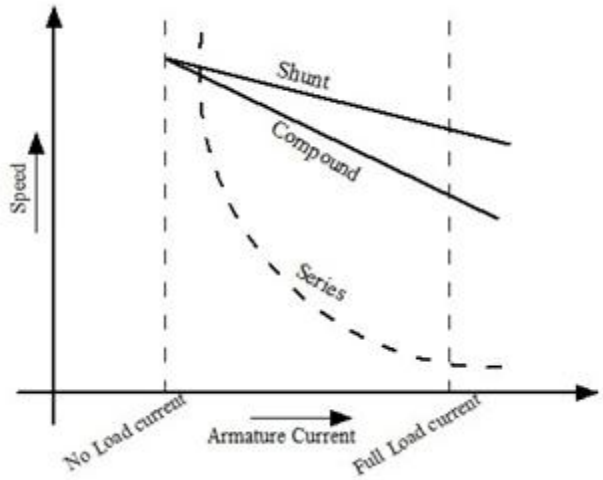

Fig. 3.9 Current-Speed curves for different motors

- For a given armature current, the starting torque of a series motor is more than that of a shunt motor. However, the starting torque of a cumulative compound motor lies between series and shunt motors as shown in Fig. 3.10.

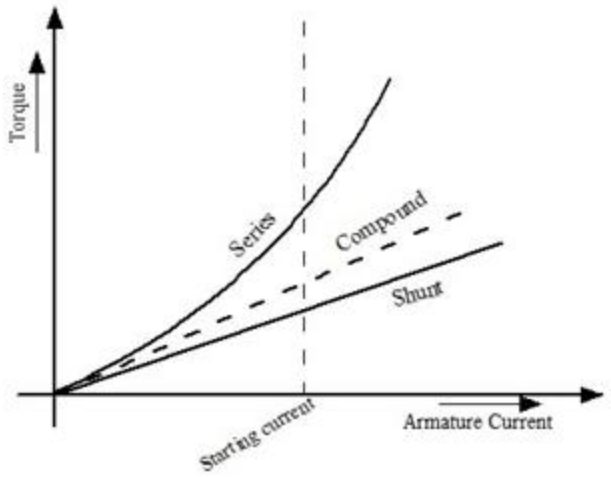

Fig. 3.10 Current-Torque curves for different motors

- Both shunt and cumulative compound motors have definite no-load speed. However, a series motor has dangerously high speed at no-load.
- Excellent speed regulation is characteristic of separately excited DC motor which lends itself well to speed control by variation of field or armature current.

3.3 Applications of DC Motors [3.2]

Separately Excited

Separately excited DC motor can race to dangerously high speeds (theoretically infinity) if current to the field coil is lost. Because of this, applications should include some form of field protection as an unprotected motor could literally fly apart.

Industrial use: Train and automotive traction applications.

Shunt motors

The characteristics of a shunt motor reveal that it is an approximately constant speed motor. It is, therefore, used

- where the speed is required to remain almost constant from no-load to full-load
- where the load has to be driven at a number of speeds and any one of which is required to remain nearly constant

Industrial use: Lathes, drills, boring mills, shapers, spinning and weaving machines etc.

Series motors

It is a variable speed motor i.e., speed is low at high torque and vice-versa. However, at light or no-load, the motor tends to attain dangerously high speed. The motor has a high starting torque. It is, therefore, used

- where large starting torque is required e.g., in elevators and electric Traction
- where the load is subjected to heavy fluctuations and the speed is automatically required to reduce at high torques and vice-versa

Industrial use: Electric traction, cranes, elevators, air compressors, vacuum cleaners, hair drier, sewing machines etc.

Compound motors

Differential-compound motors are rarely used because of their poor torque characteristics. However, cumulative-compound motors are used where a fairly constant speed is required with irregular loads or suddenly applied heavy loads.

Industrial use: Presses, shears, reciprocating machines etc.

Table 3.1 Comparison between DC and AC drives [3.3]

DC Drives	AC Drives
The power circuit and control circuit is simple and inexpensive.	The power circuit and control circuit are complex.
It requires frequent maintenance.	Less maintenance.
The commutator makes the motor bulky , costly and heavy.	These problems are not there in these motors and are inexpensive, particularly squirrel cage induction motors.
Fast response and wide speed range of control can be achieved smoothly by conventional and solid state control.	In solid state control the speed range is wide and conventional method is stepped and limited.
Speed and design ratings are limited due to commutations.	Speed and design ratings have upper limits.

3.4 Control methods for Separately Excited DC motor

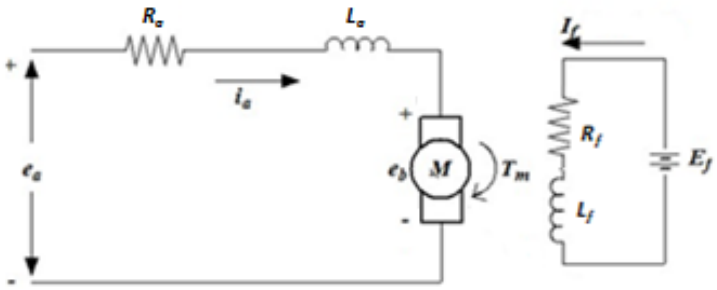

Fig. 3.11 Detailed circuitry of DC drives

The torque is produced as a result of interaction of field flux with current in armature conductors and is given by eq 3.2.

$$T_m = K_t \phi i_a \tag{3.2}$$

Where K_t is a constant depending on motor windings and geometry.

Φ is the flux per pole due to the field winding.

The direction of the torque produced depends on the direction of armature current. When armature rotates, the flux linking the armature winding will vary with time and therefore according to Faraday's law, an emf will be induced across the winding. This generated emf, known as the back emf, depends on speed of rotation as well as on the flux produced by the field and is given by eq 3.3.

$$e_b = K_t \phi \omega \tag{3.3}$$

Using KVL,

$$e_a = i_a R_a + L_a \frac{di_a}{dt} + e_b \tag{3.4}$$

In steady state condition,

$$E_a = I_a R_a + E_b \tag{3.5}$$

In terms of torque and speed, the steady state equation will be,

$$E_a = \frac{T_m}{K_t \phi} R_a + K_t \omega \phi \tag{3.6}$$

Which gives,

$$\omega = \frac{E_a}{K_t\phi} - \frac{T_m}{(K_t\phi)^2}R_a \tag{3.7}$$

Thus from Equation 3.7, it is clear that there are three methods of speed control, those are by varyingE_a, R_a, and ϕ, i.e.:-

- Armature voltage controlled (E_a).
- Armature resistance controlled (R).
- Flux controlled (ϕ).

Speed control using armature resistance by adding external resistor R_{ext} is not used very widely because of the large energy loss due to the R_{ext} that can be given as ${I_a}^2 R_{ext}$. Armature voltage control is normally used for speed up to rated speed (base speed). Flux control is used for speed beyond rated speed but at the same time the maximum torque capability of the motor is reduced since for a given maximum armature current, the flux is less than the rated value and so as the maximum torque produced is less than the maximum rated torque.

Here the main attention is given to the armature voltage control method. In the armature voltage control method, the voltage applied across the armature e_a is varied keeping field voltage constant. As equation (3.7) indicates, the torque-speed characteristic is represented by a straight line with a negative slope when the applied armature voltage is ideal, that ideal torque speed characteristic is illustrated in Fig. 3.12 [3.5].

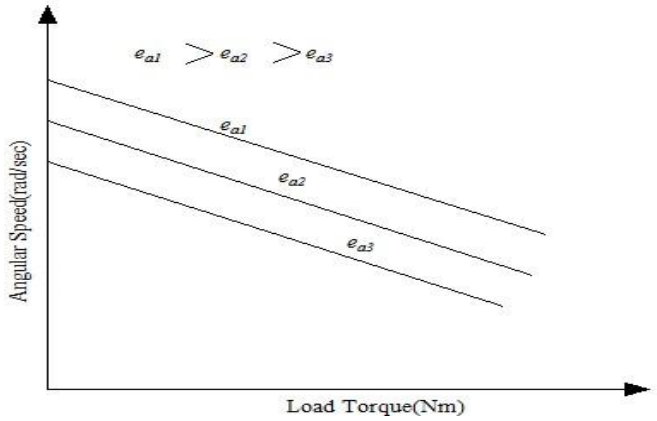

Fig. 3.12 Torque speed characteristics of the separately excited DC motor at different armature voltages

Depending upon the type of AC source or the method of voltage control, DC drives are classified as,

i. Single Phase DC drives.
ii. Three Phase DC drives.
iii. Chopper drives.

3.5 Single Phase DC drives

The general circuit arrangement for the speed control of a separately excited DC motor from a single phase source is shown in Fig. 3.13. The firing angle control of converter 1 regulates the armature voltage applied to DC motor armature. Thus, the variation of delay angle α_1 of converter 1 gives speed control below base speed and converter 2 gives the speed control above base speed. The inductor *L* is used to achieve continuous armature current as the discontinuous armature current cause more losses in armature & poor speed regulation [3.6].

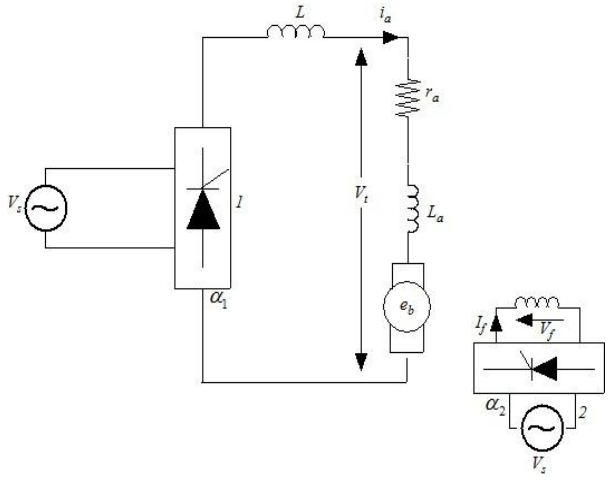

Fig. 3.13 General circuit arrangement for single phase DC drives

Depending upon the type of power electronic converter used in the armature circuit , single phase DC drives may be subdivided as below

i. Single phase half wave converter drives.
ii. Single phase semiconverter drives.
iii. Single phase full converter drives.
iv. Single phase dual converter drives.

3.5.1 Single phase half wave converter drives

A separately excited DC motor fed through single phase half wave converter, is shown in Fig. 3.14. Single phase half wave converter feeding a DC motor offers only one quadrant drive. Such type of drives are used up to about 1/2 kW DC motor.

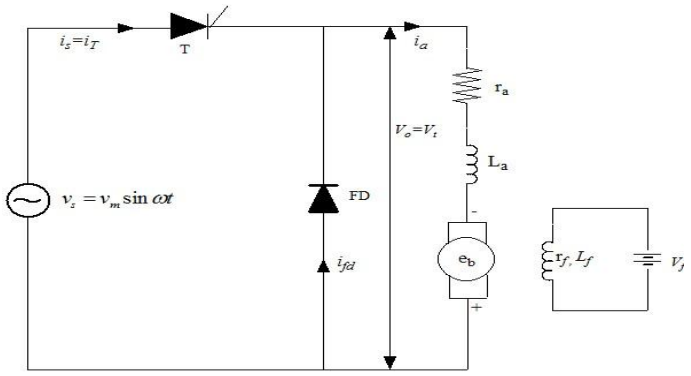

Fig.3.14 Single phase half wave converter drive

For single phase half wave converter, average output voltage of converter can be given by eq. 3.8

$$V_o = V_t = \frac{V_m}{2\pi}(1 + \cos\alpha) \qquad \text{for} \quad 0 < \alpha < \pi \tag{3.8}$$

A half wave converter in the field circuit will increase the magnetic losses of the motor due to high ripple content on the field excitation current, so an ideal DC source is preferred over half wave converter for field circuit.

3.5.2 Single phase semiconverter drive

A separately excited DC motor fed through single phase semiconverter is shown in Fig. 3.15. This converter also offers only one quadrant drive and is used up to 15 kW DC drives.

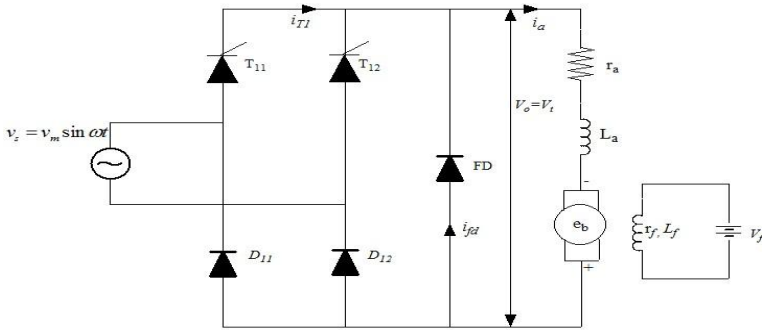

Fig. 3.15 Single phase semiconverter drive

With a single phase semiconverter in the armature circuit, equation (3.9) gives the average armature voltage as

$$V_o = V_t = \frac{V_m}{\pi}(1 + \cos\alpha) \qquad \text{for} \quad 0 < \alpha < \pi \qquad (3.9)$$

3.5.3 Single phase full converter drive

The armature voltage is varied by single phase full wave converter as shown in Fig. 3.16. It is a two quadrant drive, and it is limited to applications up to 15kW. The armature converter gives $+V_o$ or $-V_o$ and allows operation in the first and fourth quadrant. The converter in the field circuit could be semi, full or even dual converter. The reversal of the armature or field voltage allows operation in the second and third quadrant.

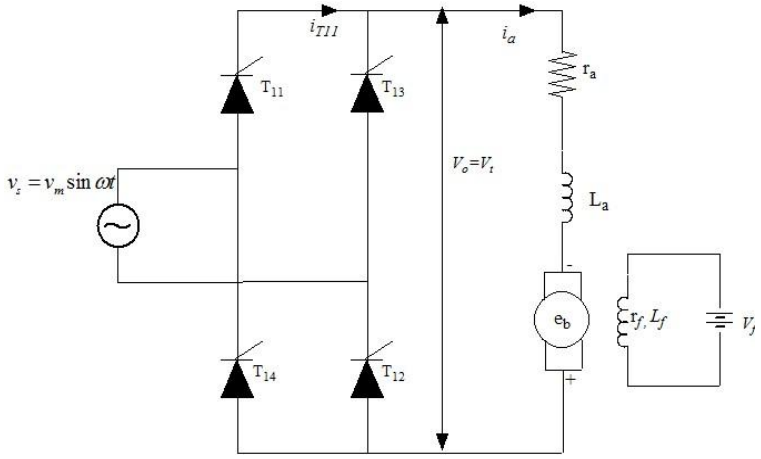

Fig. 3.16 single phase full converter drive

The average armature voltage in armature circuit for single phase full converter drive can be given as

$$V_o = V_t = \frac{2V_m}{\pi}(1 + \cos\alpha) \qquad \text{for} \quad 0 < \alpha < \pi \qquad (3.10)$$

3.5.4 Single phase dual converter drive

To realize single phase dual converter, two single phase full converters are connected as shown in Fig. 3.17.

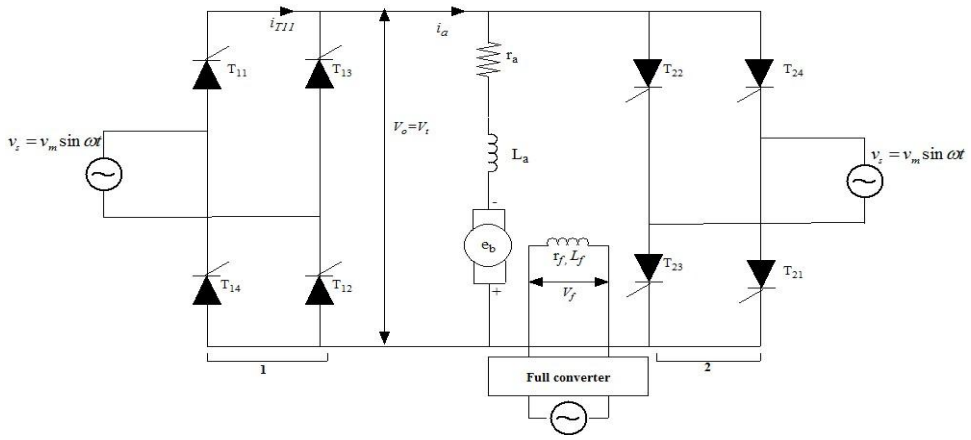

Fig. 3.17 Single phase dual converter drive

As shown in above Fig.3.17 there are two single phase full wave converters either converter 1 operates to supply a positive armature voltage V_o, or converter 2 operates to supply negative armature voltage $-V_o$. Converter 1 provides operation in first and fourth quardants, and converter 2 provides operation in second and third quardants.It is four quardant drive and provides four modes of operation: forward powering, forward braking (regenration), reverse powering, and reverse breaking (regeneration). The field converter could be a full wave converter, a semiconverter, or a dual converter.

If converter 1 operates at a firing angle of α_1, then eq. (3.11) gives the armature voltage as,

$$V_o = V_t = \frac{V_m}{\pi}(1 + \cos \alpha_1) \qquad \text{for} \quad 0 < \alpha_1 < \pi \qquad (3.11)$$

And similarly, if converter 2 operates at a firing angle of α_2 then eq. (3.12) gives the armature voltage as,

$$V_o = V_t = \frac{V_m}{\pi}(1 + \cos \alpha_2) \qquad \text{for} \quad 0 < \alpha_2 < \pi \qquad (3.12)$$

Where $\alpha_2 = \pi - \alpha_1$

3.6 Literature Review

Chin S. Moo et.al, presented an analytical approach for calculating line current waveform and frequency spectrum of full-controlled converter fed DC drive system under practical conditions. The harmonics in the line current depend on the load current, firing angle, armature inductance, and machine speed. The proposed method to investigate the harmonics generated by the DC drives by full controlled converters precludes the time consuming

calculations which are needed by numerical methods. As a result, more accurate estimation on the harmonic contents becomes feasible [3.7].

Zhifang Sun et.al, proposed an analytical method for calculating the harmonic currents in series connected AC to DC converters under unbalanced supply conditions and method of minimization of noncharacteristics harmonics in DC side using asymmetrical firing angles. With the adaptive firing angles, in quality of DC side current will be improved [3.8].

M. Nedeljkovic et.al, proposed a new method of current control for thyristor rectifier with slow varying voltage generator type loads (battery chargers/dischargers, DC motors etc.). The proposed control method was based on calculating the thyristor firing angle a predicted voltage-time area on the DC side inductor, thyristor are fired when the sum of measured instant value of DC current and the predicted current rises due to the voltage-time area on the DC side inductor becoming equal to the preset reference value [3.9].

Alfio Consoli et.al, developed an innovative converter topology that allows to improve the performance of motor drive, aimed to equip home appliances in which the energy recovery stage acts as an active power factor controller (PFC) for offline operation that is made possible by introducing a new technique to manage the free-wheeling energy that is recovered back to DC bus by suitable high frequency transformer [3.10].

K. Georgakas et.at, concluded that the use of power electronic converters to control the power flow from the AC grid to DC drives leads to increase in reactive power increase and affects the efficiency as these two important energy quantities depend on the structure of the converter topology, operating frequency and the power percentage related to the nominal power [3.11].

Manoj Daigavane et.al, presented the application of a single phase AC to DC converter using a three phase serial parallel resonant converter to variable speed DC drive. The improved power quality converter gives the input power factor unity over a wide speed range, reduces the total harmonic distortion (THD) of AC input supply current, and makes very low ripples in the armature current and voltage waveform [3.12].

Wai Phyo Aung designed and analyzed the wheeled mobile robot which is built with their wheels drive machine, DC motor. Depending on the desired design of wheeled mobile

robot(WMR) one can choose the DC motor, results are verified by using MATLAB Simulink model [3.13]

Y. Varetsky et.al, presented performance peculiarities of industrial power systems employing single-tuned for harmonics mitigation and improved reactive power compensation and concluded that it is not a healthy practice to add filter circuit to exciting power factor correction capacitors, improper choice of filter resonant frequency considering capacitor may cause significant harmonic overloading of the filter and same order filters should not be used in the system [3.14].

R. Carbone analyzed performances of the new controlled rectifier with Pspice simulation results on a DC motor drive case study of about 2.5kW of active power and under different working conditions, obtained by varying the rectifier delay angle, α, in order to control the speed and power of the motor [3.15].

Y. Kusumalatha et.al, investigated the impacts of current harmonic distortion on electric drives in paper and pulp industry and designed an active filter for minimization of harmonics generated in paper and pulp industry by industrial drives based on real time measurement of the harmonic data [3.16].

3.7 Methodology

Harmonics puts very adverse effects on the power system, the biggest problem with harmonics is voltage waveform distortion, the relation can deduce between the fundamental and distorted waveforms by mathematical tool Fast Fourier Transform (FFT), in which the square root of the sum of squares of all harmonics generated by load and then dividing that number by the nominal frequency. Using FFT total harmonic distortion (THD) contained by the nonlinear current or voltage waveform determined. Harmonics can cause overloading and overheating of load which can results as load failure.

Rectifier is the main component of any power system based system. The input stage of any AC-DC converter comprises of a full-bridge rectifier followed by a large filter capacitor. The input current of such a rectifier circuit comprises of large discontinuous peak current pulses that result in high input current harmonic distortion. The high distortion of the input current occurs due to the fact that the diode rectifiers conduct only for a short period. This

period corresponds to the time when the mains instantaneous voltage is greater than the capacitor voltage. Since the instantaneous mains voltage is greater than the capacitor voltage only for very short periods of time, when the capacitor is fully charged, large current pulses are drawn from the line during this short period of time and that will lead to poor power factor.

So from above discussion it can be concluded that if the shape of input current or voltage can be maintained as a sinusoidal wave the power factor and total harmonic distortion (THD) both can be improved.

Many input current wave shaping methods have been proposed to overcome disadvantages of conventional rectifiers like high input current harmonic components, low power factor, low rectifier efficiency etc. Those waves shaping method can be broadly classify as active, passive and hybrid methods. In the past, designers have used three passive wave shaping methods to improve the input power factor and reduce total harmonic distortion THD of conventional rectifiers [3.17]. Input passive filter method, resonant passive input filters method and Ferro resonant transformer method.

Among the passive wave shaping methods proposed earlier, the novel method is proposed in 1990 is superior to others in reducing the input current harmonics and improving the input power factor [3.18]. The novel method can efficiently improve the power factor, however, the further improvement of the input power factor is difficult to achieve, and the input current's total harmonic distortion is still high, which is the main disadvantage of the novel topology. This novel method uses an input parallel resonant tank of capacitor and inductor to remove the third harmonic component from the input current. The input power factor increases because the third harmonic component is the main reason of the low input power factor. The advantages of the this method over the conventional method include: (i) low input current THD (ii) higher input power factor, and (iii) increase in the efficiency of the rectifier. Fig. 3.18 shows the block diagram how the wave shaping method is used to improve the power factor and total harmonic distortion of DC drives.

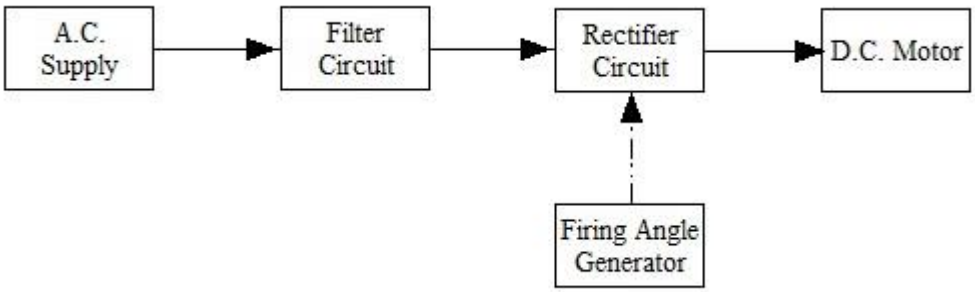

Fig. 3.18 Block diagram of methodology used

3.8 Simulation Results

To investigate the effect of armature voltage on the torque speed curve six different firing angles are used with the voltage applied to the field circuit kept constant 300V. A constant 240 V, 50 Hz AC supply is applied to the input of single phase half wave converter. The average value of converter output is controlled by changing the firing angle (α).

A cosine firing angle scheme is used to change the firing angle. The following firing angles are used to get different output voltages for armature: α = 0°, 18°, 36°, 54°, 72° and 89°. The simulink model used to get torque speed characteristic for a single phase half wave converter is shown in Fig. 3.19.

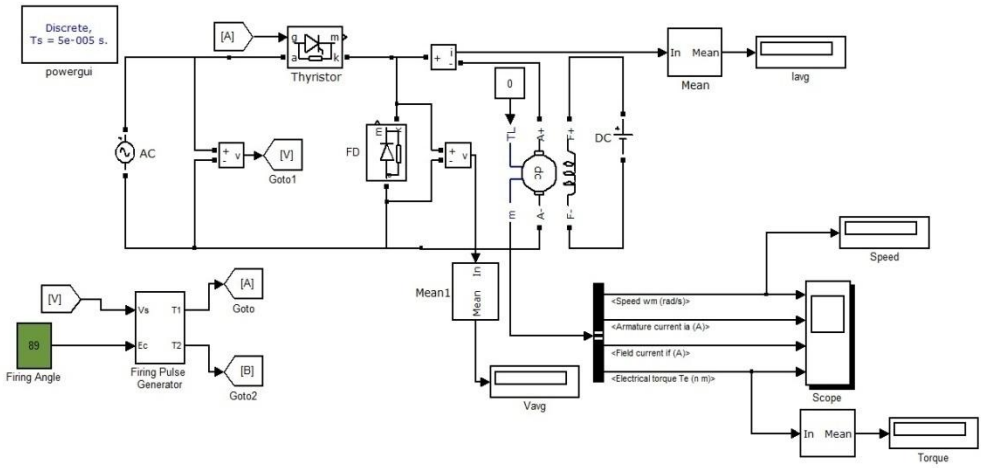

Fig. 3.19 Simulink realization of armature voltage speed control method using a single phase half wave converter drive

The torque speed curves for a single phase half wave converter drive are shown in Fig. 3.20.

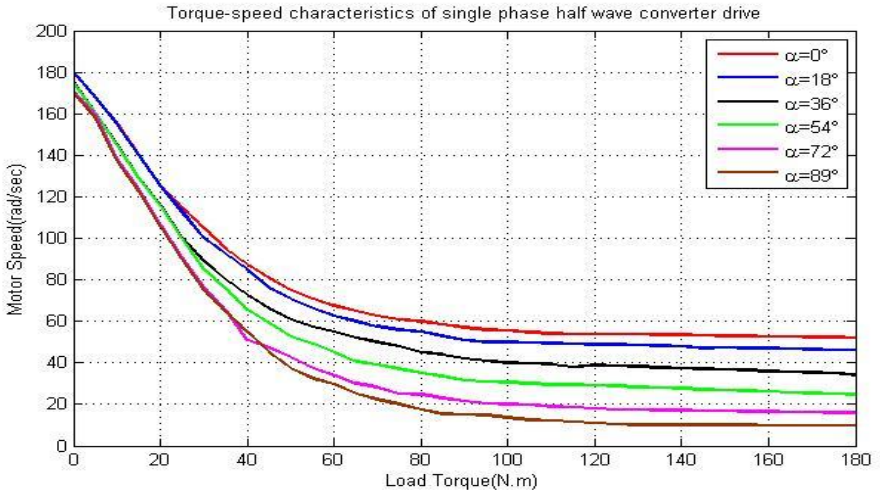

Fig. 3.20 Torque-speed characteristics for a single phase half wave converter drive

It is clear that a torque speed curve contains both linear and non linear regions. The linear region of operation for 0° firing angle approximately starts at 100 N.m load torque, but for 18° firing angle starts at 105N.m load torque, while for 36° firing angle starts at approximately at 110 N.m and so on.

The discontinuous armature current results in a highly non-linear torque speed characteristic. Fig. 3.21 and 3.22 shows the armature voltage and current obtained at 50 N.m (in the non-linear region) and 135 N.m (in linear region) with firing angle 89°. These figures clearly show the discontinuous and continuous operation of single phase half wave converter drive in non linear and linear regions, respectively.

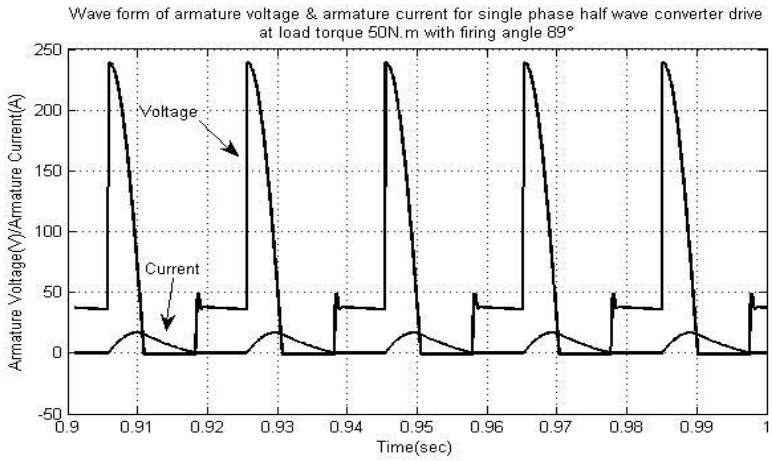

Fig. 3.21 Armature current and voltage at 50N.m with firing angle 89° for single phase half wave converter drive

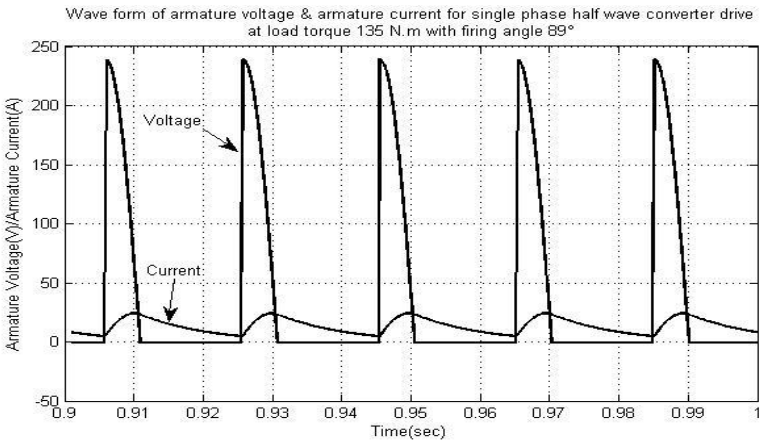

Fig. 3.22 Armature current and voltage at 135N.m with firing angle 89° for single phase half wave converter drive

To investigate the effect of armature voltage on the torque speed characteristic, six different firing angles are applied to the firing angle generator while the voltage applied to the field circuit is kept constant 300V. A constant 240V, 50Hz AC is applied to the input of single phase semi converter. The average value of the converter output is controlled by the firing angle (α). The following firing angles are used to get different output voltages for armature: α = 0°, 18°, 36°, 54°, 72° and 89°.

The simulink model used to get torque speed characteristic for a single phase half wave converter is shown in Fig. 3.23 with variation of speed with torque and firing angle which is shown in Fig. 3.24

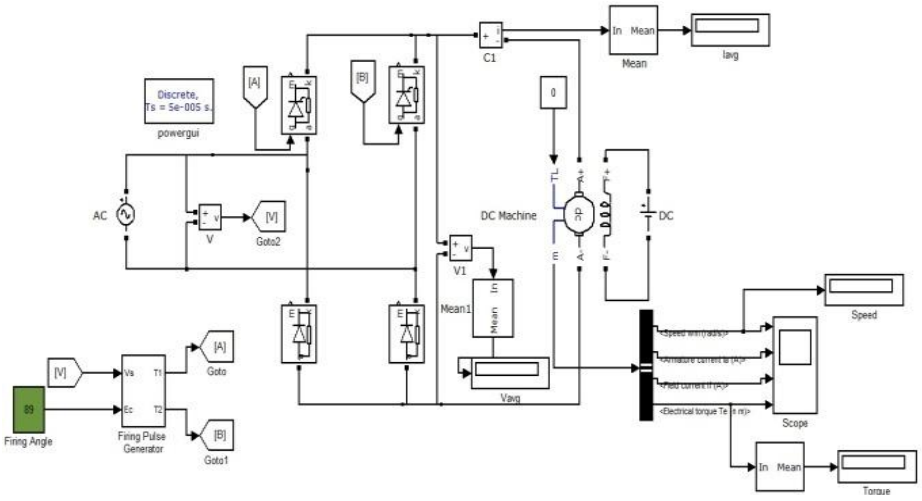

Fig. 3.23 Simulink realization of armature voltage speed control method using a single phase semiconverter drive

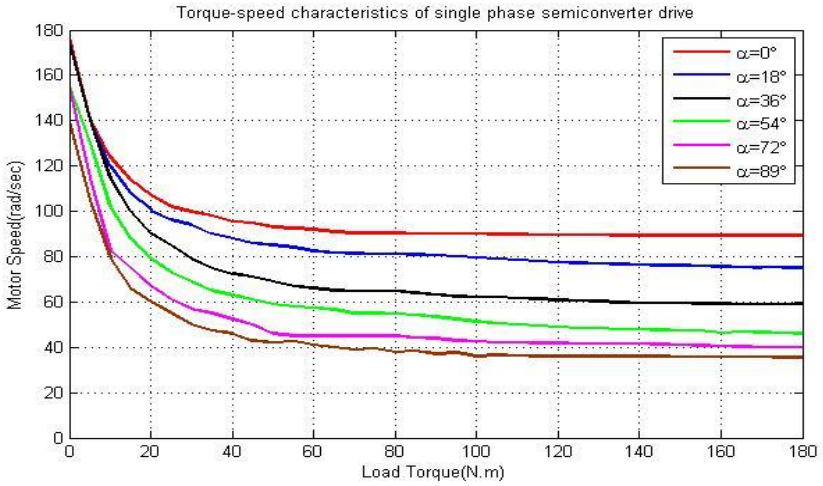

Fig. 3.24 Torque-speed characteristics for a single phase semiconverter drive

In the above shown torque speed cherecteristics, the non linear and linear operating regions are clearly visible for different firing angle. The linear operating range for single phase semiconverter drive decrease as firing angle increases. For firing angle 0° it is 60 to 180 N.m, for 18° it is 65 to 180 N.m, for 36° it is 80 to 180 N.m and for 89° it is 100 to 180 N.m. The non linearity in the speed torque characteristic is due to the discontinuity in armature current. Fig. 3.25 and 3.26 shows the armature voltage and current obtained at 50 N.m (in the non-linear region) and 135 N.m (in linear region) with firing angle 0°. These figures show the discontinuous and continuous operation of single phase semiconverter drive in non linear and linear regions, respectively.

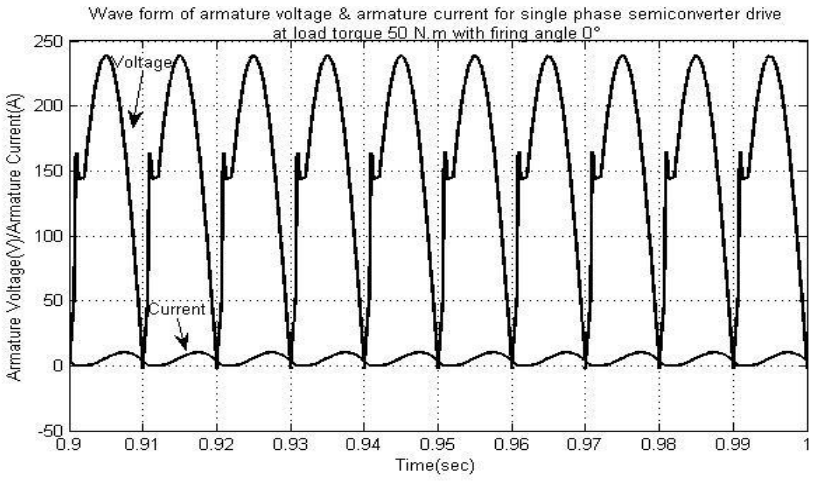

Fig. 3.25 Armature current and voltage at 50N.m with firing angle 0° for single phase semiconverter drive

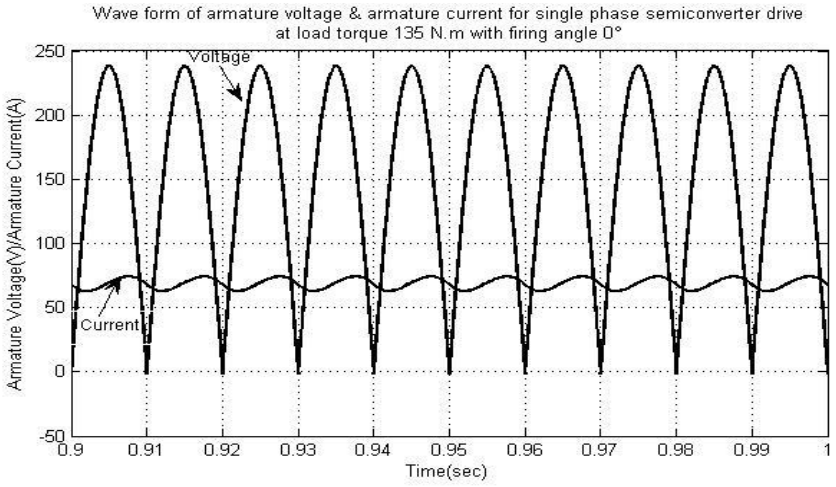

Fig. 3.26 Armature current and voltage at 135N.m with firing angle 0° for single phase semiconverter drive

The simulink model used to get torque speed characteristic for a single phase full converter drive is shown in Fig. 3.27. The effect of armature voltages on the torque speed characteristic is observed for six different firing angles, as the voltage applied to the field circuit is kept constant at 300V, and a constant 240V, 50 Hz AC is applied to input of single phase full converter. The average value of applied armature voltage is varied by varying the firing angle of full converter.

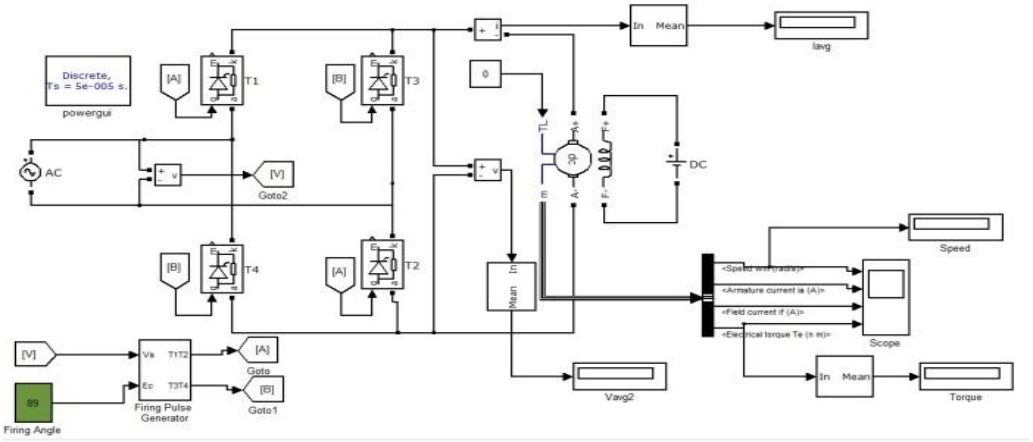

Fig. 3.27 Simulink realization of armature voltage speed control method using a single phase full converter drive

Fig. 3.28 shows the torque speed characteristics of single phase full converter drive with firing angles $\alpha = 0°$, 18°, 36°, 54°, 72°, and 89°.

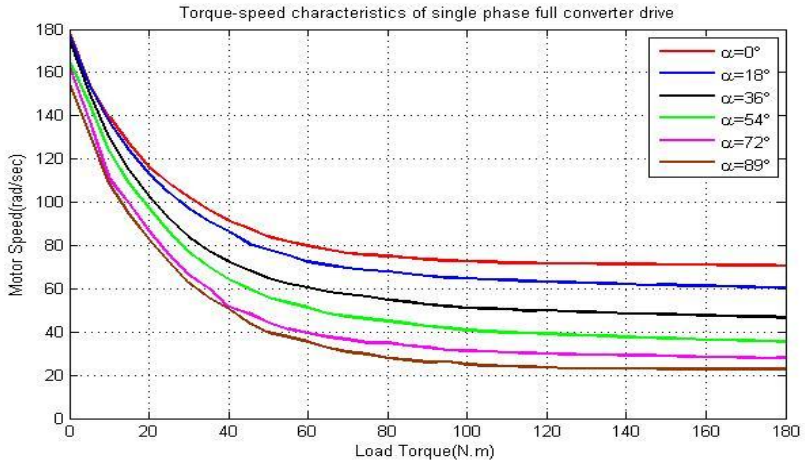

Fig. 3.28 Torque-speed characteristics for a single phase full converter drive

Linear and non linear regions for single phase full converter drive are clearly visible in the above shown torque speed curve. Non linearity is because of the discontinuity in the armature current, and also it is observed that the range of non linearity increases as firing angle is increased. For firing angle 0°, non linearity range of load torque 0 to 85 N.m, for 18° it is 0 to 100 N.m, for 36° it is 0 to 110 N.m, for 36° it is 0 to 54 N.m and for 89° it is 0 to 120 N.m. The armature voltage and current waveforms for single phase full converter drives are shown in Fig. 3.29 and 3.30, those were obtained at 50 N.m (in the non-linear region) and 135 N.m (in linear region) with firing angle 89°. These figures show the discontinuous and continuous operation of single phase full converter drive in non linear and linear regions, respectively.

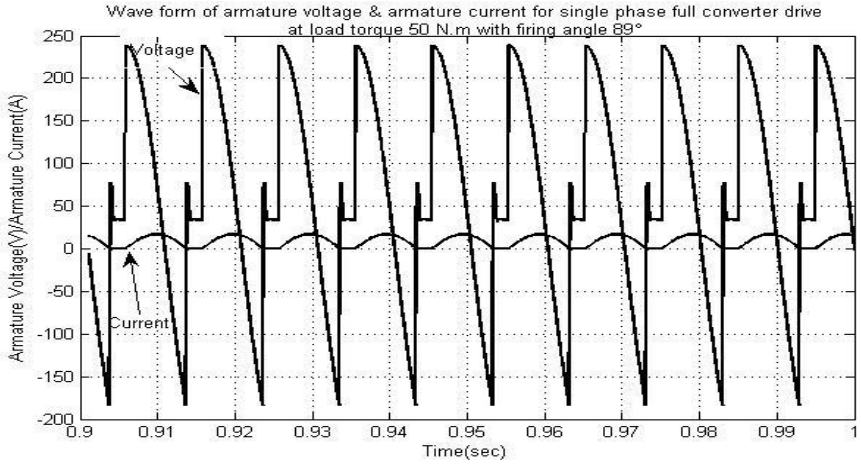

Fig. 3.29 Armature current and voltage at 50N.m with firing angle 89° for single phase full converter drive

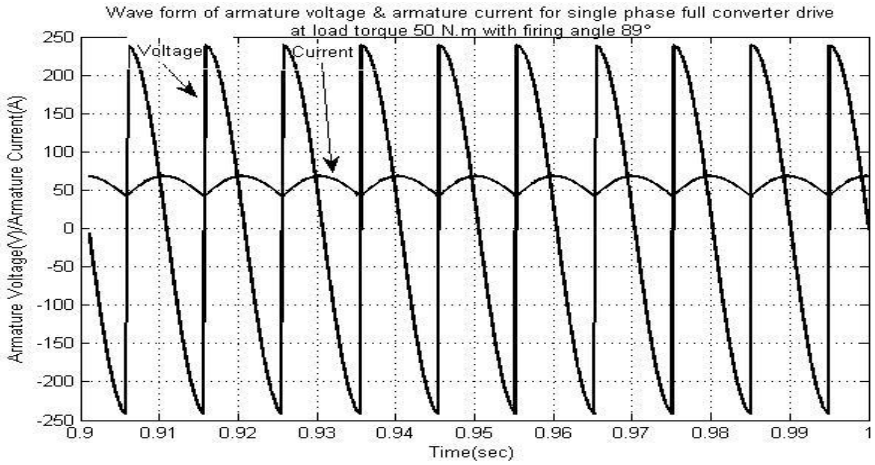

Fig. 3.30 Armature current and voltage at 135N.m with firing angle 89° for single phase full converter drive

It is clearly seen from all firing angle values that linear region of operation extends when single phase semi converter is used. The linear operating ranges of load torque for different converter drives changes with respect to firing angle.

In previous chapter, we have seen in simulation result section that improved parallel resonant filter gives the best result in terms of power factor and total harmonic distortion, so the same topology is used here with half wave converter drive, that is shown in Fig. 3.32.

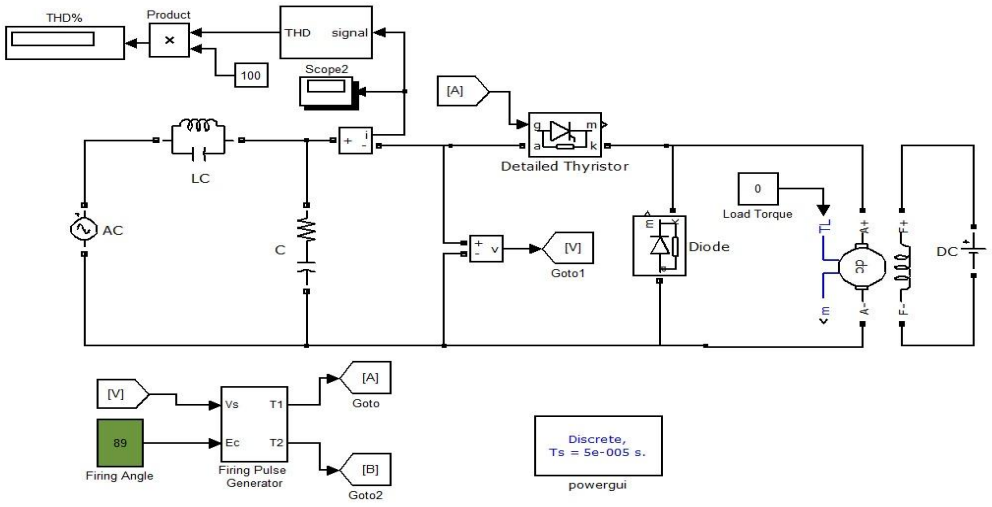

Fig 3.31 Halfwave converter drive with PFC circuit

Input current waveform of half converter drive with PFC circuit is shown in Fig. 3.31 which is almost sine wave which is desiriable and values of PF and THD are 0.78 ,11.14 respectively.

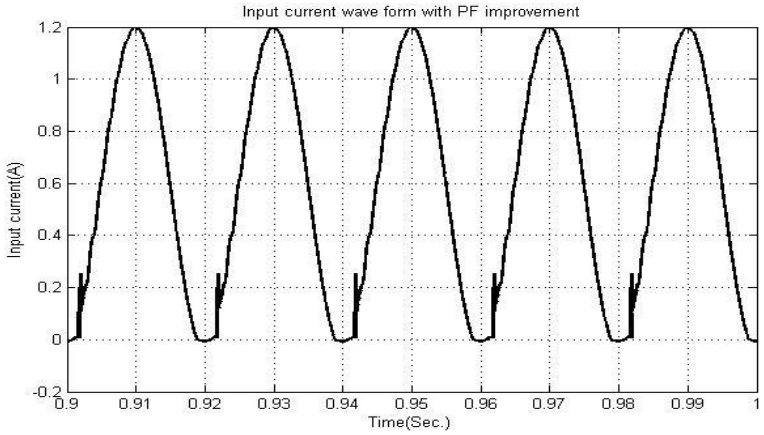

Fig 3.32 Input current waveform of Halfwave converter drive with PFC circuit

A simulink model of semiconverter drive with improved parallel resonant filter is shown in Fig. 3.33, with the input current waveform in Fig. 3.34 which is nearly sinusodial and values of PF and THD are 0.71 ,4.08 respectively.

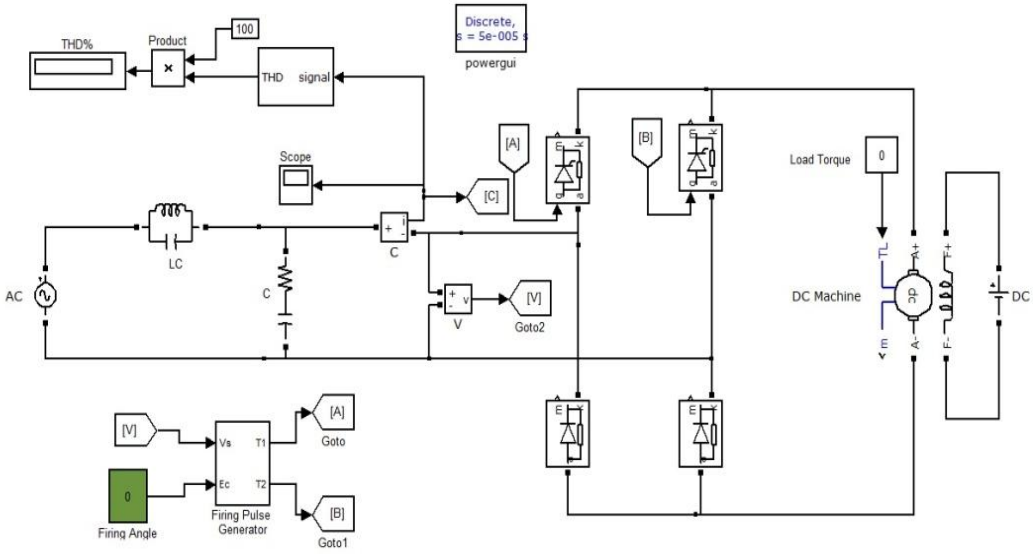

Fig 3.33 Semiconverter drive with PFC circuit

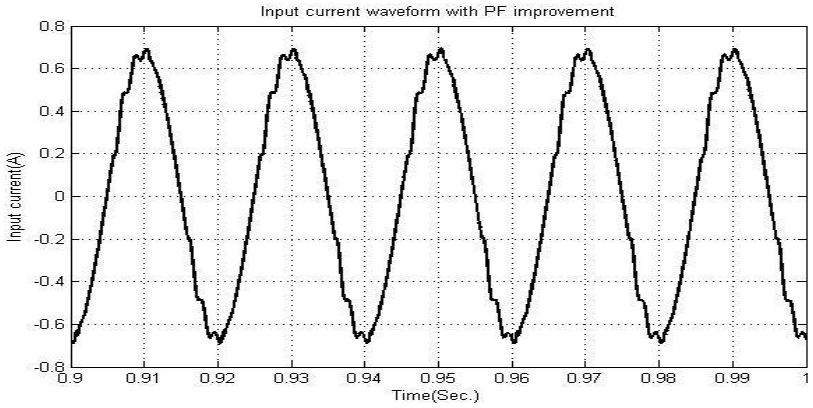

Fig 3.34 Input current waveform of Semiconverter drive with PFC circuit

Full converter drive with power factor correction circuit is shown in Fig. 3.35 with input current waveform in Fig 3.36, which is almost sine wave but more distorted as compared to smiconverter drive input current for same filter and values of PF and THD are 0.68 ,3.6 respectively.

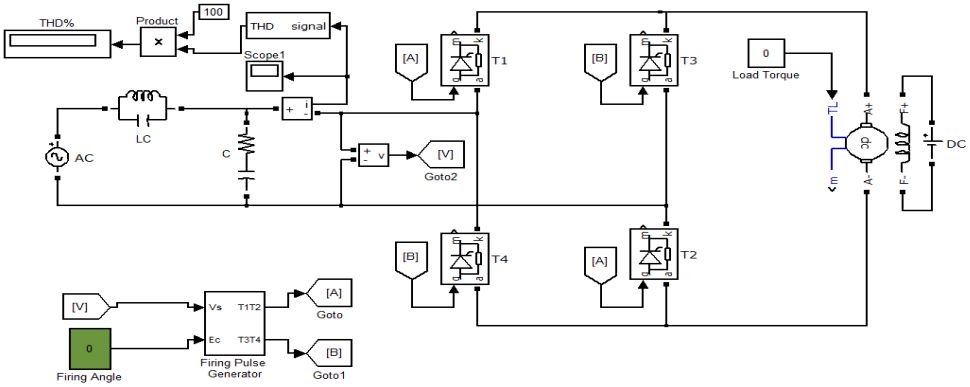

Fig 3.35 Full converter drive with PFC circuit

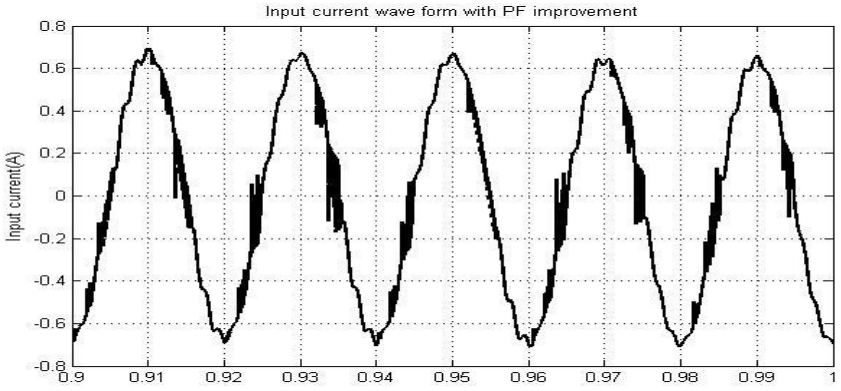

Fig 3.36 Input current waveform of Full converter drive with PFC circuit

Dual converter drive with power factor correction circuit is shown in Fig. 3.37, with input current waveform in Fig. 3.38 for one side only. The shown current waveform is sinusoidal and best as compared to previous converter drives and values of PF and THD are 0.99 ,10.73 respectively.

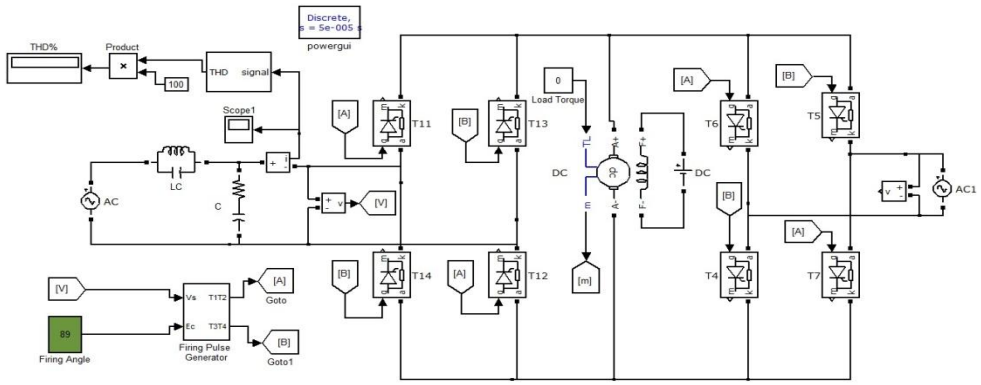

Fig 3.37 Dual converter drive with PFC circuit

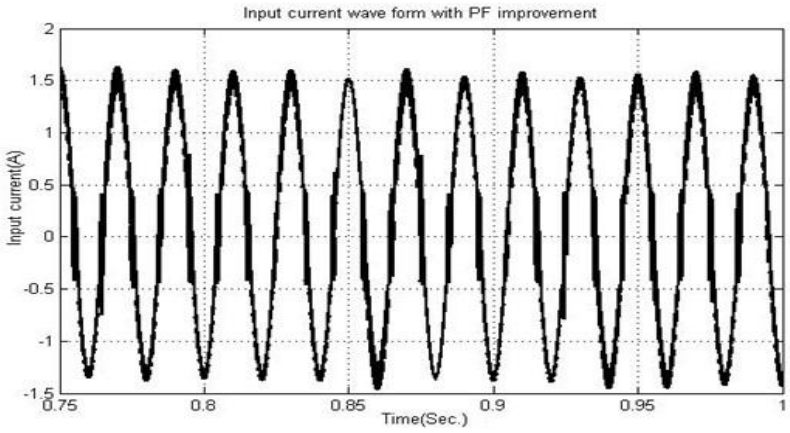

Fig 3.38 Input current waveform of Dual converter drive with PFC circuit

Reference

[3.1] Alan L. Sheldrake, *Handbook of Electrical Engineering* , John Wiley & Sons Ltd, 2003

[3.2] V. K. Mehta and Rohit Mehta, *Principle of Electrical Machines*, S. Chand & Company Limited, 2002.

[3.3] Theodore Wildi, Electrical Machines, *Drives, and Power Systems*, Prentice Hall, 2002.

[3.4] N. Mohan, "*Electric Drives: An integrative approach*", University of Minnesota Printing services, 2000.

[3.5] A. Gelen and S. Ayasun, "Effects of PWM chopper drive on the torque-speed characteristic of DC motor" *43rd International Universities Power Engineering Conference*, 2008.

[3.6] P. S. Bhimbhra, *Power Electronic,* Khanna publishers, 2010.

[3.7] Chin S. Moo, YongnN. Chang, "Harmonic Analysis On 3-Phase Full-Controlled Converter-Fed DC Drives," *IEEE TENCON'93,Proceedings, Computer, Communication, Control and Power Engineering,* Vol. 5, pp. 594-597, Oct. 1993.

[3.8] Zhifang Sun, Hongjie Liu, Kenji and Masaaki Sakui, "DC Harmonic Distortion Minimization in Series Connected Converters with AC Filters under Unbalanced Power Supply," *IEEE International Conference on Power Electronics and Drive Systems,* Vol 2, pp. 1659-1663, 2003.

[3.9] M. Nedeljkovic and Z. Stojiljkovic, "Fast current control for thyristor rectifiers," *IEE Proceedings- Electr. Power Appl.,* Vol. 150, No. 6, pp. 636-638, Nov. 2003.

[3.10] Alfio Consoli, Mario Cacciato, Antonio Testa and Francesco Gennaro, "Single Chip Integration for Motor Drive Converters With Power Factor Capability," *IEEE Transactions on Power Electronics,* Vol. 19, No. 6, pp. 1372-1379, Nov. 2004.

[3.11] K. georgakas and A. Safacas, "Efficiency and Power Factor investigation of Characteristic Converter Topologies via Simulation," *IEEE Proceedings of Internation Conference on Electrical Machines and Systems,* Vol. 2, pp. 1422-1427, Sept. 2005.

[3.12] Manoj Daigavane, Hiralal Suryawanshi and Jawed Khan, "A Novel Three Phase Series-Parallel Resonant Converter Fed DC-Drive System," *Journal of Power Electronics,* Vol. 7, No. 3, pp. 222-232, July 2007.

[3.13] Wai Phyo Anug, "Analysis on Modeling and Simulink of DC Motor and its Driving

System Used for Wheeled Mobile Robot," *World Academy of Science, Engineering and Technology 32*, pp. 299-306, 2007.

[3.14] Y. Varetsky and Z. Hanzelka, "Filter Characteristics in a DC Drive Power Supply System," *IEEE 13th International Conference on Harmonics and Quality Of Power*, pp. 1-6, Oct. 2008.

[3.15] R. Carbone, "A Passive power factor correction technique for single-phase thyristor-based controlled rectifiers," *International Journal of Circuits, Systems and Signal Processing*, Vol. 2, pp. 169-179, 2008.

[3.16] Y. Kusumalatha, Ch. Saibabu and Y. P. Obulesu, "Minimization of Harmonic Distortion of Industrial Motor Drives with Active Power Filter in Paer Mill-a Case Stude," *Proceedings of the International Multi Conference of Engineers and Computer Scientists*, Vol. II, March 2012.

[3.17] S. B. Dewan, "Optimum input and output filters for a single-phase rectifier power supply," *IEEE Trans. Industry Appl.*, vol. IA-17, no. 3, pp. 282-288, 1981.

[3.18] A. R. Prasad, P. D. Ziogas and S. Manias, "A novel Passive wave-shaping method for single phase Diode Rectifiers", *IEEE Trans. on Industrial Electronics*, Vol.37, No.6, pp. 521-530, Dec.1990.

CHAPTER 4

SYSTEM MODELING

The cascade control structure of DC motor is shown in Fig. 4.1 in which power factor correction circuit is included.

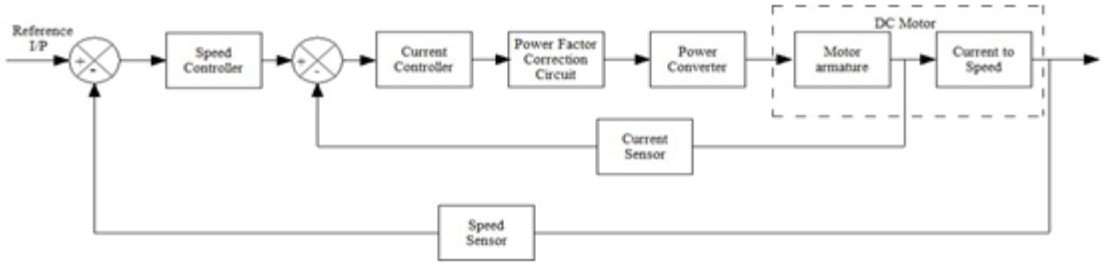

Fig. 4.1 Control block diagram of DC motor speed control with power factor correction

There are mainly five components of this control structure

i. Separately excited DC motor.
ii. Power converter.
iii. Power factor correction circuit.
iv. Current Transmitter.
v. Speed Transmitter.

All the above shown blocks are converted into S-domain to tune the controllers and analyze the control system.

4.1 DC motor modeling

In control system, the DC motors are used in two different control modes:-

- Armature control mode with fixed field current.
- Field control mode with fixed armature current.

Here armature control mode with fixed field current will be considered for analysis, as shown in Fig 4.2.

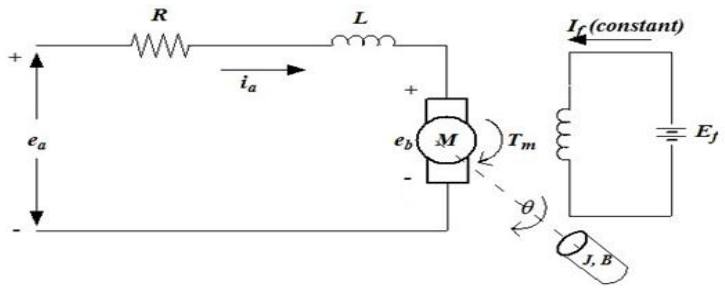

Fig 4.2 Detailed circuit of separately excited DC motor

In the above shown circuit:-

R = resistance of armature (Ω).

L =inductance of armature winding (H).

i_a = armature current (A).

i_f = field current (A).

e_a = applied armature voltage (V)

e_b = back emf (V)

T_m = torque developed by motor (Nm)

θ = angular displacement of motor shaft (rad).

ω = angular speed of motor shaft (rad/sec.)

J = equivalent moment of inertia of motor and load referred to motor shaft (kg-m^2)

B = equivalent friction coefficient of motor and load referred to motor shaft (Nm*s/rad)

In servo applications, the DC motors are generally used in the linear range of magnetization curve. Therefore, the air gap flux ϕ is proportional of field current, i.e.

$$\phi = K_f i_f \tag{4.1}$$

Where K_f is constant.

The torque T_m developed by the motor is proportional to the product of armature current and air gap flux, i.e.

$$T_m = K_1 K_f i_f i_a \tag{4.2}$$

Where K_1 is constant.

In armature controlled DC motor, the field current is kept constant, so

$$T_m = K_T i_a \tag{4.3}$$

Where K_T is known as the motor torque constant.

The motor back emf being proportional to speed is given as

$$e_b = K_b \frac{d\theta}{dt} \tag{4.4}$$

Where K_b is the back emf constant.

The differential equation of the armature circuit is

$$L\frac{di_a}{dt} + Ri_a + e_b - e_a = 0 \tag{4.5}$$

The torque equation is

$$J\frac{d^2\theta}{dt^2} + B\frac{d\theta}{dt} = T_m = K_T i_a \tag{4.6}$$

Taking the laplace transform of equations 4.4, 4.5, and 4.6 assuming initial condition zero.

$$E_b(s) = K_b s\theta(s)$$

$$(Ls + R)I_a(s) = E_a(s) - E_b(s)$$

$$(Js^2 + Bs)\theta(s) = T_m(s) = K_T I_a(s)$$

So the final transfer function will be

$$\frac{\theta(s)}{E_a(s)} = \frac{K_T}{s[(R + sL)(Js + B) + K_T K_b]} \tag{4.7}$$

Or

$$G(s) = \frac{\omega(s)}{E_a(s)} = \frac{K_T}{(R + sL)(Js + B) + K_T K_b} \tag{4.8}$$

Block diagram using equation 4.7 is shown in Fig. 4.3

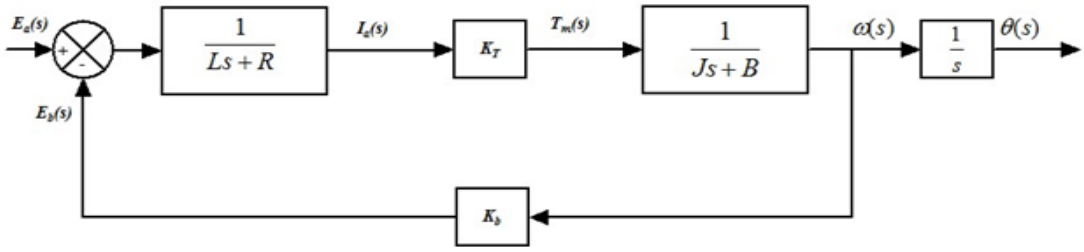

Fig. 4.3 Block diagram of DC drive with controlled output position of rotor

Block diagram using equation 4.8 is shown in Fig. 4.4

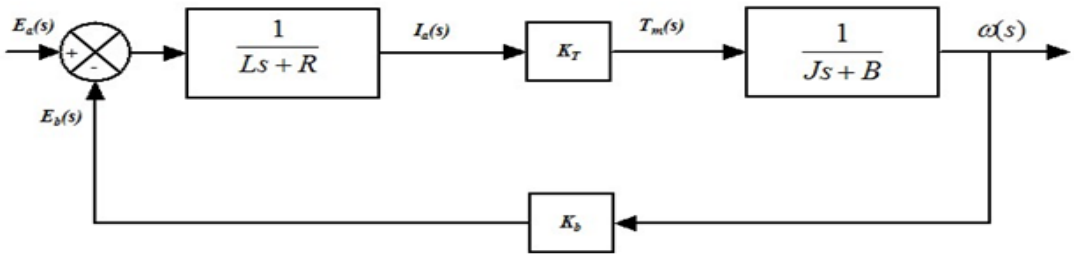

Fig 4.4 Block diagram of DC drive with controlled output speed of rotor

As shown in Fig. 4.3 the controlled output is position of the rotor of the DC drive and in Fig. 4.4 the controlled output is speed of the rotor of the DC drive, so for our further work Fig 4.4 will be considered as the system. The values of the parameters are taken as follows.

R = 2.581 Ω.

L = 0.028 H.

J = 0.003 kg-m^2

B = 0.0005 Nm*s/rad

K_t= 0.0924

K_b= 0.0924

4.2 Converter modeling

A three phase fully controlled AC to DC converter is used to convert the input AC supply into DC which will further fed to the DC drive. The circuit diagram of three phase fully controlled AC to DC converter is shown in Fig. 4.5.

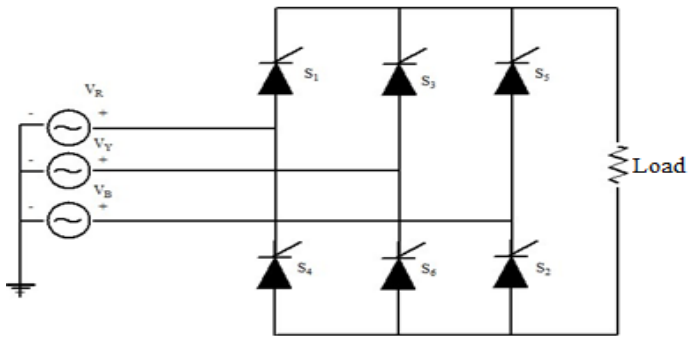

Fig. 4.5 Three phase fully controlled AC to DC converter

As the converter is a 3 phase fully controlled converter, for a typical firing angle $\alpha = 60^{\circ}$, ripple will be six times the fundamental frequency. So the duration of each ripple will be 60°, that is shown in Fig 4.6.

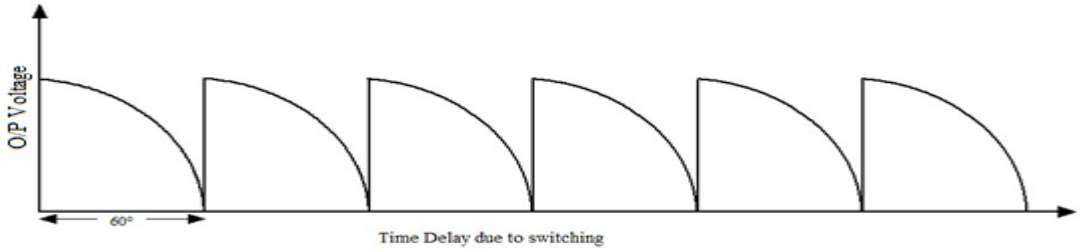

Fig 4.6 Ripples in three phase fully controlled rectifier for firing angle 60°

For 360°, Time period,

$$T = (1/50) = 0.02\text{sec.}$$

For 60°, Time period,

$$T = (0.02*60)/360 = 3.3 \text{ msec.}$$

A change in converter firing angle occurs after every 60°. It's not instantaneous, that means a delay of 3.3 msec will be there. It can have a maximum delay of 3.3 msec. or a minimum of zero.

So, an average of two values is taken to calculate T_r

$$T_r = (3.3+0)/2 = 1.7\text{msec}$$

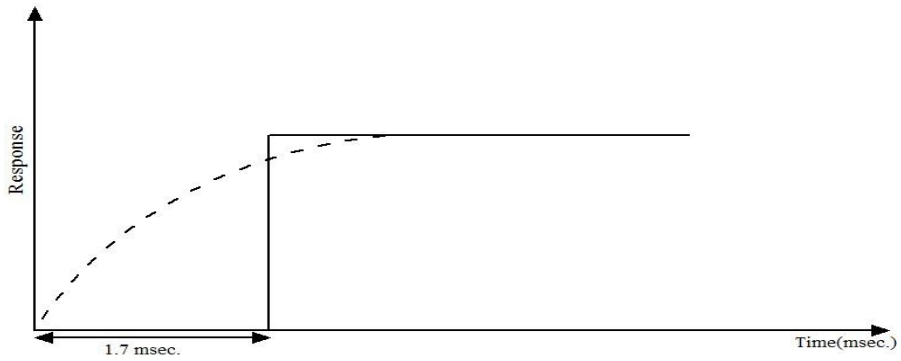

Fig 4.7 First order response of converter

The approximated response of converter is shown in Fig. 4.7. A firing command is given at t=0 ms. but due to lag, firing takes place at 1.7 msec. So this lag can be considered as a first order lag.

So converter can be represented as a first order delay with a gain. Suppose, a +24volt reference is coming from current controller. So if we are using a cosine firing with linear control, maximum output voltage should be obtained.

For a 3 phase converter,

$$\text{Output voltage} = 2*1.70*E_{rms}*\cos\alpha$$

Maximum voltage obtained when $\alpha = 0$.

$$\text{Max. Voltage} = 2*1.70*E_{rms.}$$

Control voltage is 24volt. So, gain will be

$$K_t = (2*1.7*E_{rms})/24$$

$$K_t=(2*1.7*170)/24$$

$$K_t= 24$$

So converter can be represented as first order lag with gain K_t.

$$G_c(s) = \frac{K_t}{1 + sT_r} \tag{4.9}$$

So

$$G_c(s) = \frac{24}{1 + 1.7s} \tag{4.10}$$

4.3 Power Factor correction circuit modeling

Power factor correction circuit is a filter circuit which is used to remove the harmonics from the input current which improve the power factor of the circuit in result. As discussed in chapter 2, there are various filter circuits available, but the improved parallel resonant circuit shown in fig. 2.42 gives the best results in terms of power factor and total harmonic distortion, so that topology is considered. The basic improved parallel resonant circuit is shown in Fig. 4.8.

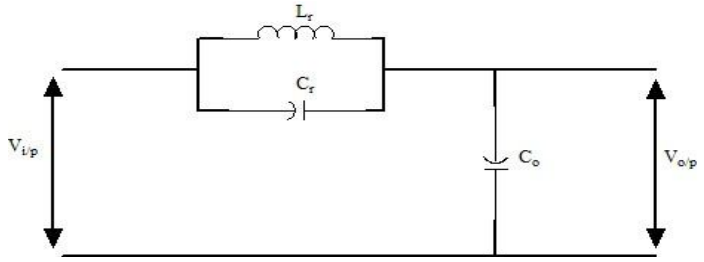

Fig 4.8 Improved parallel resonant circuit

Let

$$Z(s) = sL_r \parallel 1/sC_r$$

$$Z_1(s) = 1/sC_o$$

Applying KCL at output side,

$$\frac{V_{o/p} - V_{i/p}}{Z(s)} + \frac{V_{o/p}}{Z_1(s)} = 0$$

$$\frac{V_{o/p}}{V_{i/p}} = \frac{Z_1(s)}{Z(s) - Z_1(s)} \tag{4.11}$$

After putting the value of Z(s) & $Z_1(s)$ in equation 4.11,

$$\frac{V_{o/p}}{V_{i/p}} = \frac{s^2 L_r C_r + 1}{s^2 C_o L_r + s^2 L_r C_r + 1} \tag{4.12}$$

By putting the value of L_r, C_r and C_o from chapter 3 in equation 4.12, we get the T.F. of PFC circuit,

$$\frac{V_{o/p}}{V_{i/p}} = \frac{s^2 1.12 * 10^{-6} + 1}{s^2 5.12 * 10^{-6} + 1} \tag{4.13}$$

4.4 Current Sensor

Current sensor senses the armature current and transmits that current back to the system for error calculation. There are mainly two desirable properties of a current sensor:

i. It should reduce the high frequency ripple generated by the armature circuit.
ii. It should be able to bring the signal to the controller level.

Considering gain as K_1 and a low pass filter to remove the ripple of the armature current having T.F. $\frac{1}{1+\tau_1 s}$, the current sensor can be represented as a first order low pass filter, having transfer function

$$G_1(s) = \frac{K_1}{1 + \tau_1 s} \tag{4.14}$$

The value of K_1 and τ_1 can be selected by the user as per the requirement of the control system. By putting the value of K_1 and τ_1 in equation 4.14 we get the transfer function of current sensor as

$$G_1(s) = \frac{0.83}{1 + 3.5s} \tag{4.15}$$

4.5 Speed Sensor

Speed sensor sense the speed of the rotor and transmit that speed to the system for calculating the error so that error can be transmitted to the controller. There are mainly two desirable properties of a speed sensor,

i. It should remove the high frequency mechanical ripple generated by the rotor.
ii. It should be able to bring the speed signal to the controller level.

Considering gain as K_2 and a low pass filter to remove the ripple of rotor speed having T.F. $\frac{1}{1+\tau_2 s}$ .The speed sensor can be represented as a first order low pass filter and as speed sensor is used in outer loop in cascade control so its time constant should be greater than current sensor so transfer function of speed sensor will be

$$G_1(s) = \frac{K_2}{1 + \tau_2 s} \tag{4.16}$$

The value of K_2 and $\tau_2$can be selected by the user as per the requirement of the control system. By putting the value of $K_2$and $\tau_2$in equation 4.16 we get the transfer function of speed sensor,

$$G_1(s) = \frac{1}{1 + 25s} \tag{4.17}$$

Final control block diagram with all the subsystem transfer functions is shown in Fig 4.9.

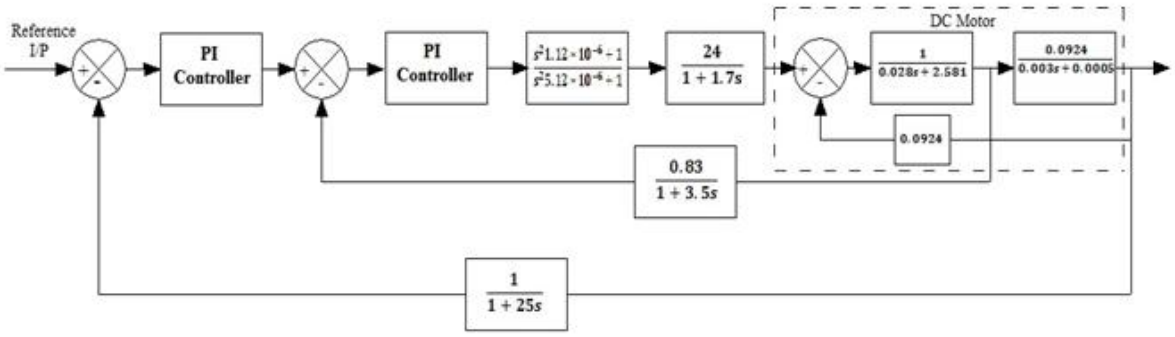

Fig 4.9 Final cascade control block diagram with transfer functions

CHAPTER 5

CONTROL SYSTEM & ITS DESIGNING

Control system engineers are responsible to control a part of an environment known as a system or plant to produce desired products for society. The prior knowledge of system always played an important role in effective controlling. A control engineer should have the knowledge of different engineering principles like electrical, mechanical, and chemical etc.

Control system can be categorized as open-loop or close-loop feedback control and feedback control systems can be further classified a single-input-single-output (SISO) or multiple-input-multiple-output (MIMO), commonly known as multivariable system [5.1].

5.1 Open –loop control system

An open-loop control system is designed to meet the desired output by using a reference signal that operates the actuators that directly control the process output. Output feedback is not present in this type of system. Figure 5.1 below shows the general structure of an open loop control system.

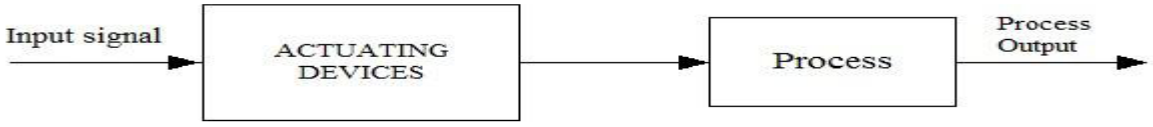

Fig 5.1 Open loop control system

5.2 Closed –loop control system

In closed loop control systems the difference of actual output and the desired output is fed back to the controller to achieve the desired output. Fig. 5.2 shows the general structure of closed loop control system.

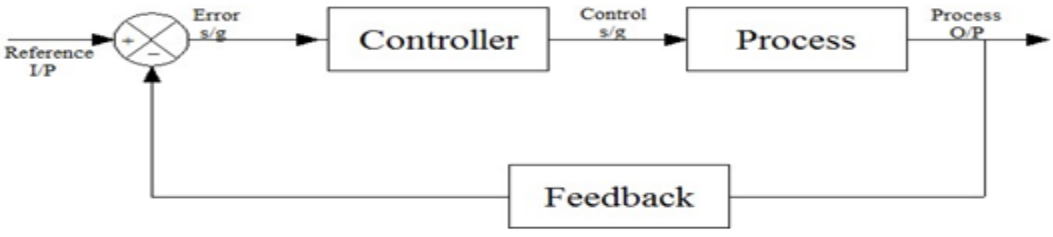

Fig 5.2 Closed loop control system

5.3 Types of control structures

There are various types of control structures are available, selection of control structure is very important. Some of control structures are listed below and further discussed with their respective advantages and disadvantages.

i. Feedback control structure
ii. Feedforward control structure
iii. Feedback + Feedforward control structure
iv. Cascade control structure

5.3.1 Feedback control structure

Feedback control is a mechanism which regulates the controlled variable by taking negative feedback from the output and taking regulatory action through the controller and changing the manipulated variable accordingly. Feedback control strategy is shown in Fig. 5.3.

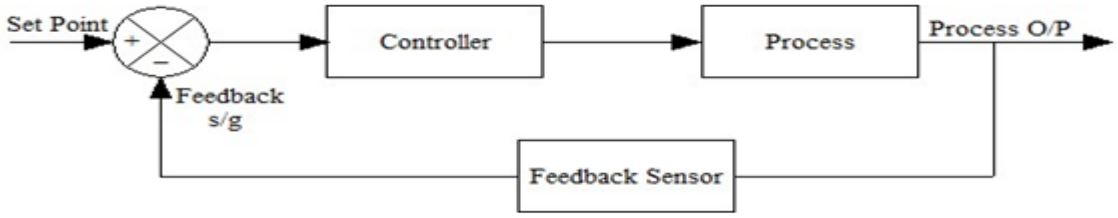

Fig 5.3 Feedback control structure

5.3.2 Feedforward control structure

The basic concept of the feed forward controller is to measure the disturbances and take corrective action before the disturbance upset the process that means the corrective action will takes place before the error occurred which is shown in Fig.5.4.

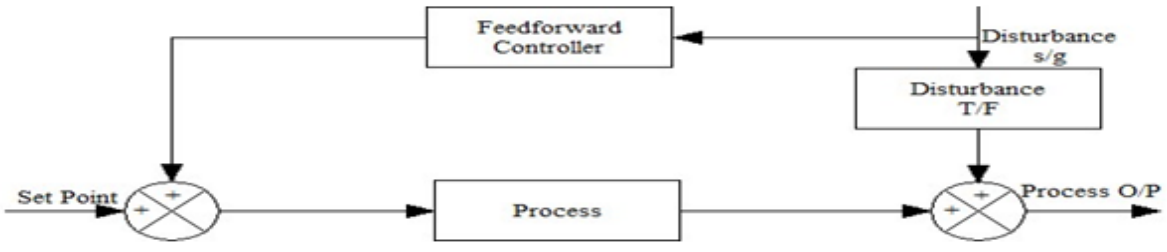

Fig. 5.4 Feedforward control structure

5.3.3 Feedback + Feedforward control structure

In some systems the disturbance can be predicated there feedforward structure gives good result but in a process some unknown sources of disturbances are always there so for that kind of systems only feedforward structure is not sufficient, for that one should use feedback structure with feedforward structure which is shown in Fig. 5.5. By using feedforward structure with feedback structure user get the advantages of both type of structure.

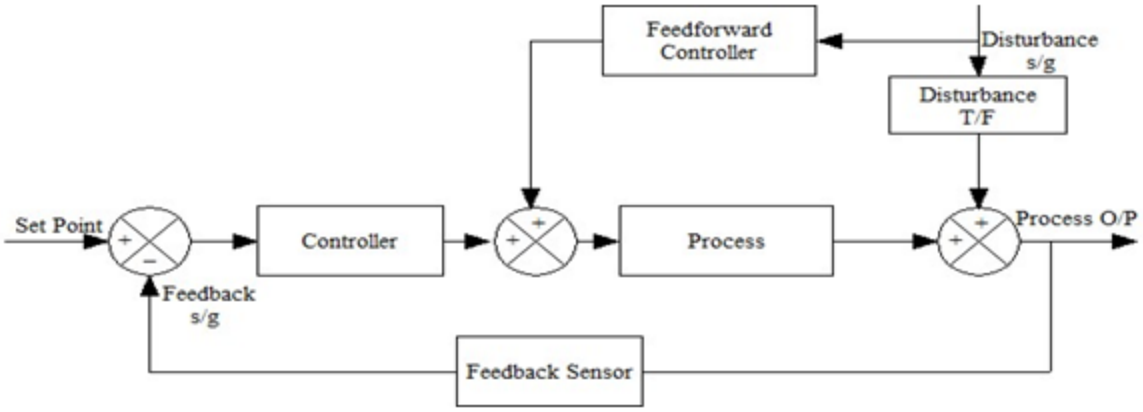

Fig. 5.5 Feedback + Feedforward control structure

5.3.4 Cascade control structure

In a cascade control which is shown in Fig. 5.6, there are two or more controllers of which one controller's output drives the set point of another controller. The controller driving the set point is called the primary, outer, or master controller. The controller receiving the set point is called the secondary, inner or slave controller. Cascade control is beneficial only if the dynamics of the inner loop are fast compared to those of the outer loop.

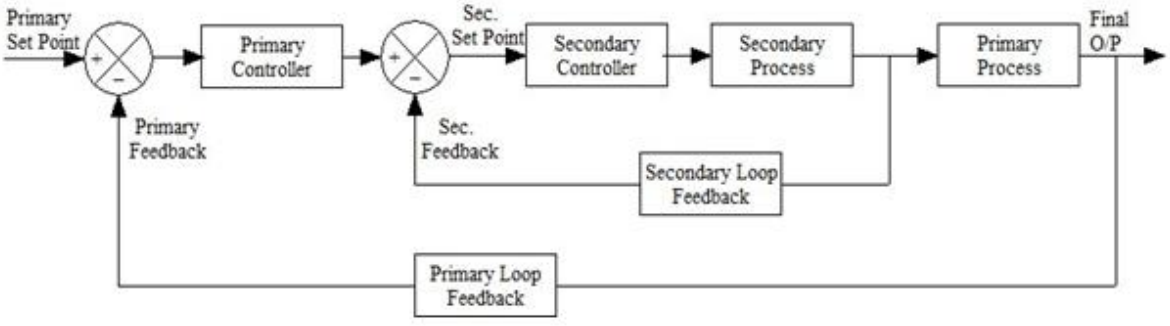

Fig. 5.6 Cascade control structure

5.4 Literature Review

Hans Butler et.al, presented an adaptive time-optimal controller for a direct-drive DC motor with the design based on model reference adaptive approach. Application of model reference adaptive control to a real direct-drive DC motor has proved successful and the controller guarantees approximate time-optimal behavior of motor if a step input is applied, independent of the load inertia and the magnitude of the step input [5.2].

Bor-Ren Lin discussed power converter control based on neural and fuzzy methods. In this paper the proposed fuzzy logic compensator is used to prevent voltage drop from nonlinear loads. The total harmonics distortion of proposed scheme is better than that of conventional controller [5.3].

Samir Mehta et.al, presented a paper in which the control problem for a series DC motor is considered , based on a nonlinear mathematical model of a series-connected DC motor. It is shown that the combination of a nonlinear transformation and state feedback reduces the nonlinear control design to linear control design [5.4].

Robert D. Lorenz discussed advances in electric drive control which have shown significant practical advantages over the previously existing technology include physics-based state variable controls design, state observer design for sensor replacement, disturbance input decoupling design, self sensing (sensorless) control, fuzzy logic and structured neural networks, and also the design methods underlying their use [5.5].

Franceso Cupertino et.al, presented paper which deals with the design of fuzzy logic-based Controllers (FLBC) for DC and AC electric drives. Industrial drives employ the cascaded PI control with a subordinated current control loop to make sure that the current does not exceed the admissible value and improve dynamic performances. The nonlinear FLBC characteristics permit one to achieve the performances of the cascaded control using only one control loop, and also authors propose a minimum number of rules and the criteria, based on physical considerations, to determine he input and output gains instead of using the trial and error procedure [5.6].

Manafeddin Namazov et.al, presents the design of a fuzzy control system to control the position of a DC motor. The motor was modeled and converted to a subsystem in Simulink.

First, a crisp proportional-derivative (PD) controller was designed and tuned using a Simulink block instead of conventional tuning methods such as hand-tuning or Ziegler-Nichols frequency response method. Then a fuzzy proportional-derivative (FPD) controller was designed and system responses of FPDs with different defuzzification methods were investigated. A disturbance signal was also applied to the input of the control system. FPD controller succeeded to reject the disturbance signal without further tuning of the parameters whereby crisp PD controller failed [5.7].

M. Nasir Uddin presents an adaptive-filter-based torque ripple minimization (TRM) of a fuzzy-logic controller (FLC) for speed control of an interior permanent magnet (IPM) motor drive. A simple and effective first-order digital infinite impulse response filter is utilized to reduce the torque ripples introduced by the FLC. The gain of the filter is adapted online based on the magnitude of the torque ripple. The optimal position of the filter in the complete drive is also determined for effective TRM [5.8].

5.5 PI controller

PI Controller (proportional-integral controller) is a feedback controller which drives the plant to be controlled by a weighted sum of the error (difference between the output and desired set-point) and the integral of that value which is given by eq. 5.1. It is a special case of the PID controller in which the derivative (D) part of the error is not used. Integral control action added to the proportional controller converts the original system into high order. Hence the control system may become unstable for a large value of K_P since roots of the characteristic eqn. may have positive real part. In this control, proportional control action tends to stabilize the system, while the integral control action tends to eliminate or reduce steady-state error in response to various inputs.

$$G_{PI}(s) = K_p + \frac{K_i}{s} \tag{5.1}$$

A proportional controller (K_P) will have the effect of reducing the rise time, but never eliminate the steady-state error. An integral control (K_i) will have the effect of eliminating the steady-state error, but it may make the transient response worse. A derivative control (K_d) will have the effect of increasing the stability of the system, reducing the overshoot,

and improving the transient response. Effects of each of controllers K_P,K_d, and K_i on a closed-loop system are shown in the table 5.1 [5.9].

Table 5.1Effects of independent P, I and D tuning

Controller Response	**Rise Time**	**Overshoot**	**Settling Time**	**Steady State Error**	**Stability**
Increasing K_P	Decrease	Increase	Small Increases	Decrease	Degrade
Increasing K_i	Small Decrease	Increase	Increase	Large Decrease	Degrade
Increasing K_d	Small Decrease	Decrease	Decrease	Minor Change	Improve

The above shown correlations may not be exactly accurate, because K_P, K_i, and K_d are dependent on each other. In fact, changing one of these variables can change the effect of the other two. For this reason, the table should only be used as a reference to determining the values for K_P, K_i and K_d.

5.6 Tuning of Controller

Here in this research work PI controller is used for both the loops i.e. the inner loop and outer loop. Closed loop oscillation based PI tuning method is a popular method of tuning PI controller. In this type of tuning method, a critical gain K_{cu} is introduced in the forward path of the control system. The high value of the gain takes the system to the verge of instability, at this stage system is said to be marginally stable so it creates oscillatory response, from that oscillatory response the value of frequency and time can be calculated. For this work Zeigler-Nichols tuning method is used for both the controllers. Table 5.2 gives the different experimental tuning rules based on closed loop oscillation method [5.10].

Table 5.2 Different closed loop oscillation based tuning methods

Type of tuning method	Kp	T_i	T_d
Zeigler-Nichols	$0.4K_{cu}$	$0.8T_c$	----
Tyreus-Luyben	$K_{cu}/3.2$	$2.2*T_c$	----
Shinkey	$K_{cu}/2$	$T_c/2.2$	----

5.6.1 Tuning of current controller

Current loop is the inner loop of our cascade control structure, so for this loop controller should be tuned first. Fig. 5.7 shows the inner current loop of the cascade control structure.

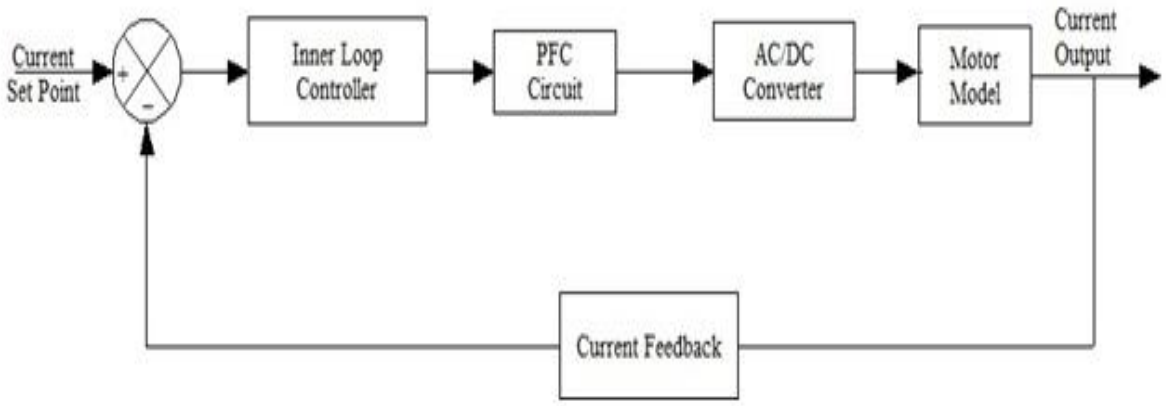

Fig. 5.7 Inner loop of cascade control structure

The current controller which is PI controller is get tuned using Zeigler-Nichols tuning method for that the value of Kp and K_i are respectively 0.10184 and 0.021132. The step response of current loop for above mentioned values of K_p and K_i is shown below in Fig. 5.8 in which the response have no overshoot and settling time is very less which is required in cascade control as it is inner loop of the cascade structure.

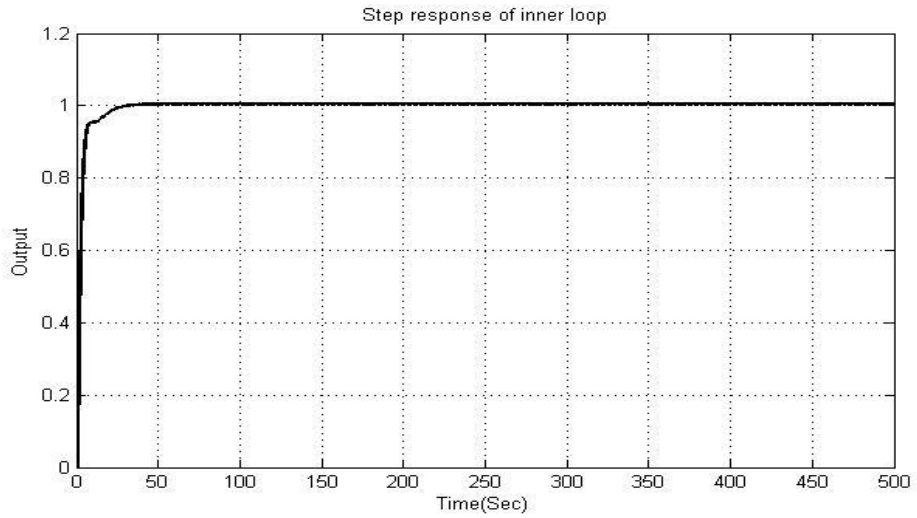

Fig. 5.8 Step response of inner loop

5.6.2 Tuning of speed controller

In the above section the inner loop of cascade structure which is current loop is tuned, now the whole inner loop including controller will be replaced by it's transfer function which is shown in Fig 5.9.

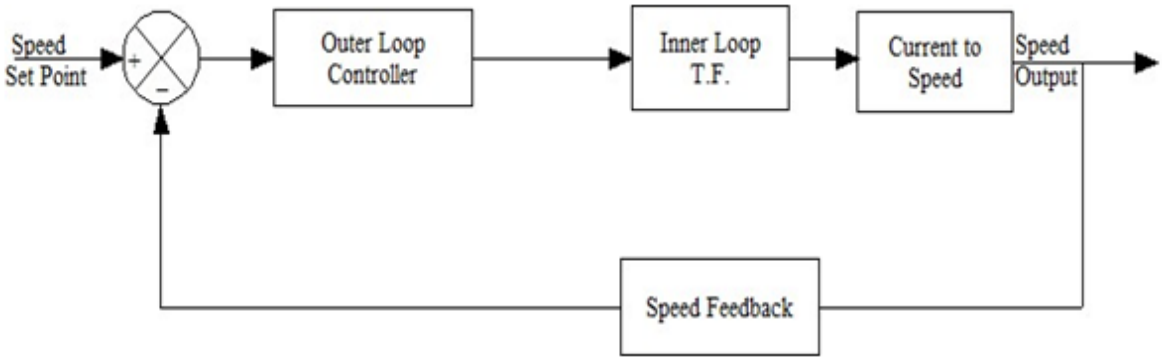

Fig. 5.9 Outer loop of cascade control structure

In this research work PI controller is used for speed control loop which is primary controlling quantity. The speed controller is get tuned using Zeigler-Nichols tuning method for that the value of Kp and K_i are respectively 0.018 and .0003. The step response of current loop for above mentioned values of K_p and K_i is shown below in Fig. 5.10.

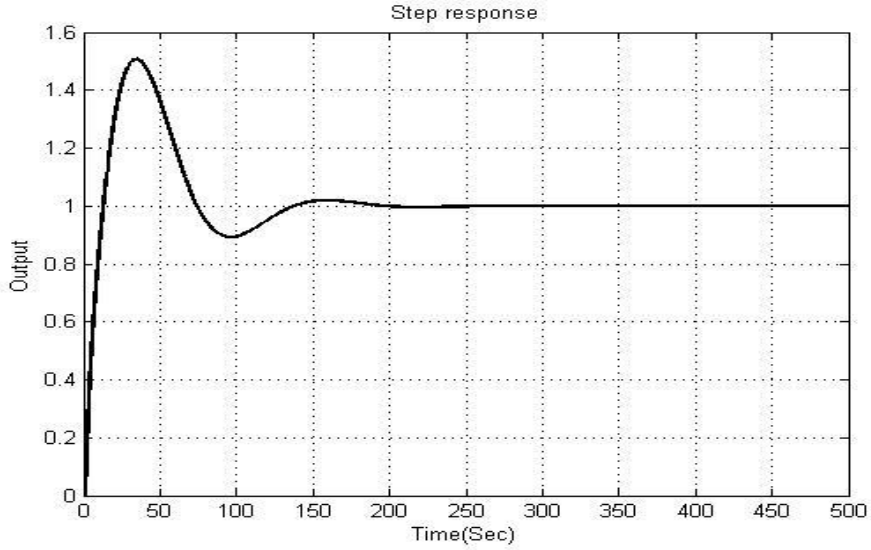

Fig. 5.10 Step response of outer loop of cascade control structure

5.7 Fuzzy Based Controller

The fuzzy logic controller provides an algorithm, which converts the expert knowledge into an automatic control strategy. Fuzzy logic is capable of handling approximate information in a systematic way and therefore it is suited for controlling non linear systems and is used for modeling complex systems, where an inexact model exists or systems where ambiguity or vagueness is common. The fuzzy control systems are rule-based systems in which a set of fuzzy rules represent a control decision mechanism for adjusting the effects of certain system stimuli. With an effective rule base, the fuzzy control systems can replace a skilled human operator. The rule base reflects the human expert knowledge, expressed as linguistic variables, while the membership functions represent expert interpretation of those variables.

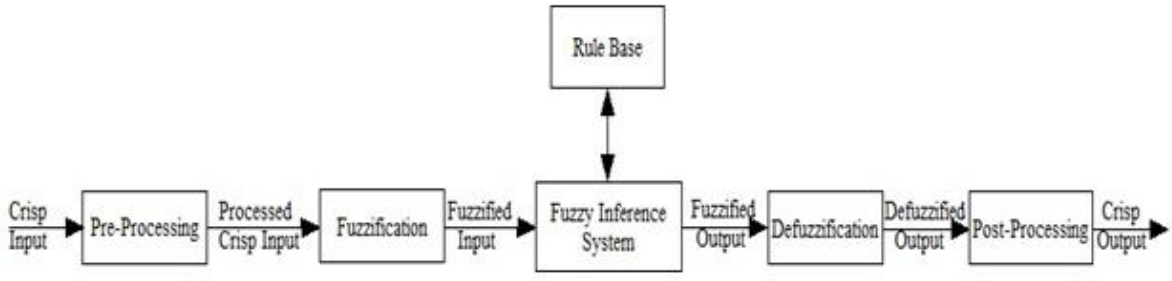

Fig. 5.11 Block diagram of fuzzy control system

Figure 5.11 shows the block diagram of fuzzy control system. The crisp inputs are supplied to the input side fuzzification unit. The fuzzification unit converts the crisp input in to fuzzy variable. The fuzzy variables are then passed through the fuzzy rule base. The fuzzy rule base computes the input according to the rules and gives the output. The output is then passed through defuzzification unit where the fuzzy output is converted to crisp output.

5.7.1 Tuning of Fuzzy Logic Controller

Seema Chopra et.al, proposed a method for tuning of fuzzy PI controller. The input scaling factors are tuned online by gain updating factor whose values are determined by fuzzy rule base [5.11]. Seema chopra et.al have proposed a neural network tuned fuzzy controller for MIMO systems from the given set of input and output data. An appropriate coupling tuned fuzzy controller is incorporated to control MIMO system to compensate for the dynamics of coupling [5.12].

5.7.2 Scaling Factor in Fuzzy Logic Controller

Scaling factor in a fuzzy logic controller is very important. Selection of suitable values for scaling factors are made based on the knowledge about the process to be controlled and sometimes through trial and error to achieve the best possible control performance. This is so because, unlike conventional non-fuzzy controllers to date, there is no well-defined method for good setting of scaling factors for fuzzy logic controllers. But the scaling factors are the main parameters used for tuning the fuzzy logic controller because changing the scaling factors changes the normalized universe of discourse, the domains, and the membership functions of input /output variables of fuzzy logic controller.

5.7.3 Fuzzy PI controller

Fig. 5.12 shows that how fuzzy PI controller can be used in cascade control strategy, as shown in figure that fuzzy PI controller is used in outer loop which is primary loop not in secondary loop. The secondary loop should be fast which is the basic requirement of cascade control structure and fuzzy PI controller takes much time as compared to conventional controller depending on the number of rules, so it is better to use fuzzy controller in outer loop which is slower one.

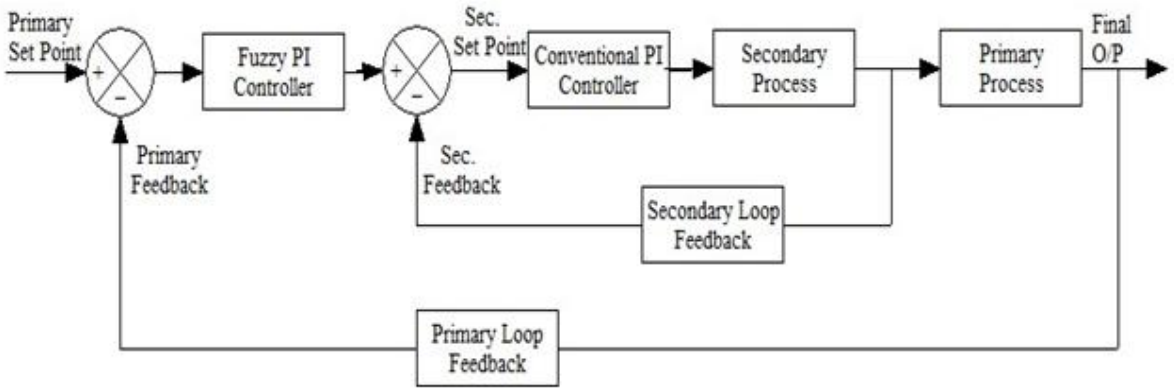

Fig. 5.12 Fuzzy PI controller with cascade control structure

Fig. 5.13 shows the fuzzy inference system developed for fuzzy controller which is similar to the Fig. 5.11.

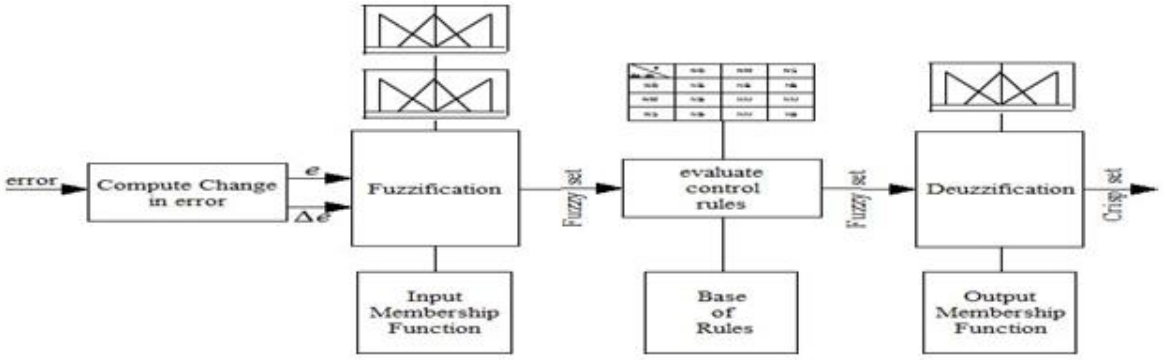

Fig. 5.13 Fuzzy inference system for fuzzy controller

Fig. 5.14 shows the structure of fuzzy logic controller, which keeps the general architecture of PI controller with some slight modifications. A mamdani based fuzzy inference system is implemented in between proportional and derivative term. The integral term is then cascaded to the output of fuzzy inference system.

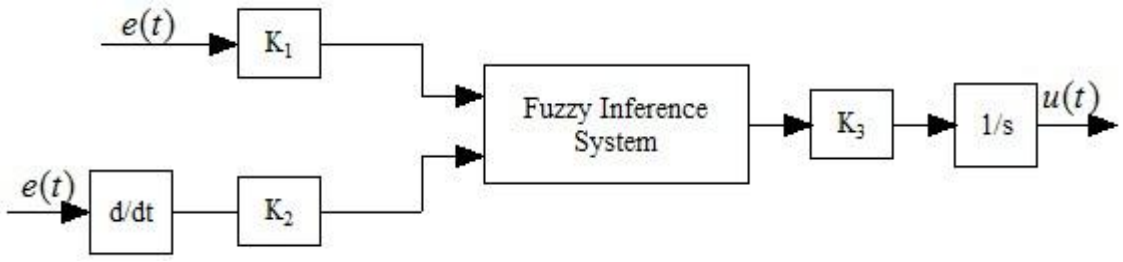

Fig. 5.14 Structure of fuzzy PI controller

K_1 and K_2 are scaling factors for the input where as K_3 is the scaling factor for the output. In this design the input and output scaling factors are determined by trial and error methods and are taken very small. The mamdani based fuzzy inference system uses linear membership function for both inputs and outputs. The ranges of the values are normalized between -1 to 1. Fig. 5.15 shows the membership functions for the inputs i.e. error and change in error and output which is controlling signal.

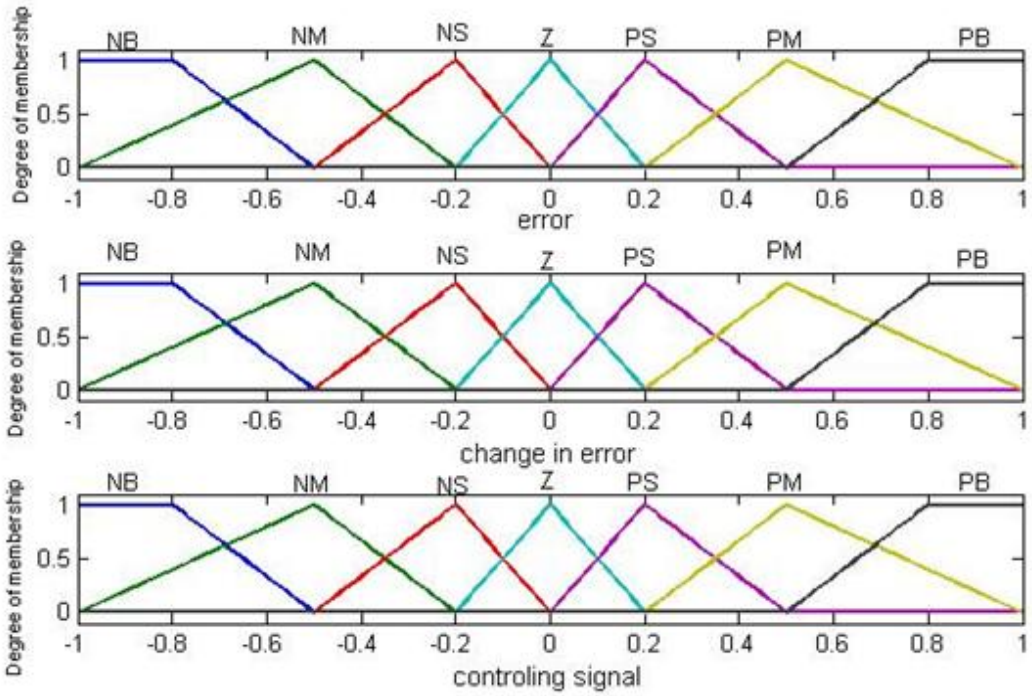

Fig. 5.15 Membership functions for inputs and output

The linguistic variables used in the membership functions are described in Table 5.3.

Table 5.3 Linguistic variables in fuzzy inference system

Error		**Change in error**		**Controlling Signal**	
NB	Negative Big	NB	Negative Big	NB	Negative Big
NM	Negative Medium	NM	Negative Medium	NM	Negative Medium
NS	Negative Small	NS	Negative Small	NS	Negative Small
Z	Zero	Z	Zero	Z	Zero
PS	Positive Small	PS	Positive Small	PS	Positive Small

PM	Positive Medium	PM	Positive Medium	PM	Positive Medium
PB	Positive Big	PB	Positive Big	PB	Positive Big

In mamdani based fuzzy inference system IF-THEN rules are created. The IF-THEN rules of mamdani type fuzzy inference system is summarized in Table 5.4.

Table 5.4 IF-THEN rules for fuzzy inference system

e / de/dt	NB	NM	NS	Z	PS	PM	PB
NB	NB	NB	NB	NB	NM	NS	Z
NM	NB	NM	NM	NM	NS	Z	PS
NS	NB	NM	NS	NS	Z	PS	PM
Z	NB	NM	NS	Z	PS	PS	PB
PS	NM	NS	Z	PS	PS	PM	PB
PM	NS	Z	PS	PM	PB	PM	PB
PB	Z	PS	PM	PB	PB	PB	PB

5.8 Simulation Results

Simulink model realization of cascade structured DC motor control is shown in Fig. 5.16 in which power factor correction circuit is not included.

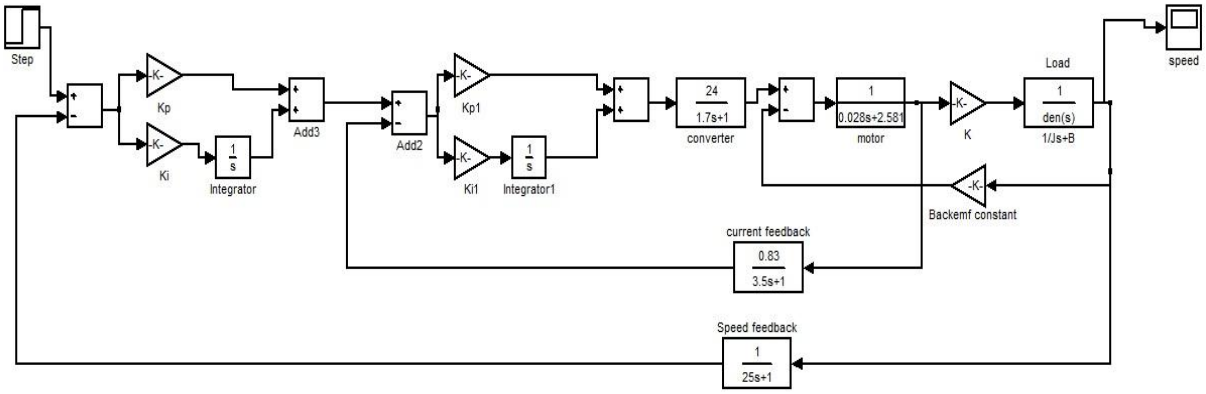

Fig. 5.16 Simulink model of DC motor control without PFC

The controller parameters are shown in Table 5.5.

Table 5.5 Parameters values of controller without PFC

Controller	K_p	K_i
Inner Loop Controller	0.10184	0.021132
Outer Loop Controller	0.018	0.0003

Fig. 5.17 shows the pulse response of cascade structured DC motor control model without power factor correction circuit.

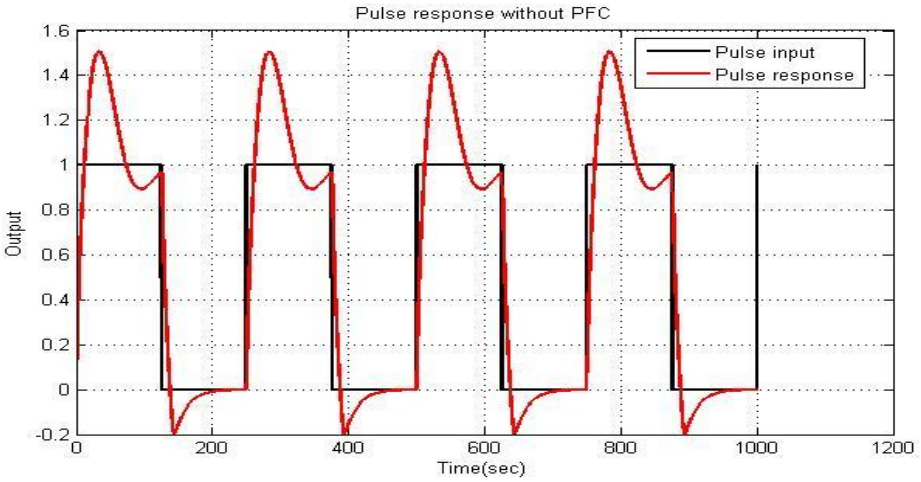

Fig. 5.17 Pulse response of controller without PFC

Simulink model realization of cascade structured DC motor control is shown in Fig. 5.18 with power factor correction circuit.

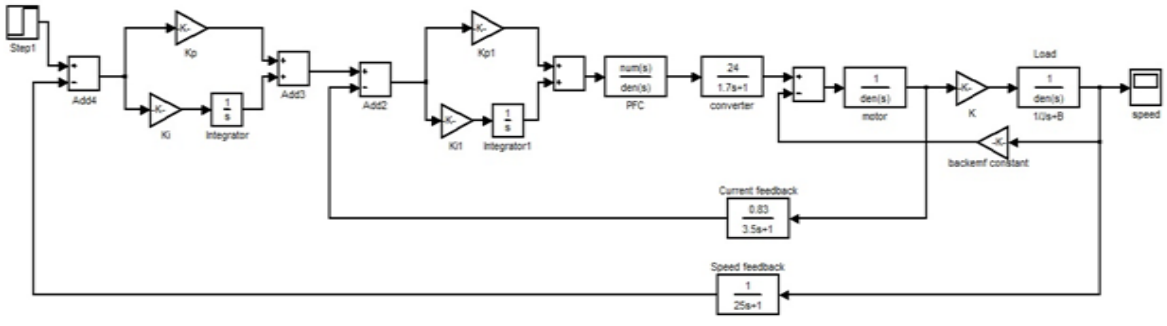

Fig. 5.18 Simulink model of DC motor control with PFC

The controller parameters are shown in Table 5.6.

Table 5.6 Parameters values of controller with PFC

Controller	**K_p**	**K_i**
Inner Loop Controller	0.10184	0.021132
Outer Loop Controller	0.015	0.0002

Fig. 5.19 shows the pulse response of cascade structured DC motor control model with power factor correction circuit.

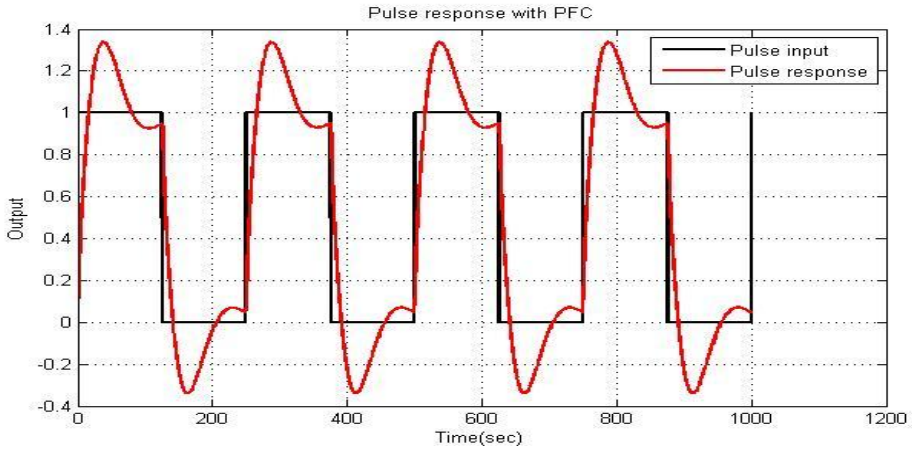

Fig. 5.19 Pulse response of controller with PFC

Simulink model realization of cascade structured Fuzzy PI DC motor control is shown in Fig. 5.20 with power factor correction circuit.

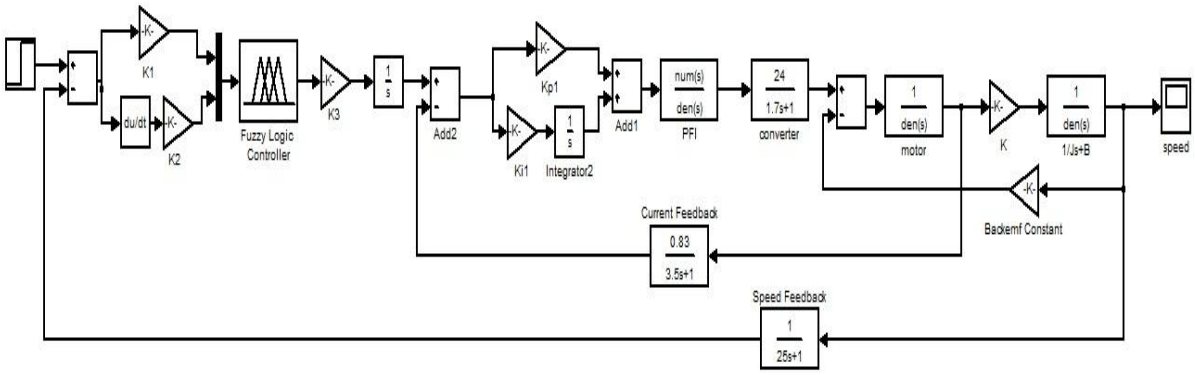

Fig. 5.20 Simulink model of Fuzzy PI DC motor control with PFC

Step response of cascade control structure having fuzzy PI controller with scaling factor K_1= 0.02, K_2= 0.01 and K_3= 0.001taking all above tabulated 49 rules in consideration is shown in Fig. 5.21.

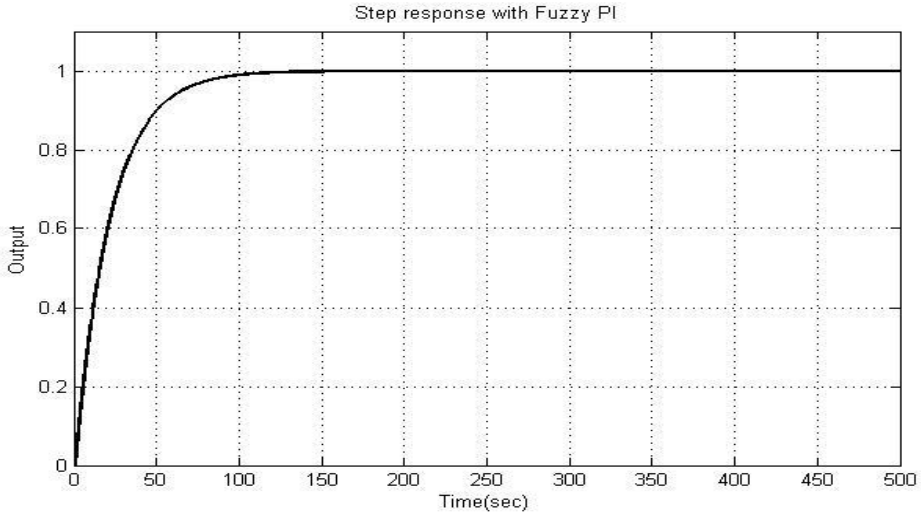

Fig. 5.21 Step response with fuzzy PI controller

References

[5.1] Dorf, Richard C. and Robert H. Bishop, *Modern Control Systems*, 9th ed., Prentice–Hall Inc., New Jersey-07458, USA, 2001.

[5.2] Hans Butler, Ger Honderd, Job van Amerongen, "Model Reference Adaptive Controlof a Direct-Drive DC Motor", *IEEE Control Systems Magazine,* 1989.

[5.3] Bor-Ren Lin, "Power Converter Control Based on Neural and Fuzzy methods", *Electric Power Systems Research 35*, pp.193-206, 1995.

[5.4] Samir Mehta, John Chiasson, "Nonlinear Control of Series DC Motor: Theory and Experiment", *IEEE Transactions on Industrial Electronics,* Vol. 45, No.1, February 1998.

[5.5] Robert D. Lorenz, "Advances in Electric Drive Control", *IEEE,* 1999.

[5.6] Francesco Cupertino, Annamaria Lattanzi, Luigi Salvatore, "A New Fuzzy Logic-Based Controller Design Method for DC and AC Impressed-Voltage

Drives", *IEEE Transactions on Power Electronics,* Vol. 15, No.6, November 2000.

[5.7] Manafeddin Namazov, Onur Basturk, "DC Motor Position Control Using Fuzzy Proportional-Derivative Controllers with Different Defuzzification methods", *TJFS: Turkish Journal of Fuzzy Systems,* Vol.1, No.1, pp.36-54, 2010.

[5.8] M. Nasir Uddin, "An Adaptive-Filter-Based Torque-Ripple Minimization of Fuzzy-Logic Controller for Speed Control of IPM Motor Drives*", IEEE Transactions on Industry Applications*, Vol.47, No.1, January 2011.

[5.9] Ang, K.H. and Chong, G.C.Y. and Li, Y. "PID control system analysis, design, and technology," *IEEE Transactions on Control Systems Technology* 13(4):pp. 559-576, 2005.

[5.10] A.B. Corripio, *Tuning of Industrial Control Systems*, Instrument Society of America, 1990.

[5.11] Seema Chopra, R Mitra and Vijay Kumar, "A robust scheme for tuning of fuzzy PI type controller," *3rd International IEEE Conference Intelligent Systems*, pp. 300-305, 2006.

[5.12] Seema Chopra, R Mitra and Vijay Kumar, "Neural network tuned fuzzy controller for MIMO system," *International Journal of Computer Systems Science and Engineering*, vol. 2, issue 1, pp. 78-85, 2007.

CHAPTER 6

RESULT AND DISCUSSION

In chapter 2 different filter topologies for power factor improvement are designed and implemented, their various parameters are compared from Table 6.1 it is observed that single phase diode rectifier circuit with improved parallel input resonant filter performs well in terms of all compared parameters.

Table 6.1 Values of all the compared parameters with their respective topologies

Topology	PF	DF	CDF	HF	THD
Conventional	0.991	0.999	0.992	0.123	0.033
With filter capacitor	0.215	0.999	0.215	4.527	176.9
With LC filter	0.362	0.967	0.375	2.471	84.09
With parallel i/p resonant filter	0.592	0.919	0.644	1.186	23.39
With series i/p resonant filter	0.64	0.953	0.679	1.08	10.12
With improved i/p resonant filter	0.931	0.999	0.94	0.36	5.591

Now best performed filter topology which improved parallel input resonant filter is implemented with different types of DC motor control strategies i.e. single phase half wave converter drives, single phase semiconverter drives, single phase full converter drives, single phase dual converter drives and improved results in terms of power factor and total harmonic distortion which are shown in Table 6.2.

Table 6.2 Comparision of PF and %THD for different drives

Type	Firing angle	PF	% THD	Improved PF	Improved %THD	% improvement PF	% Improvement THD
Half wave converter	89	0.42	104.8	0.78	11.24	85	89
Semi converter	89	0.43	56	0.71	4.08	65	92
Full wave	89	0.37	38.96	0.68	3.6	83	90

converter							
Dual converter	89	0.61	65	0.99	10.73	62	84

Table 6.3 shows the linear operating ranges for different DC drives with various firing angle which will be very useful to select the correct DC drive as per need.

Table 6.3 Linear operating range of Load torque for different converter drives and firing angles

	Load Torque(N.m)		
Type of converter Firing angle	**Half wave Drive**	**Semiconverter Drive**	**Full wave converter Drive**
0	100 to 180	60 to 180	85 to 180
18	105 to 180	65 to 180	100 to 180
36	110 to 180	80 to 180	110 to 180
54	115 to 180	100 to 180	115 to 180
72	120 to 180	80 to 180	120 to 180
89	130 to 180	100 to 180	120 to 180

In chapter 5 current controller and speed controller are designed and implemented with cascade control structure with and without power factor correction topology which is designed in chapter2 but in both the cases the values of overshoot, rising time, time delay and steady state error are not satisfactory so we went for fuzzy based controller as fuzzy base controller takes more time because of fuzzification and defuzzyfication and the inner loop of cascade control structure should be fast so fuzzy controller cannot be used in inner loop, it should be used in outer loop. Fuzzy based cascade control structure performs well as compared to conventional controller which is shown in Fig. 6.1 and its compared parameters are shown in Table 6.4.

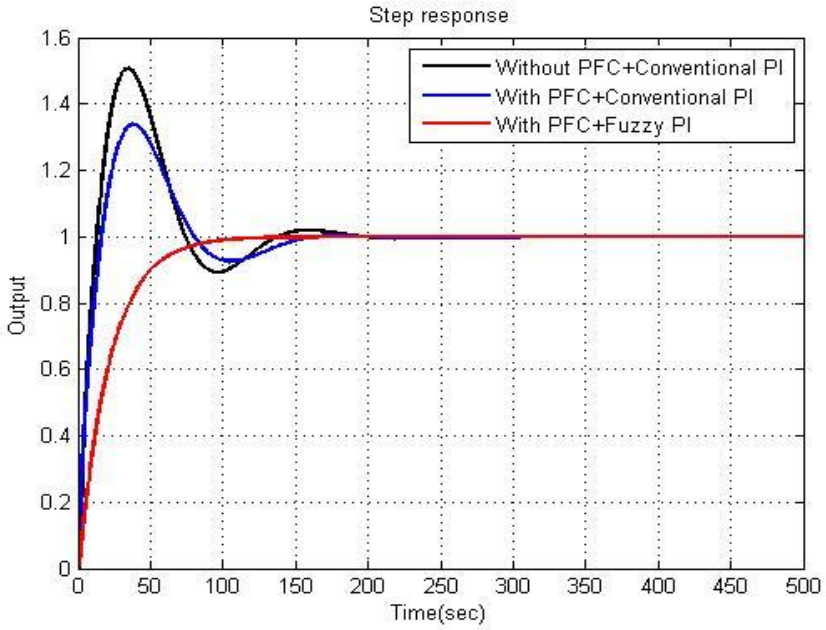

Fig. 6.1 Step response of different controllers

Table 6.4 Value of time domain parameters for different controllers

Parameters	Without PFC	With PFC	With Fuzzy PI
Maximum overshoot(%)	50.7567	30.1238	0.0
Rise time	13.1325	14.4112	90.50
Peak time	34.4908	38.1086	120
Delay time	5.3310	5.6360	10.02
Settling time	170.8280	160.52	120

From Table 6.4 gives a comparative analysis of peak overshoot, rise time, delay time, and settling time of different controllers designed to control the speed of DC motor. The conventional PI controller without PFC gives the 50% peak overshoot and 170.82 sec settling time. The peak overshoot is in a higher side on the other hand conventional PI controller with PFC gives 30% peak overshoot and 160.52 sec settling time which is on the lower side as compared the without PFC conventional PI controller but yet not satisfactory. To further reduce the peak overshoot and settling time fuzzy based controller was designed for which peak overshoot is 0% (no overshoot) and settling time reduced to 120 sec. So it

can be concluded that fuzzy controller gives the better results as compared to conventional controllers with and without PFC when a unit step input is applied and controller are evaluated in terms of peak overshoot, rise time, delay time, and settling time.

A performance index is a quantitative measure of the performance of a system and is chosen so that emphasis is given to the important system specifications. A system is considered an optimum control system when the system parameters are adjusted so that the index reaches an extreme, commonly a minimum value. To be useful a performance index must be a number that is always positive or zero. Then the best system is defined as the system that minimizes the index.

There are different performance indices of a control system and most common performance Indices are IAE (integral absolute error), ISE (integral square error), ITAE (integral time absolute error) and IE (integral error).

Table 6.5 shows the values of various errors (performance indices) with respect to different controllers.

Table 6.5 Value of various errors for different controllers

Error	**Without PFC**	**With PFC**	**With Fuzzy PI**
IE	22.13	14.92	11.09
IAE	29.62	29.12	11.09
ISE	17.23	15.77	8.41
ITAE	988.4	950.5	550.4

From the Table 6.5 it can be concluded that Fuzzy PI controller performs better as compared to other controllers as its errors (performance indices) are minimum.

Form the above discussion it can be concluded that single phase diode rectifier circuit with improved parallel input resonant filter performance well in terms of power factor improvement and total harmonic reduction also this topology performance well for DC motor thyristor based open loop control and Fuzzy PI controller with PFC results better as compared to other controllers.

CHAPTER 7

CONCLUSION AND FUTURE SCOPE

In this dissertation, a comparative study of different power factor correction circuit is done on the basis of various parameters, through that it is concluded that single phase diode rectifier circuit with improved parallel input resonant filter performed well and also that topology improve the power factor and reduce the total harmonics distortion when implemented with controlled rectifiers taking DC motor as a load, with all four types of controlled schemes those are half wave converter drive, seniconverter drive, full wave converter drive and dual converter drive.

For closed loop control of DC motor speed cascade structure is used with PI controller in which the best performed power factor correction topology is included. A comparative study is done of conventional PI controller without PFC, conventional PI controller with PFC and Fuzzy PI controller with PFC through which it is found that Fuzzy PI controller perform well in terms of various time domain parameters and various performance indices.

There are several challenges with passive power factor correction topologies and fuzzy based controller some of them are like passive power factor correction topologies worked well low power rating and also the selection of values of filter component is a big challenge, similarly the selection of scaling factor for Fuzzy PI controller is a big challenge. To overcome above stated problems one should use active power factor correction techniques with suitable switching frequency and some optimization technique should be used for the scaling factor selection.

In future scope of the dissertation, the rule base optimization can be done as the performance of the Fuzzy controller is highly dependent on the number of rules. To reduce the size of the rule base, optimal number of membership function has to be chosen and the optimal width of membership function has to be calculated. To achieve this objective system identification and estimation approach is used. The Kalman filter based H-∞ estimation technique can be used to identify and estimate the new fuzzy membership function and optimize the existing one.